



Universiteit
Leiden
The Netherlands

Brain networks in aging and dementia

Hafkemeijer, A.

Citation

Hafkemeijer, A. (2016, May 26). *Brain networks in aging and dementia*. Retrieved from <https://hdl.handle.net/1887/39720>

Version: Not Applicable (or Unknown)

License: [Licence agreement concerning inclusion of doctoral thesis in the Institutional Repository of the University of Leiden](#)

Downloaded from: <https://hdl.handle.net/1887/39720>

Note: To cite this publication please use the final published version (if applicable).

Cover Page



Universiteit Leiden



The handle <http://hdl.handle.net/1887/39720> holds various files of this Leiden University dissertation

Author: Hafkemeijer, Anne

Title: Brain networks in aging and dementia

Issue Date: 2016-05-26

BRAIN NETWORKS IN AGING AND DEMENTIA

Anne Hafkemeijer

Cover design: Renske van Dieren

Printed by: Drukkerij Mostert & van Onderen, Leiden

ISBN: 978-94-90858-46-9

The research described in this thesis was funded by the Netherlands Initiative Brain and Cognition, a part of the Netherlands Organization for Scientific Research (NWO).

Printing of this thesis was funded by Alzheimer Nederland, ChipSoft B.V., InfoCortex UG, Internationale Stichting Alzheimer Onderzoek, Nutricia Advanced Medical Nutrition, Sectra Benelux, TauRx Therapeutics Ltd., and Leiden University.

© 2016 Anne Hafkemeijer

All rights are reserved. No parts of this publication may be reproduced, stored or transmitted in any form or by any means without permission of the author. Licenses to re-use articles, as published in journals, were granted by the publishers of the journals.

Brain networks in aging and dementia

Proefschrift

ter verkrijging van

de graad van Doctor aan de Universiteit Leiden,

op gezag van de Rector Magnificus prof. mr. C.J.J.M. Stolker,

volgens besluit van het College voor Promoties

te verdediging op donderdag 26 mei 2016

klokke 13.45 uur

door

Anne Hafkemeijer

geboren te Tilburg

in 1986

Promotor

Prof. dr. S.A.R.B. Rombouts

Copromotor

Dr. J. van der Grond

Promotiecommissie

Prof. dr. M.J. de Rooij

Prof. dr. H.A.M. Middelkoop

Prof. dr. J.C. van Swieten, Erasmus Universitair Medisch Centrum Rotterdam

Prof. dr. W.M. van der Flier, VU Medisch Centrum Amsterdam

Table of contents

INTRODUCTION

Chapter 1	General introduction	7
-----------	----------------------	---

SECTION 1 FUNCTIONAL BRAIN NETWORKS

Chapter 2	Imaging the default mode network in aging and dementia. <i>Biochimica et biophysica acta 2012</i>	17
-----------	--	----

Chapter 3	Increased functional connectivity and brain atrophy in elderly with subjective memory complaints. <i>Brain connectivity 2013</i>	43
-----------	---	----

Chapter 4	Resting state functional connectivity differences between bvFTD and AD. <i>Frontiers in Human Neuroscience 2015</i>	63
-----------	--	----

Chapter 5	A longitudinal study on resting state functional connectivity in bvFTD and AD. <i>Submitted for publication</i>	85
-----------	--	----

SECTION 2 STRUCTURAL BRAIN NETWORKS

Chapter 6	Associations between age and gray matter volume in anatomical brain networks in middle-aged to older adults. <i>Aging cell 2014</i>	111
-----------	--	-----

Chapter 7	Differences in structural covariance brain networks between bvFTD and AD. <i>Human Brain Mapping 2016</i>	129
-----------	--	-----

DISCUSSION

Chapter 8	General discussion	147
-----------	--------------------	-----

Chapter 9	Nederlandse samenvatting	161
-----------	--------------------------	-----

APPENDIX	Abbreviations	169
-----------------	---------------	-----

	References	171
--	------------	-----

	Dankwoord	193
--	-----------	-----

	Curriculum vitae	195
--	------------------	-----

	List of publications	197
--	----------------------	-----

Chapter 1

General introduction

Humans are living longer than ever and life expectancy is still increasing (Mathers et al. 2015). Advancing age is a major risk factor for the development of dementia, therefore the number of dementia patients will increase in the coming years. Alzheimer's disease (AD) is the most common type of dementia and is mainly characterized by deficits in episodic and working memory (McKhann 2011). Another common type of dementia is behavioral variant frontotemporal dementia (bvFTD) (Ratnavalli et al. 2002). Patients with bvFTD typically present with changes in behavior and personality (Rascovsky et al. 2011).

Nevertheless, symptoms vary considerably, with overlap of symptoms between AD and bvFTD, including memory disturbances (Irish et al. 2014) and behavioral abnormalities (Woodward et al. 2010). Due to this heterogeneity and overlap of symptoms, clinical differentiation between both types of dementia may be challenging, particularly early in the disease.

An accurate and early diagnosis is essential, since it is a guide to prognosis and prerequisite for optimal clinical care and management. Therefore, to improve diagnostic accuracy and early differential diagnosis, there is a strong need for early markers of changes associated with different types of dementia (Raamana et al. 2014). Potential biomarker information may come from multiple sources, including clinical tests for memory impairment, bodily fluid or tissues, and voxel-based neuroimaging (Gomez-Ramirez and Wu 2014). These sources have contributed considerably to the understanding of dementia but do not yet provide enough sensitivity and specificity to establish an accurate early diagnosis. Hence, there is a need to further elucidate brain changes associated with dementia.

Cognitive functions, including memory and behavior, are increasingly understood not to be localized in one specific brain area, but rather in networks of a multitude of brain regions. Therefore, brain networks have the potential to give more insight in cognitive dysfunctioning in dementia than approaches that focused on local brain areas (Evans 2013; Fornito et al. 2015). The network degeneration or disconnection hypothesis implies that dementia starts in one part of the brain and progressively spreads to connected areas (Seeley et al. 2009). It has been suggested that different neurodegenerative diseases have specific large-scale distributed networks of degeneration (Seeley et al. 2009).

The main goal of this thesis was to improve our insights in brain networks in healthy aging and dementia. We used resting state functional magnetic resonance imaging (fMRI) and structural magnetic resonance imaging (MRI). These two innovative neuroimaging techniques allow us to investigate both functional and structural brain networks, which will be briefly introduced in the next paragraphs.

1.1. FUNCTIONAL BRAIN NETWORKS

Imaging of functional brain networks offers the opportunity to study brain function in healthy aging and has the potential to detect disease-specific network dysfunction in dementia (Seeley et al. 2009; Pievani et al. 2011). Functional networks are studied using resting state fMRI, a non-invasive technique that measures spontaneous blood oxygen level dependent (BOLD) signal fluctuations in the brain (Fox and Raichle 2007). During a resting state fMRI scan the participant is not actively participating in a particular task. Therefore, this approach is not limited to cognitive tasks that patients can successfully perform and is not restricted to studying brain areas activated by the task.

Resting state fMRI is used to study large-scale functional network interactions of brain regions throughout the entire brain. Spatially distinct brain regions with co-varying resting state fMRI signals are defined to be functional connected and represent resting state networks (RSNs). A number of RSNs are revealed and show remarkable correspondence to patterns of task activation and are consistently found across subjects, studies, and study groups (Beckmann et al. 2005; Damoiseaux et al. 2006).

Two frequently studied RSNs are the default mode network and the salience network, which include posterior hippocampal-cingulo-temporal-parietal structures and anterior frontoinsula-cingulo-orbitofrontal structures respectively. Former studies have shown disease related abnormalities in functional network interactions in the default mode network in AD (Greicius et al. 2004; Allen et al. 2007; Binnewijzend et al. 2012) and in the salience network in bvFTD (Zhou et al. 2010; Agosta et al. 2013; Filippi et al. 2013; Rytty et al. 2013).

Moreover, abnormalities in functional brain networks were found in mild cognitive impairment (Binnewijzend et al. 2012; He et al. 2014) and in asymptomatic participants at genetic risk for developing neurodegenerative diseases (Filippini et al.

2009; Sheline, Morris, et al. 2010; Chhatwal et al. 2013; Dopper et al. 2014; Rytty et al. 2014). These findings show the potential of resting state fMRI to measure network degeneration in dementia.

In this thesis, we studied functional brain networks in a standardized way using eight predefined functional networks as a reference (Beckmann et al. 2005). These standardized RSNs parcellate the whole-brain into eight networks of interest: I) medial visual network: calcarine sulcus, precuneal, and primary visual cortex, II) lateral visual network: superior and fusiform areas of lateral occipital cortex, III) auditory system network: superior temporal, insular, anterior cingulate, and auditory cortex, operculum, somatosensory cortices, thalamus, IV) sensorimotor system network: precentral and postcentral somatomotor areas, V) default mode network: rostral medial prefrontal, precuneal, and posterior cingulate cortex, VI) executive control network: medial and inferior prefrontal cortex, anterior cingulate and paracingulate gyri, and prefrontal cortex, VII and VIII) dorsal visual stream networks: frontal pole, dorsolateral prefrontal cortex, parietal lobule, paracingulate gyrus, posterior cingulate cortex (for further details, see (Beckmann et al. 2005)).

We used this model-free approach to study whole-brain functional networks without any bias towards specific brain regions. The use of these standardized networks will improve comparability between studies described in this thesis and with other studies that used these predefined networks.

1.2. STRUCTURAL BRAIN NETWORKS

Structural MRI gives insight in brain structure. Healthy aging and dementia are associated with loss of brain tissue, in which process especially the gray matter seems affected (Good et al. 2001; Krueger et al. 2010). In AD, gray matter atrophy is most often found in the hippocampus, precuneus, posterior cingulate cortex, parietal, and occipital brain regions (Buckner et al. 2005; Seeley et al. 2009; Krueger et al. 2010). Patients with bvFTD show most prominent atrophy in the anterior cingulate cortex, frontoinsula, and frontal brain regions (Seeley et al. 2009; Krueger et al. 2010).

Moreover, structural MRI data can be used to study structural brain networks based on covariance of gray matter intensity. These structural covariance networks (SCNs) take into account the inter-regional dependencies rather than the common analyses

that consider voxels separately. In this thesis, we studied structural brain networks in aging and dementia using independent component analysis (ICA), a statistical technique that decomposes a set of signals into spatial maps of maximal statistical independence (Beckmann and Smith 2004). When applied on gray matter images of different subjects, this method defines spatial components based on the structural covariance of gray matter density among subjects (Douaud et al. 2014). An advantage of this method is that it investigates whole-brain anatomical networks in an unrestricted exploratory way, without the use of a priori selected regions of interest that might introduce a selection bias (Damoiseaux and Greicius 2009).

The disease-specific patterns of gray matter atrophy in AD and bvFTD show spatial overlap with distinct structural and functional brain networks (Seeley et al. 2009). The pattern of atrophy in AD shows overlap with the default mode network in cognitively healthy controls and the typical atrophy pattern in bvFTD shows overlap with the salience network in controls (Seeley et al. 2009). This spatial colocalization of regional gray matter atrophy and structural brain networks suggests that both types of dementia target specific anatomical networks. In this thesis, we used structural brain networks to investigate inter-regional dependencies between gray matter structures in healthy aging and dementia

1.3. AIM AND OUTLINE OF THIS THESIS

The main aim of this thesis was to gain more insight in brain networks in aging and dementia. More specifically, to explore functional brain networks (*section 1*) and structural brain networks (*section 2*) in healthy aging, AD, and bvFTD patients. This thesis is organized as a collection of scientific papers, consequently a certain degree of overlapping through the most general parts of the following chapters cannot be excluded.

Section 1: functional brain networks

In the first section, we focused on functional brain networks based on resting state functional connections. *Chapter 2* gives a literature overview of studies on the default mode functional brain network in aging and dementia. The default mode network is particularly relevant for aging and dementia, since its structures are vulnerable to dementia pathology (Buckner et al. 2005). This review provides relevant background information for the work that will be presented in this thesis.

Chapter 3 describes the results of a study on functional brain networks in elderly with self-reported subjective memory complaints (SMC) who did not meet the criteria for mild cognitive impairment or dementia. The results of this study show that memory complaints are a reflection of objective alterations in functional brain networks. This suggests that functional connections are useful to investigate brain network integrity.

In next two chapters (*chapters 4 and 5*), the focus is on functional brain networks in dementia. The main project of this thesis, “Functional markers for cognitive disorders: dementia”, is a collaboration between the Leiden University Medical Center, the Alzheimer Center of the VU University Medical Center Amsterdam, and the Alzheimer Center of the Erasmus University Medical Center Rotterdam. In this multicenter study, we collected longitudinal (f)MRI data to investigate brain network differences between AD and bvFTD.

In *chapter 4*, we investigate the potential of resting state fMRI to distinguish both types of dementia in an early stage of the disease. The findings of this baseline study support the hypothesis that resting state fMRI shows disease-specific functional connectivity differences and is useful to elucidate the pathophysiology of AD and bvFTD.

Chapter 5 describes the follow-up study of our multicenter project. In this study, we show disease-specific brain regions with longitudinal changes in functional connectivity in AD and bvFTD. This suggests the potential of longitudinal resting state fMRI to delineate regions relevant for disease progression and for diagnostic accuracy.

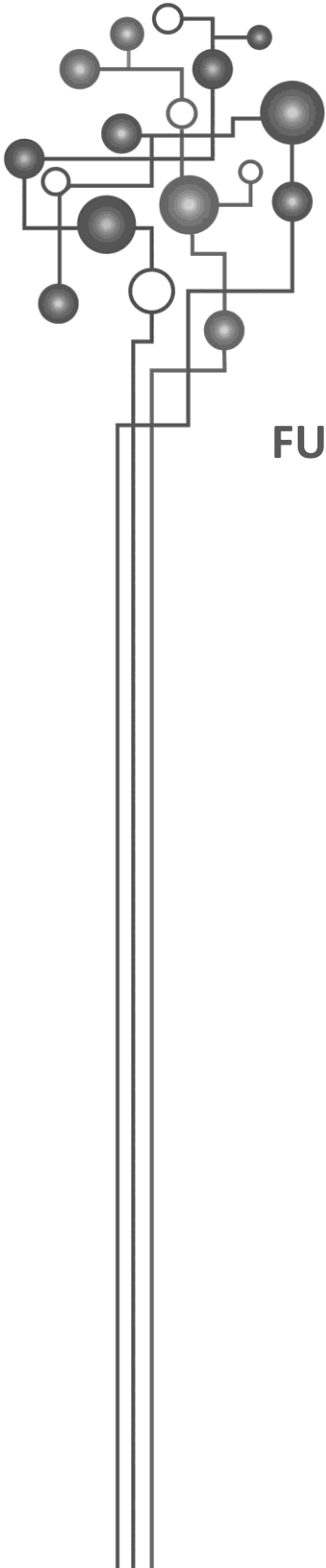
Section 2: structural brain networks

The focus of the second section is on structural networks based on covariance of gray matter intensity. In this section, we used a relatively new approach to investigate inter-regional anatomical connections.

In *chapter 6*, we investigate structural brain networks in a large group of cognitively healthy middle-aged to older adults. In this study, we show that specific anatomical networks degenerate with age, while other networks remain relatively unaffected with advancing age.

Chapter 7 describes a study on structural brain networks in bvFTD and AD. The results of this study confirm our hypothesis that both types of dementia have specific networks of degeneration and show that structural covariance gives valuable insight in the understanding of network pathology in dementia.

To conclude, *chapter 8* provides a summary and discussion of the main findings of the studies described in this thesis. In this chapter, methodological considerations and recommendations for further research will be discussed as well.



SECTION 1

FUNCTIONAL BRAIN NETWORKS

Chapter 2

Imaging the default mode network in aging and dementia

Anne Hafkemeijer, Jeroen van der Grond, and Serge Rombouts



2.1. ABSTRACT

Although in the last decade brain activation in healthy aging and dementia was mainly studied using task-activation functional magnetic resonance imaging (fMRI), there is increasing interest in task-induced decreases in brain activity, termed deactivations. These deactivations occur in the so-called default mode network (DMN). In parallel a growing number of studies focused on spontaneous, ongoing 'baseline' activity in the DMN. These resting state fMRI studies explored the functional connectivity in the DMN.

Here we review whether normal aging and dementia affect task-induced deactivation and functional connectivity in the DMN. The majority of studies show a decreased DMN functional connectivity and task-induced DMN deactivations along a continuum from normal aging to mild cognitive impairment and to Alzheimer's disease (AD). Even subjects at risk for developing AD, either in terms of having amyloid plaques or carrying the apolipoprotein E4 (APOE4) allele, showed disruptions in the DMN.

While fMRI is a useful tool for detecting changes in DMN functional connectivity and deactivation, more work needs to be conducted to conclude whether these measures will become useful as a clinical diagnostic tool in AD.

2.2. INTRODUCTION

Brain activation in healthy aging and dementia is generally studied using task-activation functional magnetic resonance imaging (fMRI). With this technique, blood oxygenation level dependent (BOLD) signal differences are studied between experimental conditions and a control condition. In general, task-related increases in BOLD signal are observed (Buckner et al. 2000; Smith 2010).

In recent years, a substantial amount of fMRI studies on aging and dementia focused on task-induced decreases in brain activity, termed ‘deactivations’ (Gusnard and Raichle 2001). Deactivations refer to the observation that brain activity decreases in the experimental condition compared to the control condition. These occur over a wide variety of tasks in specific brain regions. These regions include the medial prefrontal cortex (mPFC), posterior cingulate cortex (PCC), precuneus, anterior cingulate cortex (ACC), parietal cortex, and in a minority of studies also the hippocampus (Buckner et al. 2008). These brain structures are particularly active during ‘rest’ and deactivate during a variety of tasks (Raichle et al. 2001). This collection of brain regions has been defined as the ‘default mode network’ (DMN) (*Fig. 2.1*) (Raichle et al. 2001).

In parallel with the increasing interest in deactivations in the DMN, a vast increasing amount of studies focused on spontaneous, ongoing ‘baseline’ activity in the DMN (Fox and Raichle 2007). At rest, the brain is organized in networks of coherent spontaneous activation, highly similar to networks of task-induced activations and deactivations (Smith et al. 2009; Biswal et al. 2010). Hence, these networks, including the DMN, show functional connectivity at resting state.

In the present paper, we review aging and dementia studies of task-induced deactivation and resting state functional connectivity within the DMN. The DMN is particularly relevant for aging and dementia since DMN structures are vulnerable to atrophy, deposition of the amyloid protein, and generally show a reduced glucose metabolism (Benson et al. 1983; Minoshima et al. 1997; Buckner et al. 2005).

Task-induced deactivation of the DMN is generally studied with standardized analysis methods, focusing on decreases in BOLD signal during experimental conditions compared to control conditions. In contrast, resting state functional connectivity

studies utilize a variety of post-processing methods (Cole et al. 2010; Zhang and Raichle 2010). The majority of approaches are model-driven, with strong a priori hypotheses regarding the functional connectivity between a small brain region (seed) and the rest of the brain (seed-based analysis). Another often applied technique is independent component analysis (ICA). With this data-driven technique, the functional connectivity within large-scale networks can be analyzed.

In this review, we describe DMN resting state functional connectivity and task-induced deactivation studies in normal aging (paragraph 2.3), Alzheimer's disease (AD) patients (paragraph 2.4), and in cognitively normal subjects at risk for developing AD (paragraph 2.5 - 2.7).

In paragraph 2.5, we discuss DMN fMRI studies in healthy elderly with amyloid depositions. Amyloid, a major pathological feature of AD, is a risk factor for developing AD since these protein aggregates precede clinical AD in asymptomatic individuals. Particularly vulnerable to early amyloid deposition are posterior regions of the DMN (Buckner et al. 2005).

An overview of DMN fMRI studies in cognitively normal individuals at genetic risk for developing dementia is presented in paragraph 2.6. The apolipoprotein E4 (APOE4) allele is associated with an increased risk of early- and late-onset AD (Strittmatter et al. 1993; Okuizumi et al. 1994). In this paragraph we will focus on DMN fMRI studies in cognitively normal subjects with the APOE4 allele.

The field of aging and dementia is focusing on the characterization of the earliest stages of cognitive impairment. Mild cognitive impairment (MCI) is a transitional state between the cognitive changes of normal aging and the earlier changes associated with AD (Petersen et al. 1997). Since roughly half of the patients with a diagnosis of MCI convert into AD within 3 to 5 years, MCI is a high-risk factor for developing AD (Peterson et al. 2001). Paragraph 2.7 focuses on DMN studies in MCI patients, exploring to what extent changes in the DMN of MCI patients are similar to changes in DMN BOLD signal in AD. In paragraph 2.8, we briefly discuss DMN fMRI studies in dementia with Lewy bodies (DLB) and frontotemporal dementia (FTD).

2.3. NORMAL AGING

Resting state fMRI in normal aging

The studies that have been published on healthy aging and functional connectivity in the DMN during resting state, generally showed decreased connectivity in the DMN with aging.

In healthy elderly, a decreased functional connectivity was demonstrated in a variety of DMN brain regions. These included the PCC, superior and middle frontal gyrus, and the superior parietal region (Andrews-Hanna et al. 2007; Damoiseaux et al. 2008; Biswal et al. 2010; Koch et al. 2010). While in these studies younger and older subjects were compared, one multicenter study analyzed subjects with a continuous age range from 18 to 71 years, showing a negative association between age and DMN connectivity (Biswal et al. 2010). In none of these studies increased DMN connectivity with advancing age was observed, although increases in connectivity were noticed in regions outside the DMN (Biswal et al. 2010).

One study explored age-related effects on functional connectivity in the DMN in combination with a low level processing task (Andrews-Hanna et al. 2007). This study showed that older adults had decreased functional connectivity in anterior and posterior components of the DMN (*Fig. 2.2*). More particular, decreased connectivity was observed between mPFC and PCC, between mPFC and lateral parietal cortex, and between PCC and lateral parietal cortex.

It is well known that aging is accompanied by atrophy of the gray matter (Good et al. 2001). Since it is not exactly known how brain structure and function are related, it is important to study to which extent decreases in connectivity can be explained by gray matter atrophy. One study addressed this question by controlling for regional gray matter volume, using an average measure of gray matter volume of the DMN in each individual (Damoiseaux et al. 2008). After correction for atrophy, the fMRI observed decreases in functional connectivity remained significant, indicating that the aging-related changes in connectivity are not solely associated with reductions in gray matter volume.

Task-induced deactivation in normal aging

Task-induced deactivation in healthy aging has been reported in two studies showing decreased DMN deactivation in the elderly. Elderly subjects showed a decreased task-induced deactivation in the PCC and medial parietal regions compared to younger adults (Lustig et al. 2003). Furthermore, a gradual, age-related decreased deactivation in the DMN was observed when comparing younger, middle-aged, and older adults (Grady et al. 2006). These results suggest that there is an age-related reduction in the ability to suspend default mode activity (Grady et al. 2006).

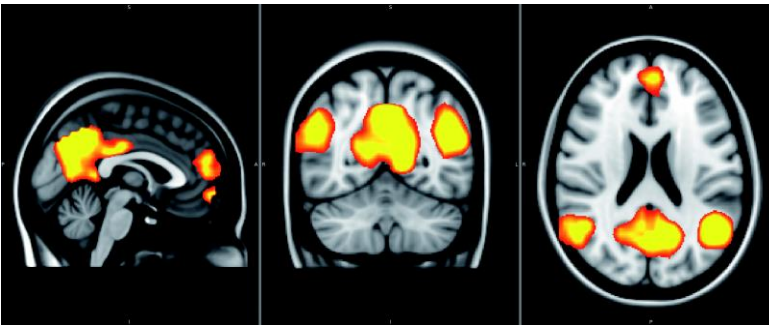


FIGURE 2.1 The default mode network

Specific brain structures that are particularly active in the resting brain and deactivate during a variety of tasks. The DMN includes the mPFC, PCC, precuneus, ACC, and the parietal cortex and in a minority of studies also the hippocampus.

Summary aging and the DMN

Aging-related changes in the DMN mainly comprise a decreased functional connectivity in a variety of brain regions, including the frontal gyrus, PCC, and parietal regions (Andrews-Hanna et al. 2007; Damoiseaux et al. 2008; Biswal et al. 2010; Koch et al. 2010). Task-related fMRI studies showed decreased deactivation patterns in the DMN (Lustig et al. 2003; Grady et al. 2006). Decreases in deactivation were especially detected in the PCC and parietal cortex. These findings suggest that there is an age-related reduction in the ability to suspend default mode activity when the experimental condition requires focused attention (Grady et al. 2006).

Together, these studies showed that with normal aging both functional connectivity at rest and BOLD deactivation are diminished in the DMN. Few data suggest that the extent to which atrophy can be observed on magnetic resonance imaging (MRI), does not explain the fMRI changes (Damoiseaux et al. 2008).

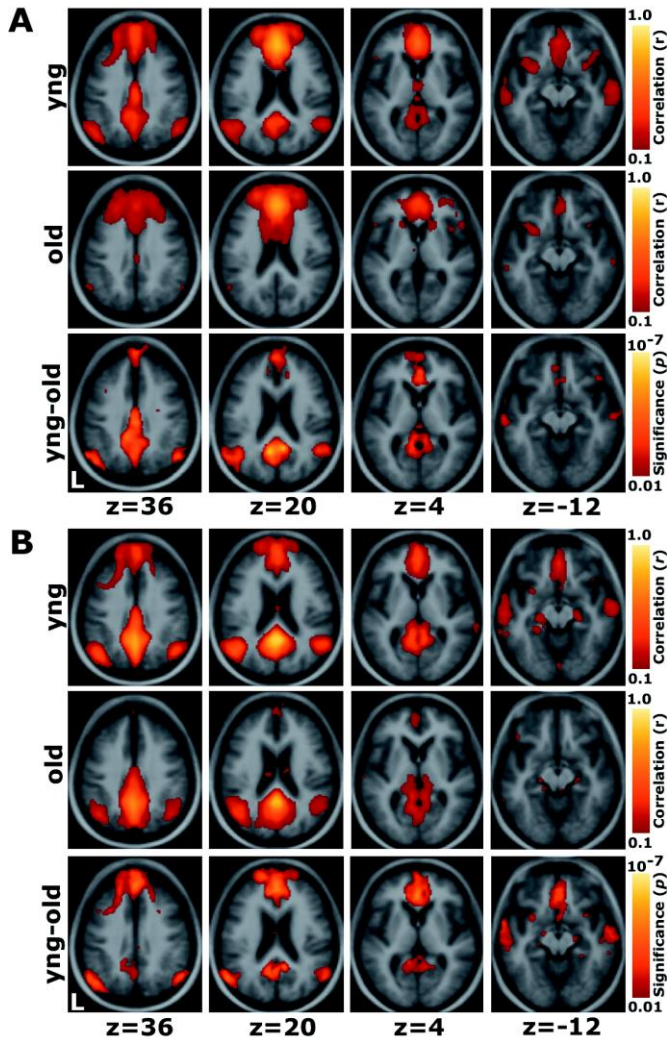


FIGURE 2.2 Whole-brain exploratory analyses reveal widespread correlation reductions in aging

Whole-brain analyses of functional correlations between the seed region and each voxel across the entire brain are graphically overlaid on a combined young and old adult anatomical image. A) For a seed placed in the mPFC, positive correlations with the mPFC time course exceeding a threshold of $r = 0.1$ are colored in red to yellow and averaged for all young participants (top) and all old participants (middle). A direct comparison between the two groups using the young-old contrast (bottom) highlights voxels at a significance level of $p < 0.01$. The young group shows higher correlations with many regions comprising the network. B) The reverse scenario when a seed is placed in the PCC / retrosplenial cortex. Functional correlations between the PCC / retrosplenial cortex and both the mPFC and the bilateral lateral parietal cortex, as well as some hint of the hippocampal formation, decline in old age. In this study statistical tests were performed on z values. Figure and legend reprinted from J.R. Andrews-Hanna, A.Z. Snyder, J.L. Vincent, C. Lustig, D. Head, M.E. Raichle, and R.L. Buckner, Disruption of large-scale brain systems in advanced aging, *Neuron* 56 (2007) page 928. Copyright 2007 Elsevier Inc. with permission from Elsevier Inc.

2.4. ALZHEIMER'S DISEASE

Resting state fMRI in Alzheimer's disease

Studying the DMN is particularly relevant for patients with AD since DMN structures are vulnerable to atrophy, deposition of the amyloid protein, and generally show a reduced glucose metabolism (Benson et al. 1983; Minoshima et al. 1997; Buckner et al. 2005). Studies that investigated DMN functional connectivity in AD showed that this connectivity was decreased. Other studies found evidence for an increase in DMN connectivity.

In AD patients with relatively mild memory complaints, the hippocampus already showed decreased functional connectivity with the mPFC, PCC, precuneus, and ventral ACC (Wang et al. 2006). When the PCC is used as seed region in this patient group, decreased connectivity was found with the mPFC, precuneus (Wang et al. 2007; Zhang et al. 2009), and parietal cortex (Wang et al. 2007). In addition, ICA demonstrated decreased DMN functional connectivity in patients with mild AD (Zhou et al. 2010). Another study that used ICA to analyze fMRI data during a low cognitive demand task, observed decreased resting state activity in the PCC and hippocampus, suggesting disrupted connectivity between these two regions (Greicius et al. 2004).

Other studies have focused on regional homogeneity throughout the entire brain, a method different from between-region connections. These studies showed an AD-related decrease in regional coherence in the PCC and precuneus (He et al. 2007; Liu et al. 2008). The decrease in coherence was correlated with disease progression, even when correcting for gray matter atrophy. In general it is highly relevant to include local gray matter volumes in the analysis since it is well known that AD patients show extensive decreases in gray matter volume in hippocampus, temporal lobe, insula, sensorimotor cortex, and occipital lobe (Karas et al. 2003). Unfortunately, none of the other studies focusing on DMN functional connectivity in AD corrected for gray matter density by including local gray matter volumes in the analysis.

Few studies investigated the association between resting state DMN connectivity and disease severity. Comparing different stages of AD showed that the decrease in DMN connectivity was associated with AD progression and severity (Allen et al. 2007; Zhang et al. 2010; Wu et al. 2011). Moderate AD patients showed more extensive decreased functional connectivity between the hippocampus and the frontal cortex than subjects

with mild AD (Allen et al. 2007). Furthermore, the decreased functional connectivity between PCC and other DMN structures including the mPFC, precuneus, and hippocampus was intensified with AD progression (Zhang et al. 2010). Decreased resting state functional connectivity was found in AD between PCC and right inferior temporal cortex (*Fig. 2.3 and 2.4*) (Wu et al. 2011). Decreased functional connectivity was positively correlated with disease severity (Wu et al. 2011).

While most resting state fMRI studies showed decreased functional connectivity in most regions of the DMN in AD, some studies showed, in addition to decreased functional connectivity, also evidence for increased functional connectivity. Seed-based studies showed increased functional connectivity between a number of DMN brain areas. This was observed between left hippocampus and right lateral PFC (Wang et al. 2006), between parietal and occipital lobes (Wang et al. 2007), and between PCC and mPFC (Zhang et al. 2009, 2010). Increased local homogeneity of the BOLD signal in AD was observed in cuneus and left fusiform gyrus (He et al. 2007).

These studies offer the compensatory-recruitment hypothesis as one of the possible explanations for this increased functional connectivity (Wang et al. 2006, 2007; He et al. 2007; Zhang et al. 2009, 2010). The increased resting state connectivity is consistent with the assumption of Grady et al. that AD patients use additional neural resources to compensate for losses of cognitive function and to maintain task performance (Grady et al. 2003). Nevertheless, this compensatory hypothesis needs to be further investigated in the context of resting state. Furthermore, to study the potential effect of local gray matter volume on the increased functional connectivity, it is highly relevant to include local atrophy as additional confound to the analysis.

Task-induced deactivation in Alzheimer's disease

DMN task-induced deactivation studies in AD showed a decrease in deactivation. Decreased deactivation in medial and lateral parietal regions was observed during an associative memory paradigm in AD patients (Celone et al. 2006). In medial parietal regions and the PCC, decreased deactivation was observed with a semantic classification task in AD patients (Lustig et al. 2003). The mPFC, PCC, precuneus, parietal cortex and hippocampus demonstrated decreased deactivation during a non-spatial working memory task and a visual encoding task for episodic memory in AD patients (Rombouts, Barkhof, et al. 2005; Rombouts et al. 2009).

Summary Alzheimer's disease and the DMN

The DMN is a particularly relevant network in AD research, since DMN structures are vulnerable to atrophy, amyloid deposition, and show a reduced metabolism in AD (Benson et al. 1983; Minoshima et al. 1997; Buckner et al. 2005). Decreased functional connectivity was observed in the mPFC, PCC, precuneus, ACC, and hippocampus (Greicius et al. 2004; Wang et al. 2006, 2007; He et al. 2007; Liu et al. 2008; Zhang et al. 2009; Zhou et al. 2010). An intensified decreased functional connectivity was observed with disease severity (Allen et al. 2007; Zhang et al. 2010; Wu et al. 2011). In addition to decreased connectivity, some studies showed increased functional connectivity in the mPFC, PCC, parietal cortex, and the hippocampus (Wang et al. 2006, 2007; He et al. 2007; Zhang et al. 2009, 2010).

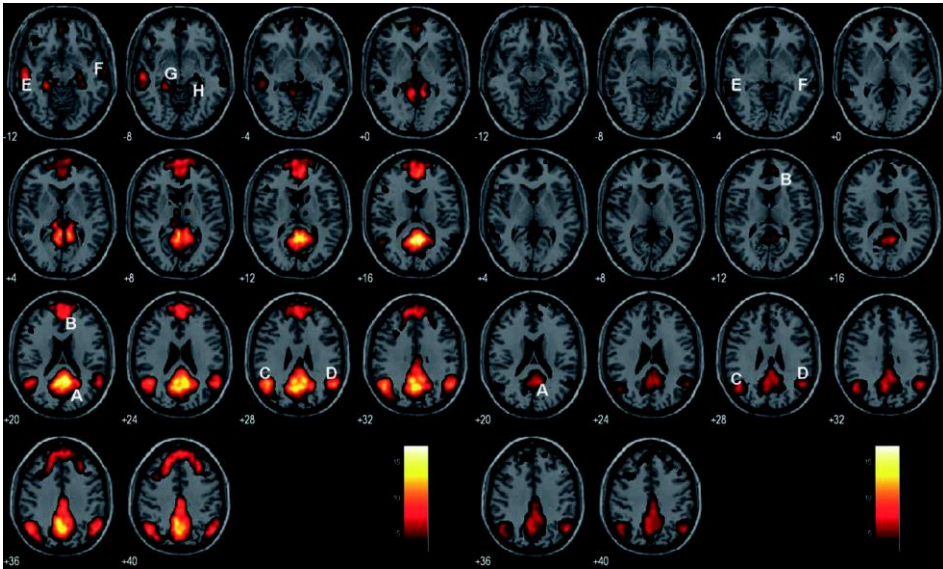


FIGURE 2.3 DMN of the normal control and AD groups

Axial images show the network for the normal control (left panel) and AD (right panel) groups, respectively. The white capital letters indicate the specific regions in the DMN. A) PCC, B) mPFC, C) left inferior parietal cortex, D) right inferior parietal cortex, E) left inferior temporal cortex, F) right inferior temporal cortex, G) left hippocampus, H) right hippocampus. T score bar is shown on the right (false discovery rate, $p = 0.05$). Figure and legend reprinted from X. Wu, R. Li, A.S. Fleisher, E.M. Reiman, X. Guan, Y. Zhang, K. Chen, and L. Yao, Altered default mode network connectivity in Alzheimer's disease – a resting functional MRI and Bayesian network study, *Human brain mapping* 32 (2011) page 1873. Copyright 2011 Wiley-Liss, Inc. with permission from Wiley-Liss, Inc.

These studies offer the compensatory-recruitment hypothesis as one of the possible explanations for the increased functional connectivity (Wang et al. 2006, 2007; He et

al. 2007; Zhang et al. 2009, 2010). Task-related fMRI studies showed decreased DMN deactivations in the mPFC, PCC, parietal cortex, and hippocampus (Lustig et al. 2003; Rombouts, Barkhof, et al. 2005; Celone et al. 2006; Rombouts et al. 2009).

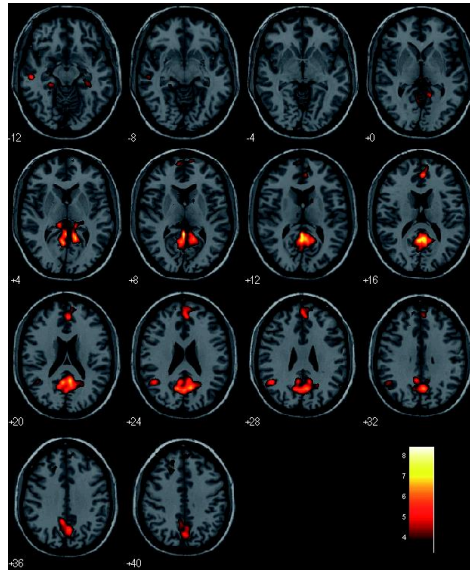


FIGURE 2.4 DMN differences between the normal control and AD groups

Difference in the functional connectivity of DMN between normal control and AD groups (normal controls vs. AD). Two sample t-test (false discovery rate, $p = 0.05$). Figure and legend reprinted from X. Wu, R. Li, A.S. Fleisher, E.M. Reiman, X. Guan, Y. Zhang, K. Chen, and L. Yao, Altered default mode network connectivity in Alzheimer's disease – a resting functional MRI and Bayesian network study, *Human brain mapping* 32 (2011) page 1874. Copyright 2011 Wiley-Liss, Inc. with permission from Wiley-Liss, Inc.

Taken together, most of these studies showed AD-related decreases in functional connectivity at rest and BOLD deactivation in the DMN, with evidence for increased functional connectivity as well. It is currently not clear to what extent these changes may be explained by atrophy, since the majority of these studies did not include this potential confound in the analysis.

2.5. AMYLOID DEPOSITION

Resting state fMRI in subjects with amyloid deposition

The deposition of amyloid protein is a major pathological feature of AD. Using positron emission tomography (PET) scans it is possible to image amyloid in the brain (Klunk et al. 2004). Interestingly, the majority of regions with amyloid deposition in AD patients are located in the DMN (Buckner et al. 2005). In addition to the amyloid plaques observed in AD, deposition of amyloid is present in cognitively normal individuals (Delaère et al. 1993). Brain regions particularly vulnerable to early amyloid deposition are posterior components of the DMN including the precuneus and PCC (Buckner et al. 2005).

A number of studies have been published that focus on the relation between amyloid deposition as imaged with PET scans, and resting state fMRI connectivity. Even when controlling for age and structural atrophy, decreased functional connectivity was observed between the PCC and mPFC, and between the PCC and hippocampus in cognitively normal elderly with high amyloid burden in frontal, lateral parietal, lateral temporal, and retrosplenial cortices compared to elderly with low amyloid burden (*Fig. 2.5*) (Hedden et al. 2009).

Another study showed decreased resting state functional connectivity between the precuneus and a number of areas in cognitively normal elderly with amyloid depositions (Sheline, Raichle, et al. 2010). These regions include ACC, parahippocampus, and hippocampus. In addition to the decreased DMN functional connectivity between PCC and mPFC, there is evidence for increased connectivity yet outside the DMN in cognitively normal subjects with amyloid depositions (Mormino et al. 2011).

A recent study explored whether cognitively normal subjects with amyloid depositions demonstrated disruptions of functional whole-brain connectivity in ‘cortical hubs’ (Drzezga et al. 2011). These ‘cortical hubs’ are brain regions with disproportionately numerous connections to other brain regions (Sporns et al. 2007; Buckner et al. 2009). When correcting for regional gray matter volume, disruptions of whole-brain connectivity were observed in the PCC and precuneus hub regions in cognitive normal individuals with amyloid depositions.

Task-induced deactivation in subjects with amyloid deposition

Only one task-related fMRI study has been published that focused on the relation between amyloid deposition and task-induced deactivation in the DMN (Sperling et al. 2009). Decreased deactivation in the DMN was observed in cognitively normal subjects with amyloid depositions in a variety of brain areas, including left mPFC, left PCC, and lateral parietal regions. These structures are similar to the structures with decreased task-induced deactivation observed in AD.

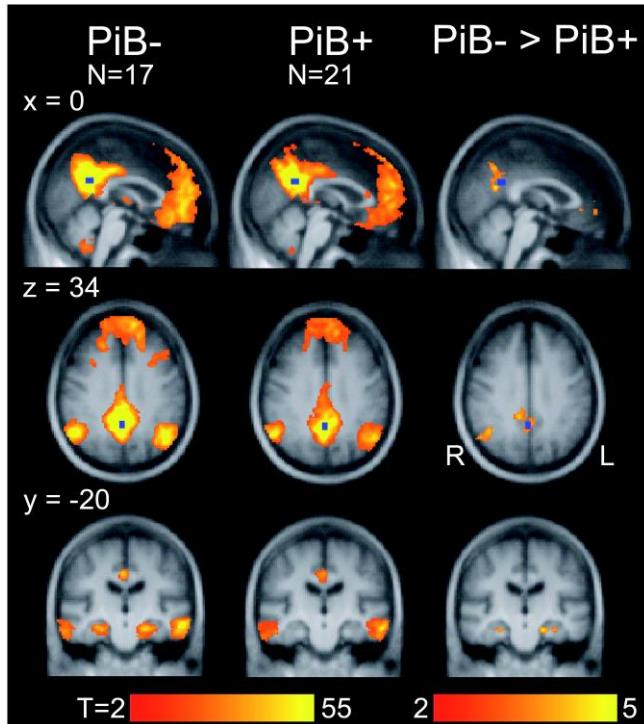


FIGURE 2.5 DMN in participants with amyloid deposition

Exploratory whole-brain analyses confirm disruption of the default network including the hippocampal formation. Maps display regions that are significantly (cluster-corrected threshold of $p < 0.05$) correlated with a seed placed in the PCC (shown in blue) for clinically normal participants with (PiB+) and without (PiB-) substantial amyloid burden. The third column displays regions with significantly greater functional correlations in the PiB- than in the PiB+ group. Regions displaying group differences included lateral parietal cortex and mPFC, as well as bilateral regions within the hippocampal formation (family-wise error correction of $p < 0.05$ corresponding to $p < 0.005$ in conjunction with a cluster constraint $k > 136$). Figure and legend reprinted from T. Hedden, K.R.A. Van Dijk, J.A. Becker, A. Mehta, R.A. Sperling, K.A. Johnson, and R.L. Buckner, Disruption of functional connectivity in clinically normal older adults harboring amyloid burden, *The journal of neuroscience* 29 (2009) page 12691. Copyright 2009 Society of neuroscience with permission from Society of Neuroscience.

Summary amyloid deposition and the DMN

Cognitively normal subjects with amyloid depositions as observed on PET scans showed, even when corrected for regional gray matter volume, decreased resting state functional connectivity in the mPFC, PCC, precuneus, ACC, and hippocampus (Hedden et al. 2009; Sheline, Raichle, et al. 2010; Drzezga et al. 2011; Mormino et al. 2011). Task-induced decreased deactivations were observed in the mPFC, PCC, and lateral parietal cortex (Sperling et al. 2009). Together, these studies suggest that amyloid pathology is related to disrupted neural responses in the DMN, even before cognitive impairment is shown.

2.6. GENETIC RISK FOR DEMENTIA

Resting state fMRI in subjects with genetic risk for dementia

Genetic studies show unequivocally that the APOE4 allele is associated with an increased risk of early- and late-onset AD (Strittmatter et al. 1993; Okuizumi et al. 1994). There has been an interest to use MRI to study brain structure and task-related fMRI to study brain function in asymptomatic carriers of the APOE4 allele. These studies show hippocampal and frontotemporal gray matter reduction (Wishart, Saykin, McAllister, et al. 2006) and a greater task-related activation in APOE4 carriers relative to non-carriers (Bookheimer et al. 2000; Fleisher et al. 2005; Wishart, Saykin, Rabin, et al. 2006). More recently, deactivation and resting state fMRI studies focused on the DMN in APOE4 carriers. These studies found altered functional connectivity and deactivations within the DMN of APOE4 carriers.

Decreased functional connectivity was observed in the DMN between PCC and precuneus, and between PCC and gyrus rectus in asymptomatic older APOE4 carriers (Fleisher et al. 2009). Furthermore, this study demonstrated increased connectivity between the PCC and other brain areas, including PFC, left parietal gyrus, and right hippocampus. Further, increased functional connectivity was observed between the hippocampus and the posterior DMN, even when corrected for gray matter atrophy (Westlye et al. 2011). A seed-based study showed decreases in functional connectivity between the precuneus and a number of DMN regions in healthy APOE4 carriers with the same age (Sheline, Morris, et al. 2010). A recent study showed decreased functional connectivity in older APOE4 carriers between the PCC and the posterior DMN that included parietal and temporal cortex (Machulda et al. 2011).

While these four studies focused on elderly APOE4 carriers, two studies investigated functional connectivity in younger APOE4 carriers (Filippini et al. 2009; Dennis et al. 2010). Using voxel-wise gray matter as confound, increased functional connectivity between DMN and hippocampus is observed in young carriers (Filippini et al. 2009). This finding is replicated by another study that showed increased connectivity between medial temporal lobe and PCC in carriers (Dennis et al. 2010). The same study also showed decreased functional connectivity between anterior and posterior cortices (Dennis et al. 2010).

Task-induced deactivation in subjects with genetic risk for dementia

Task-induced DMN deactivation in asymptomatic APOE4 carriers was investigated in some studies. Older APOE4 carriers showed decreased task-induced deactivations in the DMN compared to non-carriers. These decreased deactivations were found in left PCC and precuneus (*Fig. 2.6A*) (Pihlajamäki and Sperling 2009), mPFC (Persson et al. 2008), and parietal cortex (Persson et al. 2008; Fleisher et al. 2009). Since no support for a direct association between atrophy and deactivation magnitudes was found (Persson et al. 2008), further studies are required to establish the link between DMN deactivation changes and structural changes.

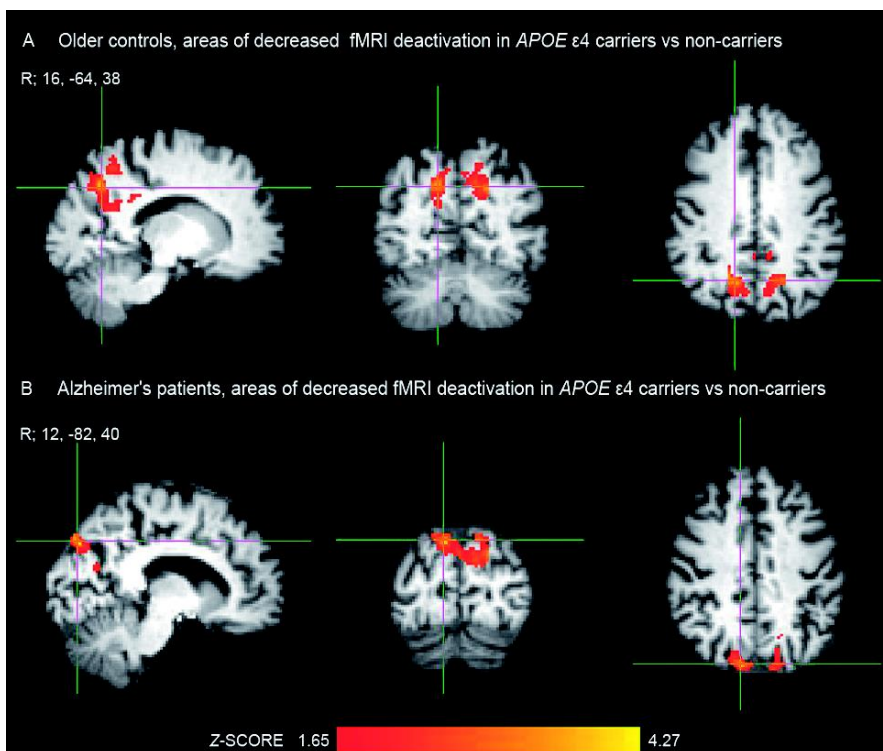


FIGURE 2.6 A) In older controls, fMRI deactivation was significantly decreased in the precuneus and PCC in APOE4 carriers compared to non-carriers. MNI (Montreal Neurological Institute standard space image) coordinate of the crosshair (x, y, z), located in the right (R) precuneal cortex, is 16, -64, 38. B) Similarly, in patients with AD, the failure of deactivation was more pronounced in APOE4 carriers than in non-carriers. Coordinate of the crosshair, located in the right posterior precuneus bordering to the parieto-occipital fissure, is 12, -82, 40. Figure and legend reprinted from M. Pihlajamäki and R.A. Sperling, Functional MRI assessment of task-induced deactivation of the default mode network in Alzheimer's disease and at-risk older individuals, *Behavioural neurology* 21 (2009) page 85. Copyright 2009 IOS Press and the authors with permission from IOS Press.

In addition to decreased deactivations detected in older asymptomatic APOE4 carriers, AD patients with an APOE4 allele also showed decreased deactivation in the PCC compared to AD patients without this allele (*Fig. 2.6B*) (Pihlajamäki and Sperling 2009).

Summary genetic risk for dementia and the DMN

Asymptomatic APOE4 carriers have an increased risk to develop early- and late-onset AD (Strittmatter et al. 1993; Okuizumi et al. 1994). Compared to non-carriers, older healthy APOE4 carriers show alterations in resting state functional connectivity. Both decreases and increases have been observed (Fleisher et al. 2009; Sheline, Morris, et al. 2010; Machulda et al. 2011; Westlye et al. 2011). In younger APOE4 carriers connectivity was increased, not decreased, between the hippocampus and the DMN (Filippini et al. 2009; Dennis et al. 2010). Deactivation in APOE4 carriers appeared diminished, not increased, in all studies (Persson et al. 2008; Fleisher et al. 2009; Pihlajamäki and Sperling 2009).

The DMN abnormalities in functional connectivity and deactivation in APOE4 carriers are established in the absence of any cognitive impairment. Furthermore, some studies showed DMN abnormalities in the absence of cerebral amyloid plaques (Persson et al. 2008; Filippini et al. 2009). This indicates that even without cognitive impairment, the presence of the genetic risk factor for dementia is related to disruptions in the DMN.

2.7. MILD COGNITIVE IMPAIRMENT

Resting state fMRI in mild cognitive impairment

Characterization the earliest stages of cognitive impairment is receiving increased attention in the field of aging and dementia research. MCI is a transitional state between the cognitive changes of normal aging and the earlier changes associated with AD (Petersen et al. 1997). Since roughly half of the patients with an MCI diagnosis convert into AD within 3 to 5 years, MCI is a high-risk condition for developing AD (Peterson et al. 2001). Structural and functional MRI studies used in the evaluation of MCI (Jack et al. 1999; De Rover et al. 2011) support the view that MCI shares features with AD, such as hippocampal atrophy. More recently, deactivation and resting state fMRI studies focusing on the DMN in MCI patients were conducted. These studies showed altered functional connectivity and deactivations within the DMN of MCI patients.

Functional connectivity between hippocampi and PCC present in healthy controls was absent in MCI patients (*Fig. 2.7*) (Sorg et al. 2007). Furthermore, MCI patients showed decreased functional connectivity between PCC and ACC, PCC and frontal cortex, mPFC and PCC, mPFC and ACC, and between mPFC and frontal cortex (Gili et al. 2011). This study also compared MCI to AD patients and revealed that the decrease in functional connectivity in MCI is less severe than in AD.

Given the changes in gray matter volume in MCI patients (Gili et al. 2011), it is relevant to further study the relation between structure and function in MCI. Three studies observed decreased connectivity in MCI, even when correcting for regional gray matter volume (Bai et al. 2008; Drzezga et al. 2011; Han et al. 2011). One of these studies observed decreased whole-brain connectivity in PCC and precuneus in MCI patients with amyloid burden (Drzezga et al. 2011). The PCC and precuneus showed decreased regional homogeneity in MCI patients after gray matter correction (Bai et al. 2008). The third study showed decreased amplitudes of low-frequency fluctuations in mPFC, PCC, precueus, and hippocampus in MCI patients (Han et al. 2011).

Recently, a longitudinal based study distinguished patients with MCI who undergo cognitive decline and conversion to AD from those who remain stable over a 2 to 3 year follow-up period (Petrella et al. 2011). MCI converters showed more severe decreased functional connectivity compared to non-converters. Furthermore, this

study observed most severe decreases in resting state functional connectivity in AD, while intermediate decreases were observed in MCI. These effects on DMN connectivity remained significant after controlling for gray matter volume.

Task-induced deactivation in mild cognitive impairment

Task-induced MRI studies showed decreased DMN deactivation in MCI patients. Comparing MCI patients to healthy elderly, decreased task-related deactivation was found in the PCC, precuneus (Rombouts, Barkhof, et al. 2005; Sala-Llonch et al. 2010), and the anterior frontal lobe (Rombouts, Barkhof, et al. 2005).

The DMN task-induced deactivation pattern is progressively decreased along the continuum from normal aging to MCI and to clinical AD (Rombouts, Barkhof, et al. 2005; Pihlajamäki and Sperling 2009). Moreover, it was shown that compared to normal older controls, less impaired MCI patients had increased task-related deactivation in medial and lateral parietal regions, whereas more impaired MCI patients showed decreased deactivation in these brain areas (Celone et al. 2006). The authors offer the compensatory-recruitment hypothesis as one of the possible explanations for the increased task-related deactivation observed in early MCI.

One study focused on cognitive reserve, which is defined as the capacity of the brain to endure neuropathology in order to minimize clinical manifestations (Bosch et al. 2010). When considering healthy elders versus MCI patients, task-induced deactivation was modulated by cognitive reserve in an opposite manner. In healthy elderly high cognitive reserve is related to decreased deactivation of the DMN. In MCI patients high cognitive reserve was related to increased activity in brain areas involved in the task and with increased deactivation in regions of the DMN. This brain reorganization facilitated by cognitive reserve may reflect behavioral compensatory mechanisms (Bosch et al. 2010).

Summary mild cognitive impairment and the DMN

MCI patients showed decreased functional connectivity within the DMN (Sorg et al. 2007; Bai et al. 2008; Drzezga et al. 2011; Gili et al. 2011; Han et al. 2011; Petrella et al. 2011). The decreased connectivity was observed in the PCC, mPFC, ACC, and hippocampus, even when controlled for gray matter atrophy. MCI converters showed severe decreased functional connectivity compared to non-converters (Petrella et al. 2011). These results suggest that resting-state fMRI could be helpful in the

classification of subjects with MCI, AD, and cognitively normal subjects (Chen et al. 2011).

Decreased task-induced deactivation in MCI patients was found in the PCC, precuneus, frontal, and parietal regions (Rombouts, Barkhof, et al. 2005; Celone et al. 2006; Pihlajamäki and Sperling 2009; Sala-Llonch et al. 2010). These DMN task-induced deactivations are progressively decreased along the continuum from normal aging to clinical AD (Rombouts, Barkhof, et al. 2005; Pihlajamäki and Sperling 2009). There is evidence that an exception is the group of less impaired MCI patients, who showed increased deactivation compared to controls (Celone et al. 2006).

2.8. OTHER SUBTYPES OF DEMENTIA

Resting state fMRI in dementia with Lewy bodies

The second most common neurodegenerative cause of dementia is dementia with Lewy bodies (DLB) (McKeith et al. 1996). A recent study showed that DLB patients had decreased functional connectivity between the precuneus and the mPFC compared to cognitively normal subjects (Galvin et al. 2011). DLB patients also showed increased connectivity between the precuneus and the frontal gyrus, and between the precuneus and the parietal sulcus.

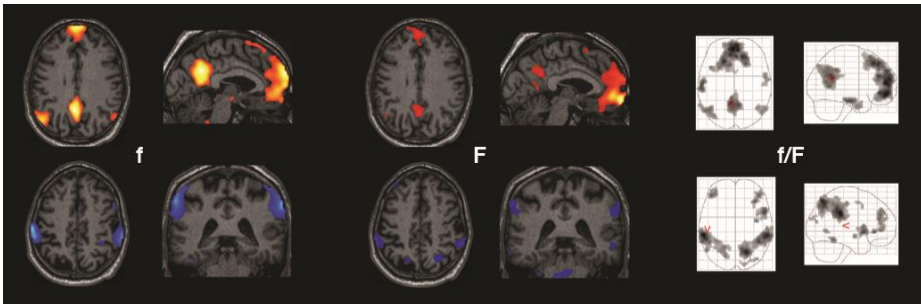


FIGURE 2.7 Resting state network of normal controls and patients with aMCI

Each group independent component image contains a pair of two spatial independent component patterns that are correlated (red) or anticorrelated (blue) with the time course of the component (data not shown). f/F) The upper row represents the correlated independent component pattern, the lower row the anticorrelated one. Independent component patterns are superimposed on a single-subject high-resolution T1 image. The black to yellow/light blue color scale represents z values, ranging from 1.8 to 8.0. Glass brain projections illustrate results of one-sample t tests on the individual back-reconstructed subject independent component patterns across both groups ($p < 0.05$, false discovery rate-corrected). Figure and legend reprinted from C. Sorg, V. Riedl, M. Muhlau, V.D. Calhoun, T. Eichele, L. Laer, A. Drzezga, H. Forstl, A. Kurz, C. Zimmer, A.M. Wohlschlagel, Selective changes of resting-state networks in individuals at risk for Alzheimer's disease, PNAS 104 (2007) page 18762. Copyright 2007 The national academy of science of the USA with permission from The national academy of science of the USA.

Resting state in frontotemporal dementia (FTD)

FTD is another subtype of dementia often seen in younger adults with early impairments in social cognitive and emotional functions. While patients with (risk for) AD commonly showed disruptions in the DMN, FTD patients showed an increased connectivity within this network, which was correlated with the clinical severity of the disease (Seeley, Allman, et al. 2007; Zhou et al. 2010). However, the so-called salience network showed decreased functional connectivity in FTD compared to AD and controls (Fig. 2.8).

Task-induced deactivation in other subtypes of dementia

At present, no studies have been published on DMN task-induced deactivation in patients with DLB or FTD.

2.9. DISCUSSION

This review gives an overview of how normal aging and dementia affect resting state functional connectivity and task-induced deactivations within the DMN. Brain structures of the DMN are particularly active during 'rest' and deactivate during a variety of tasks. This network is particularly relevant for aging and dementia since DMN structures are vulnerable to atrophy, deposition of the amyloid protein, and demonstrate reduced glucose metabolism (Benson et al. 1983; Minoshima et al. 1997; Buckner et al. 2005).

Decreased DMN functional connectivity and task-induced DMN deactivations were observed along a continuum from normal aging (Lustig et al. 2003; Grady et al. 2006; Andrews-Hanna et al. 2007; Damoiseaux et al. 2008; Biswal et al. 2010; Koch et al. 2010) to MCI (Rombouts, Barkhof, et al. 2005; Celone et al. 2006; Sorg et al. 2007; Bai et al. 2008; Pihlajamäki and Sperling 2009; Sala-Llonch et al. 2010; Chen et al. 2011; Drzezga et al. 2011; Gili et al. 2011; Han et al. 2011; Petrella et al. 2011) and to AD (Lustig et al. 2003; Greicius et al. 2004; Rombouts, Barkhof, et al. 2005; Celone et al. 2006; Wang et al. 2006, 2007; Allen et al. 2007; He et al. 2007; Liu et al. 2008; Zhang et al. 2009, 2010; Rombouts et al. 2009; Zhou et al. 2010; Wu et al. 2011). Most severe decreased resting state functional connectivity and task-induced deactivations were found in AD, intermediate decreases were observed in MCI, and normal elderly showed less decreased connectivity and deactivations. Decreased functional connectivity and deactivation in the DMN was observed even in patients at risk for developing AD, either in terms of having amyloid plaques (Hedden et al. 2009; Sperling et al. 2009; Sheline, Raichle, et al. 2010; Drzezga et al. 2011; Mormino et al. 2011) or carrying the APOE4 allele (Persson et al. 2008; Fleisher et al. 2009; Pihlajamäki and Sperling 2009; Sheline, Morris, et al. 2010; Machulda et al. 2011).

While most resting state fMRI studies showed decreased functional connectivity, some studies showed evidence for increased functional connectivity (Celone et al. 2006; Wang et al. 2007, 2006; He et al. 2007; Zhang et al. 2009, 2010; Filippini et al. 2009; Fleisher et al. 2009; Biswal et al. 2010; Dennis et al. 2010; Sheline, Morris, et al. 2010; Machulda et al. 2011; Mormino et al. 2011). In young APOE4 carriers there is evidence for increased functional connectivity (Filippini et al. 2009; Dennis et al. 2010).

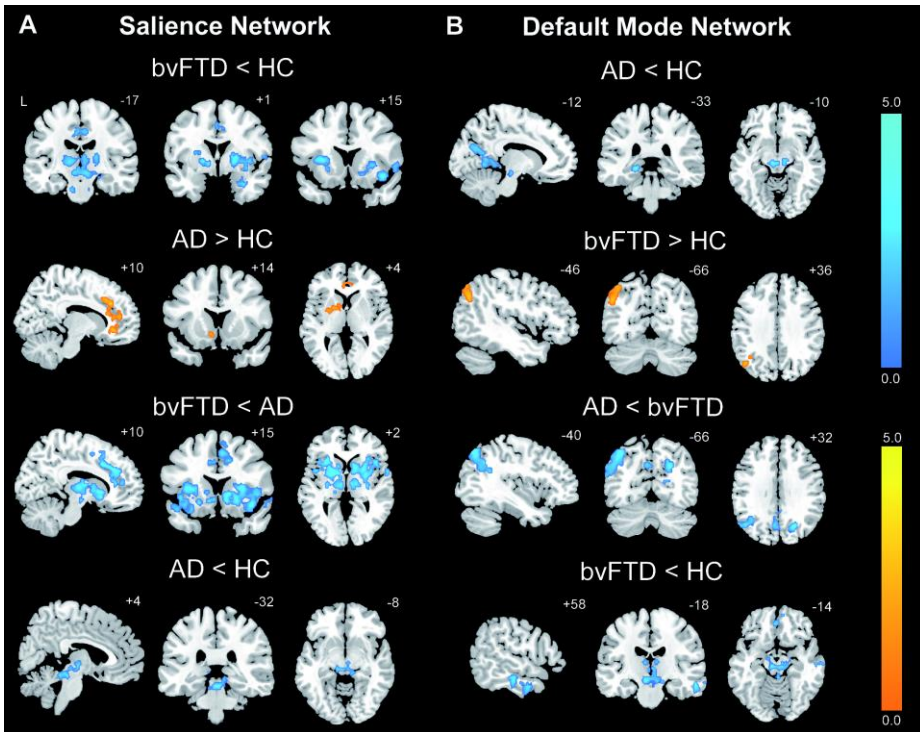


FIGURE 2.8 FT and AD feature divergent salience network and DMN dynamics

Group difference maps illustrate clusters of significantly reduced or increased connectivity for each intrinsic connectivity network. A) In the Salience Network, patients with FT and showed distributed connectivity reductions compared to healthy controls (HC) and patients with Alzheimer’s disease (AD), whereas patients with AD showed increased connectivity in AC and ventral striatum compared to healthy controls. B) In the DMN, patients with AD showed several connectivity impairments compared to healthy controls and patients with FT, whereas patients with FT showed increased left angular gyrus connectivity. Patients with FT and AD further showed focal brainstem connectivity disruptions within their ‘released’ network (DMN for FT, Salience Network for AD). Results are displayed at a joint height and extent probability threshold of $p < 0.05$, corrected at the whole-brain level. Color bars represent t-scores, and statistical maps are superimposed on the Montreal Neurological Institute template brain. Figure and legend reprinted from J. Zhou, M.D. Greicius, E.D. Gennatas, M.E. Growdon, J.Y. Jang, G.D. Rabinovici, J.H. Kramer, M. Weiner, B.L. Miller, W.W. Seeley, Divergent network connectivity changes in behavioral variant frontotemporal dementia and Alzheimer’s disease, *Brain* 133 (2010) page 1358. Copyright 2010 Oxford university press with permission from Oxford university press.

Few data suggest an increase in task-induced deactivation in early MCI patients compared to advanced MCI (Celone et al. 2006). The authors explained the increased DMN connectivity and deactivation by the compensatory-recruitment hypothesis in which additional neural resources are used to compensate for losses of cognitive function and to maintain task performance (Celone et al. 2006; Wang et al. 2006,

2007; He et al. 2007; Filippini et al. 2009; Fleisher et al. 2009; Zhang et al. 2009, 2010; Dennis et al. 2010; Mormino et al. 2011). Nevertheless, this compensatory hypothesis needs to be further investigated.

In general, fMRI is a useful tool for detecting changes in DMN functional connectivity and deactivation patterns in patients with AD. The measurement of intrinsic activity in AD patients might provide a clinical diagnostic tool as well as implications for intervention and understanding of the disease (Zhang and Raichle 2010). However, more work needs to be conducted to conclude whether these measures will become useful as a clinical diagnostic tool in AD.

A challenge for future studies lies in the understanding of the relation between changes in structure and function. While some studies corrected for regional gray matter volume (He et al. 2007; Bai et al. 2008; Damoiseaux et al. 2008; Liu et al. 2008; Persson et al. 2008; Hedden et al. 2009; Drzezga et al. 2011; Han et al. 2011; Petrella et al. 2011), most studies analyzed either structural or functional MRI data. Since it is still unclear how disruptions in functional connectivity are related to structural damage, a combined approach of different imaging techniques is necessary to get insight into the pathological processes related to dementia (Filippi and Agosta 2011).

Chapter 3

Increased functional connectivity and brain atrophy in elderly with subjective memory complaints

Anne Hafkemeijer, Irmhild Altmann-Schneider, Ania Oleksik, Lotte van der Wiel, Huub Middelkoop, Mark van Buchem, Jeroen van der Grond, and Serge Rombouts



3.1. ABSTRACT

Subjective memory complaints (SMC) are common among elderly. Although subtle changes in memory functioning can hardly be determined using neuropsychological evaluation, neuroimaging studies indicate regionally smaller brain structures in elderly with SMC. Imaging of resting state functional connectivity is sensitive to detect changes in neurodegenerative diseases, but is currently underexplored in SMC.

Here, we investigate resting state functional connectivity and brain structure in SMC. We analyzed magnetic resonance imaging data of 25 elderly with SMC and 29 age-matched controls (mean age of 71 years). Voxel-based morphometry and volume measurements of subcortical structures were employed on the structural scans using FSL. The dual regression method was used to analyze voxel-wise functional connectivity in relation to eight well-characterized resting state networks. Group differences were studied with two-sample t-tests ($p < 0.05$, Family-Wise Error corrected).

In addition to gray matter volume reductions (hippocampus, anterior cingulate cortex (ACC), medial prefrontal cortex, cuneus, precuneus, and precentral gyrus), elderly with SMC showed increased functional connectivity in the default mode network (hippocampus, thalamus, posterior cingulate cortex (PCC), cuneus, precuneus, and superior temporal gyrus), and the medial visual network (ACC, PCC, cuneus, and precuneus).

This study is the first which demonstrates that, in addition to smaller regional brain volumes, increases in functional connectivity are present in elderly with SMC. This suggests that self-reported SMC is a reflection of objective alterations in brain function. Furthermore, our results indicate that functional imaging, in addition to structural imaging, can be a useful tool to objectively determine a difference in brain integrity in SMC.

3.2. INTRODUCTION

Subjective memory complaints (SMC) refer to a subjectively noticeable decline from previous levels of memory functioning (Vestberg et al. 2010). These subjective complaints are common among elderly (Mitchell 2008a), but can hardly be confirmed by a neuropsychological evaluation (Hejl et al. 2002). The importance of SMC has been emphasized both in clinical and research-based investigations. Longitudinal population-based studies reported an association with depression (Montejo et al. 2011), future cognitive decline (Dik et al. 2001), and dementia (Jessen et al. 2010). Nevertheless, it is a subject of debate whether SMC is a clinically relevant predictor for future cognitive decline and dementia (Glodzik-Sobanska et al. 2007; Mitchell 2008b).

Neuroimaging studies in elderly with SMC showed smaller brain structures (Van der Flier et al. 2004; Jessen et al. 2006; Saykin et al. 2006; Striepens et al. 2010; Stewart et al. 2011) and increased brain activation during cognitive tasks (Rodda et al. 2009, 2011). Despite the importance of studying functional connectivity to understand brain function (Mesulam 1998), and its relevance in the context of neurodegenerative diseases (Pievani et al. 2011), functional connectivity in elderly with SMC is currently underexplored.

Here, we investigate whole-brain gray matter volumes and resting state functional connectivity in elderly with SMC. This is a cross-sectional study in a heterogeneous group of elderly with subjective complaints about their memory. Clinically, these complaints are not confirmed by a neuropsychological evaluation. Elderly with SMC are compared with an age-matched control group of healthy elderly from the general population.

It is hypothesized that imaging of functional brain connectivity is sensitive to detect early brain changes. Evidence for this is provided by studies showing differences in functional connectivity in aging, mild cognitive impairment, and dementia (Hafkemeijer, van der Grond, and Rombouts 2012), and moreover in subjects at risk for developing neurodegenerative diseases, either in terms of having amyloid plaques (Hedden et al. 2009; Sheline, Raichle, et al. 2010) or carrying a genetic mutation (Filippini et al. 2009), even when evidence for brain atrophy or cognitive decline is absent. While mostly decreased functional connectivity in the default mode network has been found in Alzheimer's disease (Greicius et al. 2004; Wang et al. 2006, 2007;

Zhang et al. 2009, 2010; Zhou et al. 2010; Wu et al. 2011), mild cognitive impairment (Sorg et al. 2007; Han et al. 2011; Petrella et al. 2011), and subjects at risk for developing neurodegenerative diseases (Fleisher et al. 2009; Hedden et al. 2009; Sheline, Morris, et al. 2010; Sheline, Raichle, et al. 2010), some studies showed evidence for increased functional connectivity in Alzheimer's disease (Wang et al. 2006, 2007; Zhang et al. 2009, 2010) and in cognitively healthy subjects at genetic risk for developing dementia (Filippini et al. 2009; Fleisher et al. 2009; Dennis et al. 2010; Westlye et al. 2011).

Based on neuroimaging studies in elderly with SMC (Van der Flier et al. 2004; Jessen et al. 2006; Saykin et al. 2006; Rodda et al. 2009, 2011; Striepens et al. 2010; Stewart et al. 2011) and studies in neurodegenerative diseases (Fox and Schott 2004; Hafkemeijer, van der Grond, and Rombouts 2012), we expect to find differences in both brain structure and functional connectivity in the default mode network, which consists of the medial prefrontal cortex (mPFC), posterior and anterior cingulate cortex (PCC and ACC), precuneus, parietal cortex, and the hippocampus (Buckner et al. 2008).

3.3. MATERIALS AND METHODS

Participants

In this cross-sectional study, we included 25 subjects with SMC (mean age = 71.4 years) and 29 control subjects (mean age = 71.3 years) (Table 3.1). Elderly with self-reported SMC who visited the outpatient clinic for memory deficits of the geriatric department of the Leiden University Medical Center were recruited for this study. The elderly came to the memory clinic with memory complaints experienced by themselves and/or notified by people in their environment. All subjects were evaluated for cognitive complaints using a standardized dementia screening that included a detailed medical history, a general internal and neurological examination, laboratory tests, a neuropsychological evaluation, and a magnetic resonance imaging (MRI) of the brain.

TABLE 3.1 Characteristics of participants

Demographic variables	Elderly with SMC (n = 25)	Control elderly (n = 29)	p value
Age (mean (SD), years)	71.4 (9.2)	71.3 (3.4)	0.993
Gender (male ; female)	14 ; 11	17 ; 12	0.850
Education (mean (SD), years)	15.3 (2.5)	14.5 (2.7)	0.268

Abbreviations: SMC = subjective memory complaints; SD = standard deviation

Cognitive functioning was assessed using neuropsychological tests, standardized for the outpatient clinic of memory deficits of the geriatric department of the Leiden University Medical Center. The standardized neuropsychological test battery included a detailed interview, the Mini Mental State Examination, the Stroop Color-Naming test, the Cambridge Cognitive Examination - Revised, the Wechsler Memory Scale, and the Trail Making Test part A and B. Age-based norms and cutoff values that define the lower range of normal test scores were available for the neuropsychological tests (Wechsler 1945; Folstein et al. 1975; Roth et al. 1986; Steinberg et al. 2005). Test results were interpreted taking into account both educational and occupational levels. When the neuropsychologist needed additional information, the standardized neuropsychological test battery was extended with the Alzheimer's Disease Assessment Scale, the California Verbal Learning Test, and the Wechsler Adult Intelligence Scale - Revised.

Diagnoses were made in a multidisciplinary consensus meeting according to the National Institute of Neurological and Communicative Disorders and Stroke-Alzheimer's Disease and Related Disorders Association (McKhann et al. 1984), the Diagnostic and Statistical Manual of Mental Disorders, fourth edition (American Psychiatric Association 1994), and the criteria of Petersen (Petersen et al. 1997). The diagnosis SMC was made by interpreting the complete screening profile with the education and past performance of the elderly taken into account. Elderly with SMC did not meet the criteria for mild cognitive impairment or dementia. Elderly with scores of above six on the Geriatric Depression Scale-15 (Sheikh and Yesavage 1986) and/or cardiovascular diseases were excluded for this study.

Control subjects were recruited from the general population and were matched in terms of age, gender, and years of education (*Table 3.1*). Normal cognitive functioning was confirmed by a neuropsychological protocol that included the Mini Mental State Examination, the Stroop Color-Naming test, and the 15-Picture Learning Test. Control subjects did not demonstrate any memory complaints and did not show any abnormalities on neuropsychological evaluation (*Table 3.2*).

TABLE 3.2 Neuropsychological test scores

Neuropsychological test	Cutoff value ^a	Elderly with SMC	Control elderly	p value
MMSE	25	27.2 (0.4)	27.9 (0.2)	0.133
Stroop Interference (t-score)	40	44.4 (3.6) ^b	49.2 (4.3)	0.449
15-PLT Immediate	8	-	10.1 (0.3)	n/a
15-PLT Delayed	8		11.3 (0.4)	n/a
WMS (memory quotient)	85 ^c	121.0 (2.8)	-	n/a
CAMCOG-R	80	91.5 (1.1)	-	n/a
TMT part A (t-score)	40	43.0 (2.1)	-	n/a
TMT part B (t-score)	40	43.4 (2.7)	-	n/a
TMT B/A (t-score)	40	46.8 (2.6)	-	n/a

Abbreviations: SMC = subjective memory complaints; MMSE = Mini Mental State Examination; 15-PLT = 15 Picture Learning Test; WMS = Wechsler Memory Scale; CAMCOG-R = Cambridge Cognitive Examination - Revised; TMT = Trail Making Test.

^a Cutoff value defines the lower range of normal test scores, ^b Stroop Color-Naming Test was performed in 13 elderly with SMC, ^c Cutoff value of 85, mean of 100 ± 15

This study was performed in compliance with the Code of Ethics of the World Medical Association (Declaration of Helsinki). Furthermore, study approval was obtained by the Medical Ethical Committee of the Leiden University Medical Center.

Data acquisition

Imaging was performed on a Philips 3 Tesla Achieva MRI scanner using a standard whole-head coil for radiofrequency transmission and reception (Philips Medical Systems, Best, the Netherlands). For each subject, a three-dimensional (3D)-T1-weighted anatomical scan was acquired with the following scan parameters: TR = 9.7 msec; TE = 4.6 msec; flip angle = 8°; voxel size 0.88 x 0.88 x 1.40 mm. In accordance with Leiden University Medical Center policy, all anatomical MRI scans were screened by a neuroradiologist from the radiology department (MvB) to rule out incidental pathology.

The scan parameters of the resting state functional magnetic resonance imaging (fMRI) scan were as follows: TR = 2.2 sec; TE = 30 msec; flip angle = 80°; voxel size 2.75 x 2.75 x 2.99 mm including 10% interslice gap, scan duration 7 minutes and 33 seconds. During the resting state scan, participants were instructed to lie still with their eyes closed and not to fall asleep. For registration purposes, a high-resolution echo planar image scan was obtained with the following scan parameters: TR = 2.2 sec; TE = 30 msec; flip angle = 80°; voxel size 1.96 x 1.96 x 2.00 mm including 10% interslice gap.

Data analysis

Before analysis, all MRI scans were submitted to a visual quality control check to ensure that no gross artifacts were present in the data. Data analysis was performed with Functional Magnetic Resonance Imaging of the Brain Software Library (FSL 4.1.8, Oxford, United Kingdom, www.fmrib.ox.ac.uk/fsl) (Smith et al. 2004). Anatomical locations were determined using the Harvard-Oxford cortical and subcortical structures atlas integrated in FSL.

Voxel-based morphometry analysis

To highlight regions with differences in gray matter volume between elderly with SMC and control elderly, structural scans were analyzed with a voxel-based morphometric (VBM) analysis (Ashburner and Friston 2000). First, the structural images were brain

extracted (Smith 2002) and tissue-type segmented (Zhang et al. 2001b). To correct for the partial volume effect (i.e., voxels 'containing' more than one tissue-type), the tissue-type segmentation was carried out with partial volume estimation. For each partial volume voxel, the proportion of each tissue-type is estimated, that is, a partial volume vector is formed, with each element being a 'fraction' of a specific tissue type and having a sum of one (Zhang et al. 2001a). The segmented images have values that indicate the probability of a given tissue-type (i.e., they are not binary).

The resulting gray matter partial volume images were aligned to the gray matter MNI standard space image (Montreal Neurological Institute, Montreal, QC, Canada) (Jenkinson et al. 2002), followed by nonlinear registration (Andersson et al. 2007a). The resulting images were averaged to create a study-specific template. More precisely, to create the study-specific gray matter template the same number of participants from each group (25 elderly with SMC and 25 (randomly selected) control elderly) was used in order to avoid any bias during the registration step that would have favored one of the groups. Next, all native gray matter images were nonlinearly registered to this study-specific gray matter template (Ashburner and Friston 2000; Good et al. 2001). Due to the nonlinear spatial registration, the volume of some brain structures may grow, while others may shrink. To be able to test for regional differences in the absolute gray matter volumes, a further processing step is needed to compensate for these enlargements and contractions (modulation). In this additional step, each voxel of each registered gray matter image was multiplied by the Jacobian of the warp field, which defines the direction (larger or smaller) and the amount of modulation. The modulated segmented images were spatially smoothed with an isotropic Gaussian kernel with a full width at half maximum of 7 mm.

A general linear model (GLM) approach as implemented in FSL was used to compare maps of elderly with SMC and control elderly. Two-sample t-tests were used for this analysis, including age and gender as covariate in the statistical model. Voxel-wise non-parametric permutation testing (Nichols and Holmes 2001) with 5000 permutations was performed, correcting for multiple comparisons across space (statistical threshold set at $p < 0.05$, Family-Wise Error (FWE) corrected), using the Threshold-Free Cluster Enhancement (TFCE) technique (Smith and Nichols 2009), applying a minimum cluster size of 40 mm^3 .

Volume measurement of subcortical structures

An automatic segmentation method (FIRST as implemented in FSL), was applied to measure volumes of seven subcortical structures: the hippocampus, amygdala, thalamus, putamen, globus pallidus, nucleus accumbens, and the caudate nucleus (Patenaude et al. 2011). First, the structural scans were registered to the MNI standard space image. After subcortical registration, a subcortical mask was applied to locate the different subcortical structures. This was followed by segmentation based on shape models and voxel intensities. After registration and segmentation of all structural scans, all segmented subcortical regions were visually checked for errors in registration and segmentation. After volumetric analysis, the volume in mm^3 of each subcortical structure was obtained. To determine whether the subcortical structures volumes in elderly with SMC differ from those of the control elderly, univariate general linear modeling was used (IBM SPSS Statistics Version 18, IBM Corp., Somers, NY, USA). Age and gender were included as covariate in the statistical model.

Functional connectivity analysis

The preprocessing of the resting state data consisted of motion correction (Jenkinson et al. 2002), brain extraction (Smith 2002), spatial smoothing using a Gaussian kernel with a full width at half maximum of 6 mm, and high-pass temporal filtering (cutoff frequency of 0.01 Hz). After preprocessing, the functional images were registered to the corresponding high-resolution echo planar images, which were registered to the T1-weighted images, which were registered to the 2 mm isotropic MNI standard space image (Jenkinson et al. 2002). These registration parameters were combined to obtain the registration matrix from native (fMRI) space to MNI space and its inverse (from MNI space to native space).

The functional connectivity analysis was performed using the dual regression method of FSL, a technique that allows a voxel-wise comparison of resting state functional connectivity (previously described in (Filippini et al. 2009)). Functional connectivity can be studied using the dual regression technique based on a data-driven independent component analysis. Another approach to study functional connectivity in a more standardized way is the use of standard resting state networks as reference. Here, resting state functional connectivity is determined in terms of similarity of the blood oxygenation level dependent (BOLD) fluctuations in the brain in relation to characteristic fluctuations in eight predefined resting state networks. Our choice of

resting state networks was based on high reproducibility of these networks from independent component analysis of different data sets (Beckmann et al. 2005; Damoiseaux et al. 2006). These standardized resting state networks parcellate the brain into eight templates that represent over 80% of the total brain volume (Khalili-Mahani et al. 2012): 1) medial visual network, 2) lateral visual network, 3) auditory network, 4) sensorimotor system, 5) default mode network, 6) executive control network, 7 and 8) dorsal visual stream networks (Beckmann et al. 2005). To account for noise, a white matter and a cerebrospinal fluid template were included in the analysis (Fox et al. 2005; Cole et al. 2010; Birn 2012).

In the dual regression, individual time series were first extracted for each template, using the eight resting state networks (Beckmann et al. 2005) and the two additional white matter and cerebrospinal fluid maps (Fox et al. 2005; Cole et al. 2010; Birn 2012), in a spatial regression against the individual fMRI data set (regression 1). The resulting matrices described temporal dynamics for each template and individual. Next, the ten temporal regressors (eight from the resting state networks and two additional noise regressors) were used in a linear model fit against the individual fMRI data set (regression 2), to estimate the spatial maps for each individual. This gives ten 3D images per individual, with voxel-wise the z scores of functional connectivity to each of the templates. The higher the absolute value of the z score, the stronger the connectivity to a network.

In the final stage of the functional connectivity analysis, the same statistical model as used in the VBM analysis was applied. To obtain group averages, a one-sample non-parametric t-test was used, and a two-sample t-test was applied to obtain group differences for each of the resting state networks, using a GLM approach as implemented in FSL. Age and gender were included as covariate in the model. To statistically account for potential effects of local structural differences within and between the two groups, gray matter volume of each voxel was included as subject wise and voxel-wise covariates in the GLM design (Oakes et al. 2007). The `feat_gm_prepare` script of FSL was used to compute individual gray matter density maps. Per network, the group comparison was masked by the union of the one-sample maps from each group for that network (i.e., voxels that fell within the group map of the elderly with SMC and/or the group map of the control elderly). Voxel-wise non-parametric permutation testing was performed using `FSL-randomise` (5000

permutations) (Nichols and Holmes 2001). All statistical maps were FWE corrected using $p < 0.05$, based on the TFCE statistic image (Smith and Nichols 2009), applying a minimum cluster size of 40 mm^3 .

3.4. RESULTS

Demographic characteristics

Table 3.1 shows the characteristics of the participants. There were no differences between elderly with SMC and control elderly with regard to age, gender, and years of education. Both groups did not show abnormalities in neuropsychological evaluation (Table 3.2).

Voxel-based morphometry

The whole-brain voxel-wise structural analysis yielded group differences in gray matter volume in several regions across the brain (Fig. 3.1). Elderly with SMC show a volume reduction of the right hippocampus, right amygdala, bilateral ACC, mPFC, cuneus, precuneus, and precentral gyrus compared with the control elderly. Left hippocampal volume reduction was visible in the images that were not corrected for FWE ($p < 0.01$, uncorrected images not shown).

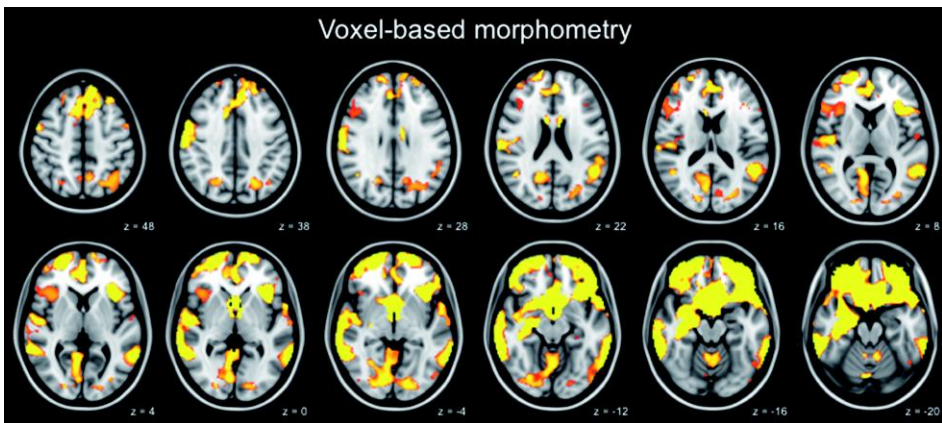


FIGURE 3.1 Elderly with SMC show loss of brain structure

Brain areas showing reduced gray matter volume in elderly with SMC compared with control elderly. The left side of the brain corresponds to the right hemisphere and vice versa. Images are overlaid on the transverse slices of the MNI standard anatomical image. Z-coordinates of each slice in the MNI standard space are given. Voxel-based morphometry results are thresholded using $p < 0.05$, FWE corrected, based on the TFCE statistic image. Age and gender were included as covariate in the statistical model. P values are color-coded from 0.05 FWE corrected (red) to < 0.0001 FWE corrected (yellow).

Within the SMC group, correlations between individual neuropsychological test scores and regional gray matter volume were found at the liberal uncorrected threshold. A positive correlation with the scores of the Wechsler Memory Scale (uncorrected $p = 0.0002$) was found in the cerebellum (365 voxels). In the inferior and middle temporal gyrus (218 voxels), we found a positive correlation with the scores of the Trail Making Test (uncorrected $p = 0.0002$). A positive correlation was found with the scores of the Stroop Color-Naming test (uncorrected $p = 0.0002$) in the frontal pole (57 voxels). These correlations did not survive correction for multiple comparisons.

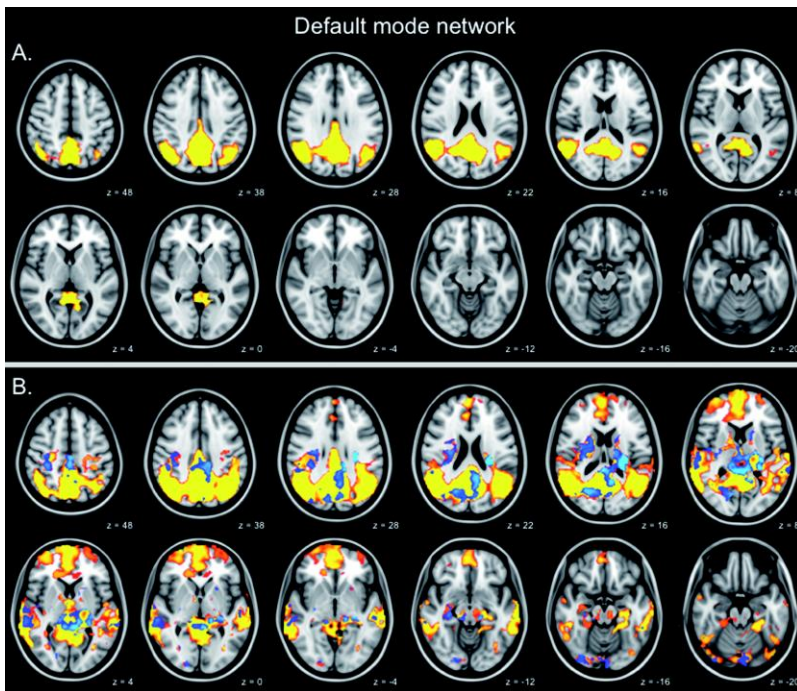


FIGURE 3.2 Increased functional connectivity in the default mode network

Functional connectivity in the default mode network in healthy control elderly (yellow areas in A) and elderly with SMC (yellow areas in B). P values of the functional connectivity are color-coded from 0.05 FWE corrected (red) to < 0.0001 FWE corrected (yellow). Note that the anterior part of the default mode network in elderly with SMC is significantly connected, while this region appears not connected in the control elderly. However, the anterior region appears connected in control elderly at the [$p = 0.08$, FWE corrected] level (not shown). Elderly with SMC show increased functional connectivity compared with control elderly (blue areas in B, p values are color-coded from 0.05 FWE corrected (dark blue) to < 0.0001 FWE corrected (light blue), full list of structures in Table 3.4). Images are overlaid on the transverse slices of the MNI standard anatomical image. The left side of the brain corresponds to the right hemisphere and vice versa. Z-coordinates of each slice in the MNI standard space are given.

Volumes of subcortical structures

Right hippocampal volume reduction in the elderly with SMC was confirmed in the analysis of subcortical structure volumes ($p = 0.002$) (Table 3.3). In addition, the volume of the left hippocampus was smaller in elderly with SMC ($p = 0.017$). While the whole-brain structural analysis suggested amygdala volume reduction, this could not be confirmed with the automatic segmentation method. In agreement with the whole-brain voxel-wise analysis, no volume differences were found in the other subcortical structures.

TABLE 3.3 Mean volumes of subcortical structures

Brain structure	Mean (SD) volume (cm ³)		p value
	Elderly with SMC (n = 25)	Control elderly (n = 29)	
Right hippocampus	3.67 (0.48)	3.96 (0.31)	0.002
Left hippocampus	3.57 (0.62)	3.85 (0.37)	0.017
Right amygdala	1.28 (0.21)	1.23 (0.22)	0.350
Left amygdala	1.32 (0.22)	1.27 (0.19)	0.280
Right thalamus	7.28 (0.95)	7.11 (0.57)	0.237
Left thalamus	7.50 (1.07)	7.37 (0.59)	0.413
Right putamen	4.59 (0.71)	4.74 (0.54)	0.309
Left putamen	4.52 (0.76)	4.69 (0.69)	0.300
Right globus pallidus	1.98 (0.49)	1.88 (0.17)	0.293
Left globus pallidus	1.96 (0.50)	1.86 (0.23)	0.310
Right nucleus accumbens	0.32 (0.16)	0.29 (0.07)	0.399
Left nucleus accumbens	0.38 (0.13)	0.41 (0.11)	0.335
Right caudate nucleus	3.65 (0.50)	3.63 (0.42)	0.713
Left caudate nucleus	3.34 (0.36)	3.35 (0.41)	0.944

Abbreviations: SD = standard deviation; SMC = subjective memory complaints

Functional connectivity

Given the extensive gray matter differences, we included gray matter volume as a voxel-wise covariate in the fMRI analysis to correct for its potential effect on functional connectivity. Voxel-wise group comparisons revealed increased functional connectivity in two resting state networks in elderly with SMC compared with the control elderly (the default mode network (Fig. 3.2) and the medial visual network (Fig. 3.3)). No decreases in functional connectivity were found in elderly with SMC. In the other six resting state networks no changes in functional connectivity were observed.

TABLE 3.4 Increased functional connectivity in elderly with SMC compared with control elderly

Network	Brain structure ^a	Side	Peak voxel coordinates (MNI)			Peak T score
			x	y	z	
Default mode network	Hippocampus	R	30	-22	-10	4.01
	Thalamus	R	1	-20	6	3.03
	Thalamus	L	0	-20	6	3.13
	Posterior cingulate cortex	R	1	-22	44	3.19
	Posterior cingulate cortex	L	-1	-26	44	3.23
	Cuneus	R	26	-68	16	3.73
	Cuneus	L	-8	-74	22	3.07
	Precuneus	L	-6	-64	24	2.72
	Superior temporal gyrus	R	60	-30	2	4.05
	Medial visual network	Anterior cingulate cortex	R	1	8	30
Anterior cingulate cortex		L	-1	8	30	4.06
Posterior cingulate cortex		R	2	-20	36	4.13
Posterior cingulate cortex		L	-1	-20	36	3.98
Cuneus		R	0	-88	6	3.54
Cuneus		L	-4	-96	18	4.33
Precuneus		R	2	-60	6	3.12
Precuneus		L	-2	-56	6	3.39

Abbreviations: MNI = Montreal Neurological Institute standard space image; R = right; L = left

^a Full list of structures with increased functional connectivity in elderly with SMC (Fig. 3.2 and 3.3). Between group effects are corrected for gray matter volume, thresholded using $p < 0.05$, FWE corrected, based on the TFCE statistic image. For each peak voxel x-, y-, and z-coordinates in the MNI standard space image are given.

Regions showing increased functional connectivity in the default mode network included the right hippocampus, bilateral thalamus, PCC, cuneus, left precuneus, and right superior temporal gyrus (Fig. 3.2B, full list of structures in Table 3.4). The medial visual network structures with increased functional connectivity included the bilateral ACC, PCC, cuneus, and precuneus (Fig. 3.3B, full list of structures in Table 3.4). To further illustrate group differences per network, subjects' mean z scores of regions with increased functional connectivity are plotted separately for the default mode network and the medial visual network (Fig. 3.4). Within the SMC group, no correlations between individual neuropsychological test scores and functional connectivity were found.

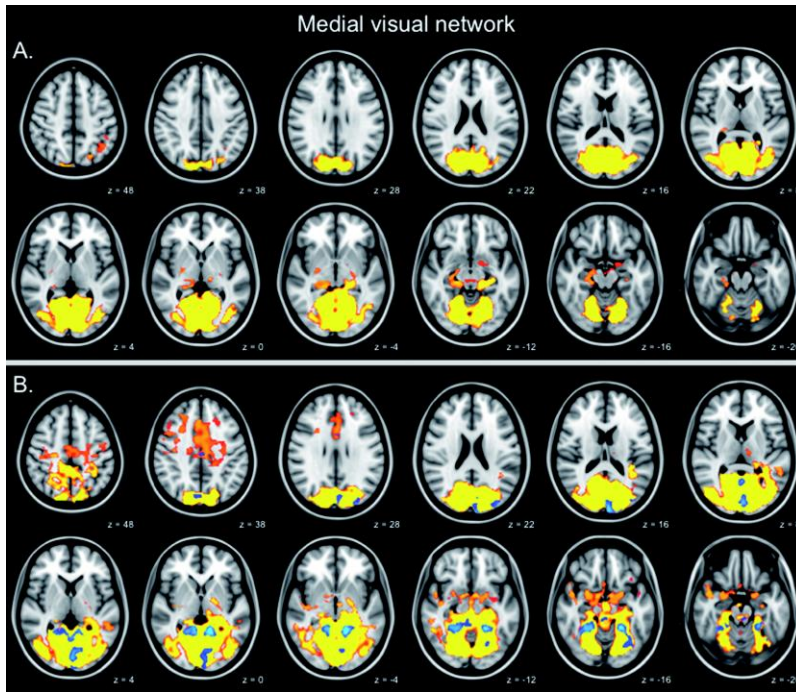


FIGURE 3.3 Increased functional connectivity in the medial visual network

Functional connectivity in the medial visual network in healthy control elderly (yellow areas in A) and elderly with SMC (yellow areas in B). P values of the functional connectivity are color-coded from 0.05 FWE corrected (red) to < 0.0001 FWE corrected (yellow). Elderly with SMC show increased functional connectivity compared with control elderly (blue areas in B, p values are color-coded from 0.05 FWE corrected (dark blue) to < 0.0001 FWE corrected (light blue), full list of structures in Table 3.4). Images are overlaid on the transverse slices of the MNI standard anatomical image. The left side of the brain corresponds to the right hemisphere and vice versa. Z coordinates of each slice in the MNI standard space are given.

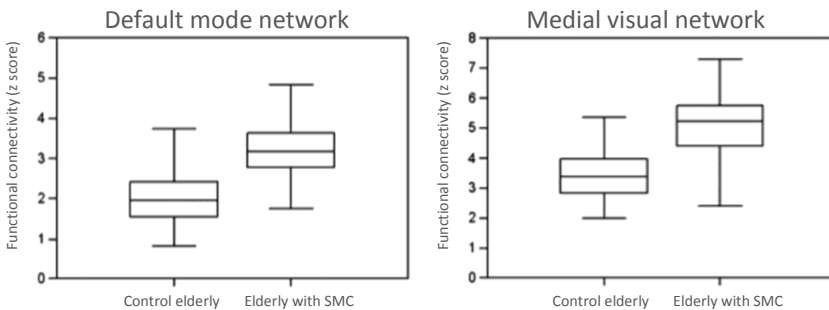


FIGURE 3.4 Boxplots of increased functional connectivity in elderly with SMC

For each subject mean z scores were extracted from the brain areas with increased functional connectivity in elderly with SMC (blue areas in Fig. 3.2 and 3.3). Boxplots for the default mode network and the medial visual network, show median, lower and upper quartile, and sample minimum and maximum.

3.5. DISCUSSION

The present study is the first which demonstrates that, in addition to structural brain deficits, increases in functional connectivity are present in elderly with SMC. These findings were observed even in a heterogeneous group of elderly with subjective complaints about their memory. This suggests that self-reported SMC is a reflection of objective alterations in brain function.

Our findings of atrophy of the hippocampus, ACC, mPFC, cuneus, precuneus, and precentral gyrus in elderly with SMC are in line with previous studies showing atrophy of the hippocampus (Van der Flier et al. 2004; Saykin et al. 2006; Striepens et al. 2010; Stewart et al. 2011), and less frequently also in the left medial frontal gyrus (Saykin et al. 2006), right cuneus (Saykin et al. 2006), right precentral gyrus (Saykin et al. 2006), and entorhinal cortex (Jessen et al. 2006; Striepens et al. 2010) in elderly with SMC. The voxel-based morphometry analysis showed smaller amygdala volumes, which could not be confirmed with the volume measurements of subcortical structures. This makes it unlikely that amygdala atrophy is present in elderly with SMC.

The volume reductions observed in the present study suggest that self-reported SMC is a reflection of objective alterations in brain structure. These findings of atrophy could be of clinical importance, as atrophy of these regions is associated with dementia (Fox and Schott 2004). Moreover, cognitively healthy elderly who during a ten-year follow-up developed mild cognitive impairment or Alzheimer's disease, were at baseline characterized by gray matter atrophy of these regions (Tondelli et al. 2012). The correlation between gray matter volume and individual cognitive performance in the elderly with SMC could have strengthened the clinical relevance of our findings. However these correlations were found in small areas throughout the brain and did not survive correction for multiple comparisons. Further investigation is highly recommended to confirm the weak correlations found in this study.

Studying resting state functional connectivity is important to understand brain function, (Mesulam 1998) and is relevant in the context of neurodegenerative diseases (Pievani et al. 2011). While brain activation is studied in elderly with SMC with task-related fMRI (Rodda et al. 2009, 2011), resting state functional connectivity is underexplored in these elderly. The present study is the first to demonstrate that, even in a heterogeneous group of elderly with SMC, functional connectivity is

increased. Mostly decreased functional connectivity has been found in mild cognitive impairment and dementia (Hafkemeijer, van der Grond, and Rombouts 2012) and in one study in elderly with SMC applying the magnetoencephalography technology (Bajo et al. 2011); however there is evidence for increased functional connectivity in Alzheimer's disease (Wang et al. 2006, 2007; Zhang et al. 2009, 2010) and in cognitively healthy subjects at risk for developing dementia as well (Filippini et al. 2009; Fleisher et al. 2009; Dennis et al. 2010; Westlye et al. 2011).

It has been suggested that increased task-related activation reflects a greater cognitive effort to compensate for subclinical losses of cognitive function and to maintain task performance (Bondi et al. 2005). This idea is supported by findings of increased functional connectivity in the hippocampus, amygdala, mPFC, and retrosplenial cortex in young cognitively healthy subjects at genetic risk for developing neurodegenerative diseases (Filippini et al. 2009). This compensatory mechanism has been suggested as explanation for reduced interhemispheric inhibition (Talelli et al. 2008) and may also explain the increased functional connectivity found in elderly with SMC in the current study. An alternative explanation is that the increased functional connectivity is a pathological state that may cause further brain damage (Gallagher et al. 2010; Yassa et al. 2010). Nevertheless, this compensatory hypothesis and the clinical meaning of increased functional connectivity in SMC need to be further investigated.

Since it is not exactly known how brain structure and function are related, the functional connectivity data were analyzed with regional gray matter volume as covariate in the model, to statistically account for the potential effect of local structural differences. Our observations showed that the functional connectivity differences are not simply explained by differences in gray matter volume. The changes in functional connectivity are found in brain areas that are part of the default mode network. The differences in functional connectivity between hippocampus and PCC is in accordance with the affected hippocampal white matter integrity found with diffusion tensor imaging in mild cognitive impairment and Alzheimer's disease (Mielke et al. 2009). These findings could be of clinical relevance, as changes in functional connectivity in the default mode network have repeatedly been demonstrated in patients with Alzheimer's disease, and moreover in cognitively healthy subjects at risk for developing neurodegenerative diseases (Hafkemeijer, van der Grond, and Rombouts 2012). However, it should be noticed that these changes are not specific for

elderly with SMC, as changes in functional connectivity are found in a wide range of diseases from neurodegenerative disorders to psychiatric diseases (Broyd et al. 2009).

The medial visual network showed differences in functional connectivity. This may appear as a remarkable finding, as histological studies showed that the occipital cortex is one of the latest brain regions affected in Alzheimer's disease (Braak and Braak 1991). However, previous studies repeatedly showed that functional connectivity and reactivity is altered in the occipital lobe in mild cognitive impairment, and mild, moderate, and severe Alzheimer's disease (Horwitz et al. 1995; Prvulovic et al. 2002; Rombouts, Goekoop, et al. 2005; Bokde et al. 2008, 2010; Zhang et al. 2010), showing that fMRI changes may occur in the earlier phases of dementia in the occipital lobe, and may not necessarily follow the same sequential pattern as found in histological studies.

3.5.1. CONCLUSION

Here, we demonstrated that, in addition to structural brain deficits, increases in functional connectivity are present in elderly with SMC. The present study is the first which demonstrates that functional connectivity is increased in the default mode and medial visual network in these elderly. Our findings in elderly with SMC suggest that self-reported SMC is a reflection of objective alterations in brain function. Furthermore, our results indicate that functional imaging, in addition to structural imaging, can be a useful tool to objectively determine a difference in brain integrity in elderly with SMC. Further investigation is necessary to confirm the present findings, to establish the pathophysiology and clinical meaning of SMC, and to establish the potential role of fMRI in the predictive models of dementia.

Chapter 4

Resting state functional connectivity differences between behavioral variant frontotemporal dementia and Alzheimer's disease

Anne Hafkemeijer, Christiane Möller, Elise Dopper, Lize Jiskoot, Tijn Schouten,
John van Swieten, Wiesje van der Flier, Hugo Vrenken, Yolande Pijnenburg,
Frederik Barkhof, Philip Scheltens, Jeroen van der Grond, and Serge Rombouts



4.1. ABSTRACT

Alzheimer's disease (AD) and behavioral variant frontotemporal dementia (bvFTD) are the most common types of early-onset dementia. Early differentiation between both types of dementia may be challenging due to heterogeneity and overlap of symptoms. Here, we apply resting state functional magnetic resonance imaging (fMRI) to study functional brain connectivity differences between AD and bvFTD.

We used resting state fMRI data of 31 AD patients, 25 bvFTD patients, and 29 controls from two centers specialized in dementia. We studied functional connectivity throughout the entire brain, applying two different analysis techniques, studying network-to-region and region-to-region connectivity. A general linear model approach was used to study group differences, while controlling for physiological noise, age, gender, study center, and regional gray matter volume.

Given gray matter differences, we observed decreased network-to-region connectivity in bvFTD between a) lateral visual cortical network and lateral occipital and cuneal cortex, and b) auditory system network and angular gyrus. In AD, we found decreased network-to-region connectivity between the dorsal visual stream network and lateral occipital and parietal opercular cortex. Region-to-region connectivity was decreased in bvFTD between superior temporal gyrus and cuneal, supracalcarine, intracalcarine cortex, and lingual gyrus.

We showed that the pathophysiology of functional brain connectivity is different between AD and bvFTD. Our findings support the hypothesis that resting state fMRI shows disease-specific functional connectivity differences and is useful to elucidate the pathophysiology of AD and bvFTD. However, the group differences in functional connectivity are less abundant than has been shown in previous studies.

4.2. INTRODUCTION

The most common types of early-onset dementia are Alzheimer's disease (AD) and behavioral variant frontotemporal dementia (bvFTD) (Ratnavalli et al. 2002). Patients with AD typically present with deficits in episodic and working memory (McKhann 2011), whereas bvFTD is mainly characterized by changes in behavior, personality, and motivation (Rascovsky et al. 2011). However, symptoms may vary considerably, with overlap of symptoms between AD and bvFTD, including memory disturbances (Irish et al. 2014) and behavioral abnormalities (Woodward et al. 2010). Due to this heterogeneity and overlap of symptoms, clinical differentiation between both types of dementia may be challenging, particularly early in the disease. Therefore, to improve diagnostic accuracy and early differential diagnosis, there is a strong need for early markers of brain changes associated with the two types of dementia.

A substantial amount of dementia research used neuroimaging to elucidate the pathophysiology of bvFTD and AD (McMillan et al. 2014; Raamana et al. 2014). Neuroimaging of brain structure shows typical AD pathology in the hippocampus, precuneus, posterior cingulate cortex (PCC), parietal, and occipital brain regions (Buckner et al. 2005; Seeley et al. 2009; Krueger et al. 2010). BvFTD pathology is most often found in the anterior cingulate cortex (ACC), frontoinsula, and frontal brain regions (Seeley et al. 2009; Krueger et al. 2010).

Imaging of functional brain connectivity may be sensitive to detect disease-specific network changes in neurodegenerative diseases (Pievani et al. 2011). Former studies have shown abnormalities in functional connectivity in a posterior hippocampal-cingulo-temporal-parietal network known as the default mode network in AD (Greicius et al. 2004; Allen et al. 2007; Binnewijzend et al. 2012; Hafkemeijer, van der Grond, and Rombouts 2012) and in an anterior frontoinsular-cingulo-orbitofrontal network often called the salience network in bvFTD (Zhou et al. 2010; Agosta et al. 2013; Filippi et al. 2013; Rytty et al. 2013). Moreover, abnormalities in functional brain networks were found in mild cognitive impairment (Binnewijzend et al. 2012; He et al. 2014), subjective memory complaints (Hafkemeijer et al. 2013), and asymptomatic subjects at genetic risk for developing neurodegenerative diseases (Filippini et al. 2009; Sheline, Morris, et al. 2010; Chhatwal et al. 2013; Dopper et al. 2014; Rytty et al. 2014), even in the absence of brain atrophy or cognitive decline.

Previous studies compared functional brain networks between dementia patients and controls, most often focusing on a priori defined regions or networks of interest, showing decreased functional connectivity in the default mode network in AD and in the salience network in bvFTD (Greicius et al. 2004; Allen et al. 2007; Binnewijzend et al. 2012; Agosta et al. 2013; Rytty et al. 2013). The direct comparison of functional connectivity between patients with AD and bvFTD, which is relevant for clinical differentiation, has been studied less often (Zhou et al. 2010; Filippi et al. 2013). In these studies, bvFTD patients have consistently shown decreased salience network connectivity compared with AD, while findings of default mode network connectivity have been inconsistent (Zhou et al. 2010; Filippi et al. 2013).

Therefore, to further explore functional connectivity in both types of dementia, the aim of this study was to compare whole-brain functional connectivity between AD and bvFTD. To study functional connections throughout the entire brain, voxel-based network-to-region (Greicius et al. 2004; Seeley et al. 2009; Zhou et al. 2010; Filippi et al. 2013) and region-to-region analyses (Supekar et al. 2008; Brier et al. 2014; Zhou et al. 2015) were applied. Given the differences in gray matter atrophy in AD and bvFTD (Buckner et al. 2005; Seeley et al. 2009; Krueger et al. 2010), we studied functional connectivity while controlling for gray matter volume. We expected connectivity differences in the posterior temporal-parietal regions of the brain in AD, and in the anterior cingulate and frontoinsula regions in bvFTD.

4.3. MATERIALS AND METHODS

Participants

We used resting state functional magnetic resonance imaging (fMRI) scans of 31 patients with probable AD, 25 patients with probable bvFTD, and 29 control participants (*Table 4.1*). All subjects were recruited from two Dutch centers specialized in dementia; the Alzheimer Center of the VU University Medical Center Amsterdam, and the Alzheimer Center of the Erasmus University Medical Center Rotterdam.

All patients underwent a standardized dementia screening including medical history, informant-based history, physical and neurological examination, blood tests, extensive neuropsychological assessment, and magnetic resonance imaging (MRI) of the brain. Diagnoses were established in a multidisciplinary consensus meeting according to the core clinical criteria of the National Institute on Aging and the Alzheimer's Association workgroup for probable AD (McKhann 2011) and according to the clinical diagnostic criteria for bvFTD (Rascovsky et al. 2011). To minimize center effects, all diagnoses were re-evaluated in a panel including clinicians from both Alzheimer centers. The control participants were screened to exclude memory complaints, drug or alcohol abuse, major psychiatric disorders, and neurological or cerebrovascular diseases. They underwent an assessment including medical history, physical examination, extensive neuropsychological tests, and an MRI of the brain, comparable to the work-up of patients.

Cognitive functioning of all participants was assessed using neuropsychological tests. The neuropsychological test battery included Mini Mental State Examination (MMSE) (Folstein et al. 1975), Frontal Assessment Battery (FAB) (Dubois et al. 2000), Clinical Dementia Rating scale (CDR) (Morris 1993), Geriatric Depression Scale (GDS) (Reisberg et al. 1982), the Dutch version of the Rey Auditory Verbal Learning Test (Rey 1958), Visual Association Test (Lindeboom et al. 2002), Wechsler Adult Intelligence Scale III subtest digit span (Wechsler 1997), Trail Making Test part A and B (Army Test Battery 1994), Stroop Color-Naming test (Stroop 1935), Categorical and Letter fluency (Thurstone and Thurstone 1962), and the Letter Digit Substitution Test (Jolles et al. 1995).

This study was performed in compliance with the Code of Ethics of the World Medical Association (Declaration of Helsinki). Ethical approval was obtained from the local

ethics committees (VU University Medical Center Amsterdam (CWO-nr 11-04, METC-nr 2011/55) and Leiden University Medical Center (2011/55 P11.146)). Written informed consent from all participants was obtained.

TABLE 4.1 Characteristics of the study population

Characteristic	HC (n=29)	AD (n=31)	bvFTD (n=25)	AD vs bvFTD (p value)
Age (years)	62.8 (5.1)	65.3 (7.0)	61.8 (7.3)	0.076
Gender (male/female)	17/12	19/12	19/6	0.249
Study center (VUMC/LUMC) ^a	16/13	20/11	16/9	0.969
Level of education ^b	5.4 (1.2)	4.9 (1.3)	5.1 (1.5)	0.580
Duration of symptoms (months)	n/a	41.9 (30.7)	49.4 (48.3)	0.355
MMSE (max score: 30)	28.8 (1.4)	22.7 (2.8)	24.4 (3.7)	0.068
FAB (max score: 18)	n/a	13.3 (3.4)	13.8 (2.8)	0.592
CDR (max score: 3)	0.0 (0.0)	0.8 (0.3)	0.7 (0.4)	0.545
GDS (max score: 15)	1.3 (1.5)	2.8 (2.9)	3.8 (3.3)	0.279
RAVLT immediate recall (15)	9.0 (2.3)	4.6 (1.6)	5.7 (1.8)	0.017
RAVLT delayed recall (15)	8.6 (3.2)	1.9 (1.8)	3.9 (3.5)	0.009
RAVLT total (75)	44.9 (11.3)	22.8 (8.2)	28.7 (9.1)	0.017
VAT (6)	5.9 (0.5)	3.3 (2.0)	4.8 (1.9)	<0.001
Digit span, forward (30)	12.1 (3.7)	10.0 (2.9)	10.6 (3.8)	0.519
Digit span, backward (30)	8.2 (3.4)	6.2 (2.7)	7.1 (3.1)	0.286
TMT A ^c	37.6 (14.0)	56.8 (32.3)	63.2 (52.0)	0.604
TMT B ^c	79.5 (26.8)	145.4 (65.3)	137.7 (67.5)	0.744
Stroop I ^c	46.6 (7.8)	56.1 (13.9)	58.7 (25.0)	0.637
Stroop II ^c	60.2 (9.6)	80.3 (31.4)	83.0 (41.6)	0.793
Stroop III ^c	98.3 (20.1)	156.5 (48.8)	153.1 (95.2)	0.883
Categorical fluency ^d	24.2 (5.4)	13.9 (5.1)	13.0 (4.7)	0.537
Letter fluency ^d	12.8 (5.1)	9.7 (4.0)	6.8 (4.3)	<0.001
LDST ^d	34.1 (6.8)	19.0 (9.3)	25.9 (7.1)	0.020

Abbreviations: AD = Alzheimer's disease; bvFTD = behavioral variant frontotemporal dementia; HC = healthy controls; MMSE = Mini Mental State Examination; FAB = Frontal Assessment Battery; CDR = Clinical Dementia Rating Scale; GDS = Geriatric Depression Scale; RAVLT = Rey Auditory Verbal Learning Test; VAT = Visual Association Test; TMT = Trail Making Test; LDST = Letter Digit Substitution Test. Values are means (standard deviation) for continuous variables or numbers for dichotomous variables.

^aImaging was performed either in the Alzheimer Center of the VU University Medical center (VUMC) or in the Leiden University Medical Center (LUMC) in the Netherlands. ^bLevel of education was determined on a Dutch 7-point scale ranging from 1 (less than elementary school) to 7 (university or technical college). ^cTime in seconds. ^dNumber of correct responses in 1 minute.

Data acquisition

Imaging was performed on a 3 Tesla scanner either in the VU University Medical Center (Signa HDxt, GE Healthcare, Milwaukee, WI, USA) or in the Leiden University Medical Center (Achieva, Philips Medical Systems, Best, the Netherlands), using a standard 8-channel head coil.

For each subject, a three-dimensional T1-weighted anatomical image was acquired. Imaging parameters in the VU University Medical Center were: TR = 7.8 msec, TE = 3 msec, flip angle = 12°, 180 slices, resulting in a voxel size of 0.98 x 0.98 x 1.00 mm. Imaging parameters in the Leiden University Medical Center were: TR = 9.8 msec, TE = 4.6 msec, flip angle = 8°, 140 slices, resulting in a voxel size of 0.88 x 0.88 x 1.20 mm. In the Leiden University Medical Center an additional high-resolution echo planar imaging scan was acquired for registration purposes (TR = 2.2 sec, TE = 30 msec, flip angle = 80°, 84 slices, resulting in a voxel size of 1.96 x 1.96 x 2.00 mm, including 10% interslice gap).

Resting state fMRI T2*-weighted scans were acquired using whole-brain multislice gradient echo planar imaging. Imaging parameters in the VU University Medical Center were: TR = 1.8 sec, TE = 35 msec, flip angle = 80°, 34 slices, resulting in a voxel size of 3.30 x 3.30 x 3.30 mm, including 10% interslice gap, 200 volumes, scan duration 6 minutes. Imaging parameters in the Leiden University Medical Center were: TR = 2.2 sec, TE = 30 msec, flip angle = 80°, 38 slices, resulting in a voxel size of 2.75 x 2.75 x 2.99 mm, including 10% interslice gap, 200 volumes, scan duration 7 minutes and 33 seconds. Participants were instructed to lie still with their eyes closed and not to fall asleep during the resting state scan.

Data analysis

Before analysis, all MRI scans were submitted to a visual quality control check to ensure that no gross artifacts were present in the data. Data analysis was performed with Functional Magnetic Resonance Imaging of the Brain Software Library (FSL 5.0.1, Oxford, United Kingdom) (Smith et al. 2004) and Matlab version R2011b (MathWorks, Natick, MA, USA). Anatomical regions were determined using the Harvard-Oxford cortical and subcortical structures atlas integrated in FSL.

Gray matter volume

Structural MRI scans were analyzed with a voxel-based morphometry (VBM) analysis (Ashburner and Friston 2000) to study group differences in gray matter volume. First, the structural images were brain extracted and tissue-type segmented (Zhang et al. 2001b). The resulting gray matter partial volume images were aligned to the gray matter MNI standard space image (Montreal Neurological Institute, Montreal, QC, Canada) (Jenkinson et al. 2002), followed by non-linear registration (Andersson et al. 2007a). The images were averaged to create a study-specific template.

Next, all native gray matter images were non-linearly registered to this study-specific gray matter template (Ashburner and Friston 2000; Good et al. 2001). To correct for the contractions and enlargements due to the non-linear registration, each voxel of each registered gray matter image was multiplied by the Jacobian of the warp field, which defines the direction (larger or smaller) and the amount of modulation. The modulated segmented images were spatially smoothed with an isotropic Gaussian kernel with a full width at half maximum of 7 mm.

To study group differences in gray matter volume, a general linear model (GLM) approach using analysis of variance F-tests with post hoc Bonferroni adjusted t-tests was applied. Age, gender, and study center were included as covariate in the statistical model. Voxel-wise non-parametric permutation testing (Nichols and Holmes 2001) with 5000 permutations was performed using FSL-randomise correcting for multiple comparisons across space (statistical threshold set at $p < 0.05$, Family-Wise Error (FWE) corrected), using the Threshold-Free Cluster Enhancement (TFCE) technique (Smith and Nichols 2009).

Preprocessing of resting state fMRI data

The preprocessing of the resting state data consisted of motion correction (Jenkinson et al. 2002), brain extraction, spatial smoothing using a Gaussian kernel with a full width at half maximum of 3 mm, and high-pass temporal filtering (cutoff frequency of 0.01 Hz). To quantify movement in the fMRI signal, the mean square of the absolute head movement was calculated. Patients with AD showed a mean square of 0.16 mm, patients with bvFTD 0.25 mm, and controls 0.19 mm. No significant group differences in movement values were found.

After preprocessing, the functional images were registered to the corresponding T1-weighted images using Boundary-Based Registration (Greve and Fischl 2009). The T1-weighted images were registered to the 2 mm isotropic MNI standard space image using non-linear registration (Andersson et al. 2007b) with a warp resolution of 10 mm. High-resolution echo planar images (only available for subjects scanned in the Leiden University Medical Center) were used for an additional registration step between functional images and T1-weighted images. In order to achieve better comparison across voxels, subjects, and centers, standardization on a voxel-by-voxel basis has been recommended (Yan et al. 2013). We used the Z-standardization approach in which individual resting state fMRI time series were normalised (standardized to z scores) on a voxel-by-voxel basis using the mean and standard deviation of each individual resting state signal across time (previously described in (Yan et al. 2013)).

Single-session independent component analysis was performed on the preprocessed resting state data to decompose the data into distinct components for denoising purposes (Beckmann and Smith 2004). The standard training-dataset of FMRIB's ICA-based Xnoiseifier 1.05 (FIX) was used to auto-classify components into "good" (i.e., functional signal) and "bad" (i.e., noise) components (Salimi-Khorshidi et al. 2014). FIX removed unique variance related to "noise" components and motion confounds from the preprocessed fMRI data to denoise the resting state data and to increase the signal-to-noise ratio. Manual classification of data from 18 participants, equally distributed over groups and centers, showed that between 75 and 100 % of the hand-labeled "noise" components and none of the "signal" components were removed.

Functional connectivity analysis: network-to-region connectivity

Voxel-based group differences in network functional connectivity were studied using the dual regression method of FSL (previously described in (Filippini et al. 2009)). We used eight standard resting state networks as reference to study functional connectivity in a standardized way (Khalili-Mahani et al. 2012; Hafkemeijer et al. 2013). Resting state functional connectivity was determined in terms of similarity of the blood oxygenation level dependent (BOLD) fluctuations in the brain in relation to characteristic fluctuations in the eight predefined resting state networks (Beckmann et al. 2005; Damoiseaux et al. 2006).

These standardized resting state networks parcellate the brain into eight templates that represent over 80% of the total brain volume (Khalili-Mahani et al. 2012): network I) calcarine sulcus, precuneal cortex, and primary visual cortex (medial visual network), network II) superior and fusiform areas of lateral occipital cortex (lateral visual network), network III) superior temporal cortex, insular cortex, ACC, auditory cortex, operculum, somatosensory cortices, thalamus (auditory system network), network IV) precentral and postcentral somatosensory somatomotor areas (sensorimotor system network), network V) rostral medial prefrontal cortex, precuneal cortex, PCC (default mode network), network VI) medial and inferior prefrontal cortex, anterior cingulate and paracingulate gyri, prefrontal cortex (executive control network), networks VII and VIII) frontal pole, dorsolateral prefrontal cortex, parietal lobule, paracingulate gyrus, PCC (dorsal visual stream networks) (for further details, see (Beckmann et al. 2005; Khalili-Mahani et al. 2014)). To account for noise, even after FIX, a white matter and a cerebrospinal fluid template were included in the analysis (Fox et al. 2005; Birn 2012).

In the dual regression, individual time series were first extracted for each template, using the eight resting state networks (Beckmann et al. 2005) and the two additional white matter and cerebrospinal fluid maps (Fox et al. 2005; Birn 2012), in a spatial regression against the individual fMRI data set (regression 1). The resulting matrices described temporal dynamics for each template and individual. Next, the ten temporal regressors were used to fit a linear model to the individual fMRI data set (regression 2), to estimate the spatial maps for each individual.

This results in ten 3D images per individual, with for each voxel z scores representing the functional connectivity to each of the templates. The higher the absolute value of the z score, the stronger the connectivity to a network. Z scores were calculated for voxels both inside and outside the networks. Z scores of voxels outside a network indicate the strength of the functional connections between that outside region and the average of the network, while z scores of voxels inside the network indicate the strength of the connection between the average of the network and that region within the network. If functional connectivity is decreased in specific voxels inside the network, this indicates a less homogeneous fMRI signal in the network (i.e., less functional connectivity).

To study group differences in functional connectivity, a GLM approach using analysis of variance F-tests with post hoc Bonferroni adjusted t-tests was applied. The data used in this study were collected from two centers. Although the distribution of participants between centers did not differ significantly between groups, we followed previous approaches to account for the potential effects of center and included center in all statistical models (Kim et al. 2009; Zhou et al. 2010). In addition to center, age and gender were included as covariate. To account for potential effects of local structural gray matter differences within and between the two groups, segmented structural data were used to include gray matter volume of each voxel as subject-wise and voxel-wise covariates in the GLM design (Oakes et al. 2007). Voxel-wise non-parametric permutation testing (Nichols and Holmes 2001) with 5000 permutations was performed using FSL-randomise correcting for multiple comparisons across voxels (statistical threshold set at $p < 0.05$, FWE corrected), using the TFCE technique (Smith and Nichols 2009).

Functional connectivity analysis: region-to-region connectivity

In addition to the network analysis, we studied connections throughout the entire brain using correlation analyses. The whole-brain was divided into 110 cortical and subcortical brain areas based on the probabilistic Harvard-Oxford cortical and subcortical structural atlas integrated in FSL (which we split into left and right hemisphere regions) to calculate the functional connectivity between pairs of anatomically defined brain areas. The preprocessed and denoised resting state data were voxel-based weighted with the gray matter partial volume estimate obtained with the FMRIB's Automated Segmentation Tool. Then, to calculate the average signal per probabilistic brain area, we averaged each voxel weighted by their probability per region (with a minimum of 25%) resulting in 110 time courses per subject.

The full correlation between each pair of the 110 time signals was calculated, forming a weighted correlation matrix for each subject. Fischer-Z transformation was used to transform the correlations to z scores. The GLM approach using analysis of variance F-tests (IBM SPSS Statistics Version 20, IBM Corp., Somers, NY, USA) with post hoc Bonferroni adjusted t-tests was applied to compare functional connectivity between pairs of anatomical regions in bvFTD and AD. The same statistical model as used in the network analysis was applied with age, gender, and study center included as covariates. To correct for multiple comparisons, we applied the false discovery rate

(FDR) approach ($p < 0.05$) (Genovese et al. 2002). Group average of the control group was used as reference value in the post hoc plots.

4.4. RESULTS

Demographic characteristics

Demographic data for all participants are summarized in *Table 4.1*. There were no significant differences between the groups with regard to age, gender, study center distribution, level of education, and duration of symptoms (all $p > 0.05$). As expected, both dementia groups performed worse on cognitive tests compared with controls (all $p < 0.05$). Patients with AD performed worse compared with bvFTD patients on memory tests (Rey Auditory Verbal Learning Test ($p = 0.009$) and Visual Association Test ($p < 0.001$)) and furthermore on the Letter Digit Substitution Test ($p = 0.020$). Patients with bvFTD performed worse compared with AD patients on Letter fluency ($p < 0.001$), which is an attention and executive function test. No significant differences between both dementia groups were found on the other cognitive tests ($p > 0.05$).

Gray matter volume

The voxel-wise structural analysis revealed group differences in gray matter volume (*Fig. 4.1*). Patients with AD showed less gray matter in precuneal cortex, PCC, frontal medial cortex, temporal gyrus, hippocampus, lateral occipital cortex, and operculum cortex compared with controls (*Fig. 4.1A*). Patients with bvFTD showed less gray matter in ACC, insular cortex, frontal pole, frontal gyrus, temporal pole, temporal gyrus, and temporal fusiform gyrus compared with controls (*Fig. 4.1B*). AD patients had less gray matter compared with bvFTD in precuneal cortex, PCC, and angular gyrus (*Fig. 4.1C*). Patients with bvFTD had less gray matter compared with AD in anterior cingulate gyrus, frontal pole, and superior frontal gyrus (*Fig. 4.1D*).

Functional connectivity: network-to-region connectivity

Functional connectivity analysis showed main effect of group for resting state network II, network III, network V, and network VIII. For the other four resting state networks, no group differences in functional connectivity were observed. The results of post hoc testing showed decreased functional connectivity in bvFTD compared with controls between network III (auditory network) and inferior temporal gyrus, middle temporal gyrus, superior temporal gyrus, postcentral gyrus, and supramarginal gyrus (*Table 4.2*). In AD, functional connectivity was decreased compared with controls between network V (default mode network) and posterior cingulate gyrus, precuneal cortex, and lateral occipital cortex (*Table 4.2*).

The results of post hoc testing showed decreased functional connectivity in bvFTD compared with AD between network II (lateral visual cortical network) and the lateral occipital cortex and cuneal cortex (*Table 4.2, Fig. 4.2A*). Patients with AD showed decreased functional connectivity between network VIII (dorsal visual stream network) and lateral occipital cortex and parietal opercular cortex (*Table 4.2, Fig. 4.2B*). We also observed ‘negative’ (i.e., anti-correlated) connectivity: bvFTD patients showed less negative functional connectivity between network III (auditory system network) and the angular gyrus (*Table 4.2, Fig. 4.2C*).

To illustrate group differences between both types of dementia and how network-to-region connectivity compares to controls, subjects’ mean z scores of regions with differences in functional connectivity between the two patient groups are plotted in *Fig. 4.2D*. Boxplots show mean z scores from: lateral occipital cortex and cuneal cortex (blue areas in A), lateral occipital and parietal opercular cortex (blue areas in B), and angular gyrus (blue areas in C).

Functional connectivity: region-to-region connectivity

In a second analysis, we studied connections throughout the entire brain using correlation analyses between 110 cortical and subcortical brain areas and found a main effect of group. The results of post hoc testing showed decreased pairwise connectivity in bvFTD compared with AD between the right superior temporal gyrus (*Fig. 4.3A*, blue area, coronal slice) and the right cuneal cortex (*Fig. 4.3A*, yellow, $p < 0.0001$), left cuneal cortex ($p = 0.0002$), the right supracalcarine cortex (*Fig. 4.3A*, blue, $p = 0.0002$), left supracalcarine cortex ($p = 0.0001$), the right intracalcarine cortex (*Fig. 4.3A*, pink, $p = 0.0001$), and the right lingual gyrus (*Fig. 4.3A*, green, $p = 0.0002$).

To further illustrate these group differences and how region-to-region connectivity compares to controls, functional connectivity with the right superior temporal gyrus is plotted in separate boxplots (*Fig. 4.3B*) for the cuneal cortex (yellow), supracalcarine cortex (blue), intracalcarine cortex (pink), and lingual gyrus (green).

FIGURE 4.1 Group differences in gray matter volume
 Differences in gray matter volume between behavioral variant frontotemporal dementia (FTD), Alzheimer’s disease (AD), and healthy controls (HC) (TFCE, FWE corrected). A) Patients with AD showed less gray matter in precuneal cortex, PCC, and frontal medial cortex compared with controls. B) Patients with bvFTD showed less gray matter in ACC, insular cortex, frontal pole, frontal gyrus, and middle temporal gyrus compared with controls. C) AD patients had less gray matter compared with bvFTD in precuneal cortex and PCC. D) Patients with bvFTD had less gray matter compared with AD in anterior cingulate gyrus and frontal pole.

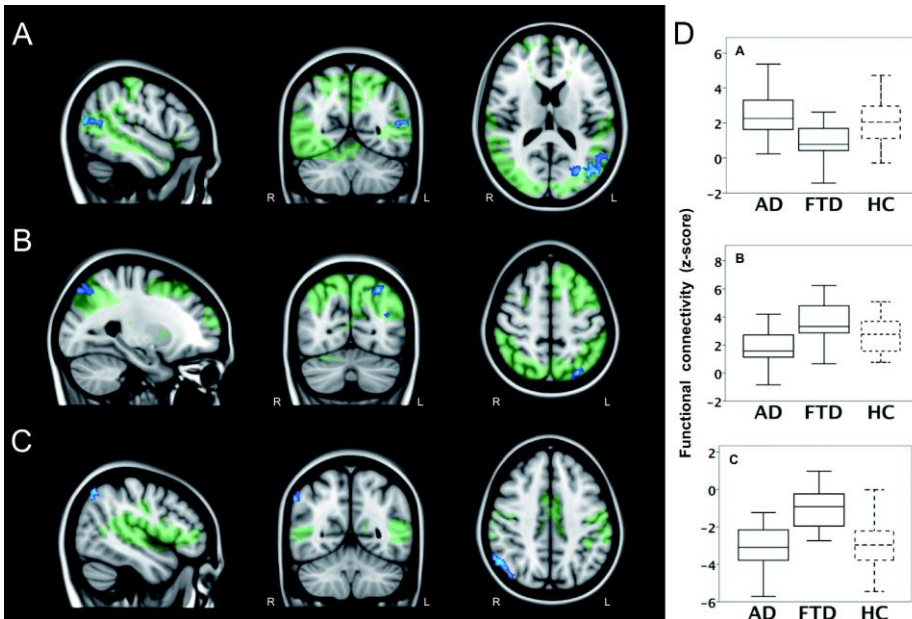
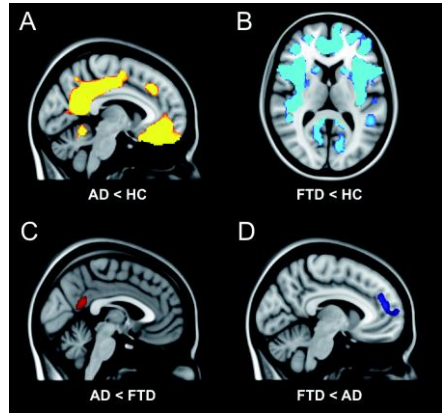


FIGURE 4.2 Functional connectivity in bvFTD versus AD: network-to-region connectivity

Differences in functional connectivity between green networks and blue voxels in behavioral variant frontotemporal dementia (FTD) and Alzheimer’s disease (AD) (TFCE, FWE corrected). A) Decreased functional connectivity between lateral visual cortical network (green) and lateral occipital cortex and cuneal cortex (blue) in bvFTD compared with AD. B) Decreased functional connectivity between dorsal visual stream network (green) and lateral occipital cortex and parietal opercular cortex (blue) in AD compared with bvFTD. C) Less negative functional connectivity between auditory system network (green) and angular gyrus (blue) in bvFTD compared with AD. Images are overlaid on the MNI standard anatomical image. D) Subjects’ mean z scores were extracted from brain areas with group differences in functional connectivity (blue areas). Boxplots show median, lower and upper quartile, and sample minimum and maximum z scores for patients with AD, patients with bvFTD, and healthy controls (HC, dotted lines).

TABLE 4.2 Group differences in network functional connectivity

Network	Brain structure ^a	Side	Peak voxel coordinates (MNI)			Peak T score
			x	y	z	
Default mode network AD < HC	Posterior cingulate gyrus	R	-2	-44	42	3.55
	Precuneal cortex	L	-16	-62	12	2.90
	Lateral occipital cortex	R	50	-74	26	3.74
Auditory system network bvFTD < HC	Inferior temporal gyrus	L	-42	-60	0	3.82
	Middle temporal gyrus	L	-52	-60	6	3.05
	Superior temporal gyrus	L	-60	-2	0	3.63
	Postcentral gyrus	L	-50	-18	34	4.37
	Supramarginal gyrus	L	-52	-30	36	4.05
	Lateral visual cortical network bvFTD < AD	Lateral occipital cortex / Angular gyrus	L	-40	-76	12
	Cuneal cortex	L	0	-86	32	4.39
	Cuneal cortex	R	22	-72	24	4.63
	Lateral occipital cortex	R	46	-78	10	3.86
Dorsal visual stream network AD < bvFTD	Lateral occipital cortex	L	-28	-72	52	5.05
	Parietal opercular cortex	L	-54	-24	24	4.36
	Lateral occipital cortex	L	-38	-70	22	4.18
Auditory system network bvFTD < AD	Angular gyrus	R	52	-62	44	5.22

Abbreviations: MNI = Montreal Neurological Institute standard space image; AD = Alzheimer's disease; HC = healthy controls; bvFTD = behavioral variant frontotemporal dementia; R = right; L = left

^aFull list of structures with group differences in network functional connectivity. Between group effects are independent of physiological noise, age, gender, study center, and gray matter volume. For each peak voxel x-, y-, and z-coordinates in the MNI standard space image are given.

4.5. DISCUSSION

We studied functional connections throughout the brain in AD and bvFTD and showed that functional connectivity is different between both types of dementia. Given the gray matter atrophy, we observed decreased connectivity in bvFTD compared with AD between a) the lateral visual cortical network and the lateral occipital cortex and cuneal cortex, and b) between the auditory system network and the angular gyrus. Patients with AD showed decreased functional connectivity between the dorsal visual stream network and lateral occipital cortex and parietal opercular cortex. The decreased cuneal connectivity found in bvFTD patients was also found with the region-to-region connectivity analysis showing decreased connectivity between superior temporal gyrus and cuneal cortex, supracalcarine, intracalcarine cortex, and lingual gyrus. These findings support the hypothesis that resting state fMRI shows disease-specific functional connectivity differences and is useful to elucidate the pathophysiology of AD and bvFTD.

The region-to-region connectivity analysis showed decreased temporal gyrus connectivity in patients with bvFTD. This part of the brain is particularly vulnerable for FTD pathology, with gray matter atrophy located in this area (Whitwell et al. 2011; Farb et al. 2013). Decreased functional connectivity in the temporal lobe has earlier been found in bvFTD when compared with controls (Whitwell et al. 2011; Farb et al. 2013). In AD, we did not find differences in region-to-region connectivity, although decreased connectivity with the hippocampus has been reported by others (Allen et al. 2007).

The network-to-region analysis showed that functional connectivity of the angular gyrus was decreased (less negative) in patients with bvFTD. Differences in angular gyrus functional connectivity have been found in bvFTD compared with healthy controls (Farb et al. 2013; Rytty et al. 2013). An association between angular gyrus functional connectivity and stereotypical behavior has been found in bvFTD (Farb et al. 2013), suggesting an important role of the angular gyrus in the typical behavior of patients with bvFTD. However, the exact role of the angular gyrus in the behavior of bvFTD is not clear. Longitudinal changes in bvFTD have been found to be related to insular, not angular, connectivity (Day et al. 2013). Moreover, decreased angular functional connectivity was found in AD when compared with healthy controls (Wang et al. 2015) or with bvFTD patients (Zhou et al. 2010).

Functional connectivity between the dorsal visual stream network and the lateral occipital cortex and parietal opercular cortex is increased in bvFTD compared with AD. A recent study reported atrophy in the opercular cortex in patients with bvFTD, but no differences in functional connectivity in this brain area were reported in that study (Rytty et al. 2013). The opercular cortex overlies the insula, which is one of the brain regions first affected in bvFTD (Seeley et al. 2008). Patients with bvFTD show differences in insula functional connectivity compared with healthy controls (Farb et al. 2013) and patients with AD (Zhou et al. 2010). The differences in functional connectivity in this brain area may relate to the impaired social behavior that typically occurs in bvFTD, since the insula has an important role in social-emotional processing (Couto et al. 2013).

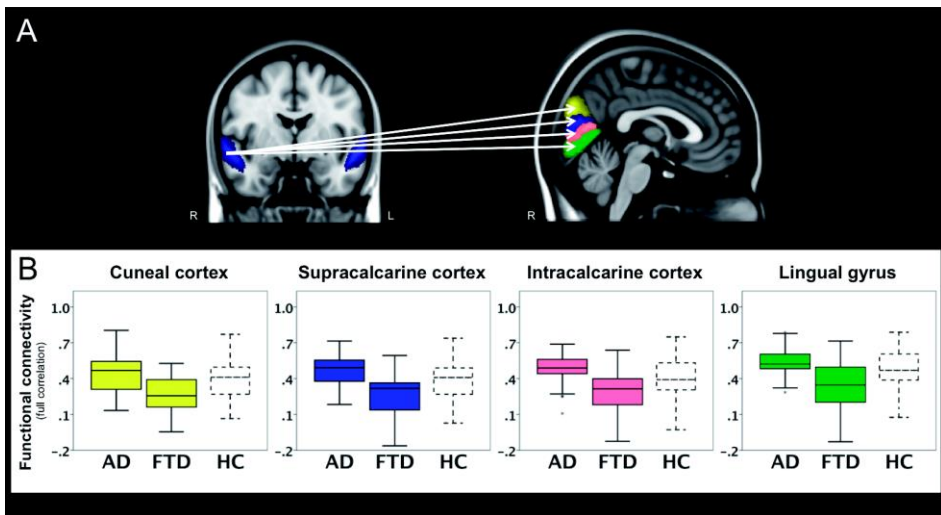


FIGURE 4.3 Functional connectivity in bvFTD versus AD: region-to-region connectivity

Differences in pairwise functional connectivity between behavioral variant frontotemporal dementia (FTD) and Alzheimer’s disease (AD). A) Decreased functional connectivity between right superior temporal gyrus (blue area, coronal slice) and cuneal cortex (yellow), supracalcarine cortex (blue), intracalcarine cortex (pink), and lingual gyrus (green) in bvFTD compared with AD. Images show brain areas based on the probabilistic Harvard-Oxford structural atlas overlaid on coronal and sagittal slices of the MNI standard anatomical image. B) Subjects’ correlation scores were extracted from brain areas with differences in functional connectivity between the two patient groups (right cuneal, supracalcarine, intracalcarine cortex, and lingual gyrus). Boxplots show median, lower and upper quartile, and sample minimum and maximum correlation scores for patients with AD, patients with bvFTD, and healthy controls (HC, dotted lines).

We found differences in functional connectivity in the so-called auditory system network that encompassed temporal cortex, insular cortex, ACC, auditory cortex,

operculum, somatosensory cortices, and thalamus, areas which are related to social-emotional processing (Seeley, Menon, et al. 2007). We found decreased negative, not positive, functional connectivity between this network and the angular gyrus in patients with bvFTD. It has been suggested that negative functional connectivity indicates an anti-correlation between brain areas (Fox et al. 2005; Hampson et al. 2010). The interpretation of anti-correlations in resting state data is not straightforward (Fox et al. 2009; Yan et al. 2013) and its biological meaning is a subject of debate (Chai et al. 2012).

In addition to the direct comparison of AD and bvFTD patients, we compared functional connectivity between patients and control participants. As expected, we found decreased connectivity in AD compared with controls between the default mode network and posterior cingulate gyrus, precuneal cortex, and lateral occipital cortex. In bvFTD, functional connectivity was decreased compared with controls between the auditory network (temporal cortex, insular cortex, ACC, auditory cortex, operculum, somatosensory cortices, thalamus) and temporal gyrus, supramarginal gyrus, and postcentral gyrus. These findings reproduced connections that are comparable with other studies that compared functional brain networks between dementia patients and controls, showing decreased functional connectivity in the posterior temporal-parietal default mode network in AD and in the anterior cingulo-frontoinsula salience network in bvFTD (Greicius et al. 2004; Allen et al. 2007; Binnewijzend et al. 2012; Agosta et al. 2013; Rytty et al. 2013).

Decreased functional connectivity between regions within the default mode network has been found in AD compared with bvFTD (Zhou et al. 2010). The present study and the study by Filippi and colleagues (Filippi et al. 2013) were not able to replicate these default mode network disease-related differences. Although functional connectivity between patient and controls differed as expected, the group differences between AD and bvFTD were smaller than those in previous studies. This variability among studies may be due to multiple factors, including variations in the study cohort. Compared with other resting state fMRI studies in bvFTD and AD (Zhou et al. 2010; Filippi et al. 2013), we included a relatively large sample of patients in an early stage of the disease with very mild to mild symptoms. Hence it is possible that they are less severely affected compared with those in other studies. Furthermore, since early differential diagnosis between AD and bvFTD may be challenging, the possibility of misdiagnosis of

the patients cannot be ruled out. The diagnosis FTD or AD can only be confirmed by brain autopsy after a person dies. In this study, postmortem data were not available. Nevertheless, all patients underwent an extensive dementia screening. Only dementia patients that fulfilled the most recent criteria for bvFTD (Rascovsky et al. 2011) and AD (McKhann 2011) were included.

As expected, both dementia groups performed worse on cognitive functioning compared with controls. Patients with AD showed lowest scores on MMSE, which is a general measurement of cognitive performance (Folstein et al. 1975). Moreover, AD patients performed worse in memory functioning compared with controls and bvFTD. Patients with bvFTD performed, as expected, worse on executive functioning compared with controls. We further expected lower executive functioning scores in the bvFTD group compared with AD, however, AD patients did not differ from bvFTD in most executive functioning tests.

Overall, the AD patients showed low scores in all cognitive domains, not only in the memory domain, but also in executive functioning. Although executive functioning could be useful to differentiate AD from bvFTD (Iavarone et al. 2004; Slachevsky et al. 2004), some studies reported that executive functioning, measured with FAB, does not discriminate AD from bvFTD patients (Lipton et al. 2005; Castiglioni et al. 2006). It has been suggested that testing multiple cognitive domains is required to differentiate both types of dementia rather than focus on one cognitive test (Lipton et al. 2005). In the current study, all patients underwent extensive neuropsychological assessment. Diagnoses were established according to the core clinical criteria for probable AD (McKhann 2011) and for bvFTD (Rascovsky et al. 2011) and therefore were not based on one single neuropsychological test score.

This study showed data that were collected in two centers. The strengths of multicenter studies are the larger number of participants that can be included and the increased generalizability of the study findings. However, multicenter studies have also limitations, since the data will be less homogeneous than in single center studies. To increase homogeneity between centers in the current study, we evaluated all patients in a multidisciplinary panel including clinicians from different centers specialized in dementia, we used a standardization approach in order to achieve better comparison across voxels, subjects, and centers (Yan et al. 2013), and we added center as

covariate in all statistical models, following previous approaches (Kim et al. 2009; Zhou et al. 2010).

4.5.1. CONCLUSION

In the present study, we used resting state fMRI to study functional connections throughout the entire brain and showed that resting state functional brain connectivity is different between AD and bvFTD. Our findings support the hypothesis that resting state fMRI shows disease-specific functional connectivity differences and is useful to elucidate the pathophysiology of AD and bvFTD. However, the findings of the present study suggest that group differences in functional connectivity between both dementia types are less abundant than has been shown in previous studies.

Chapter 5

A longitudinal study on resting state functional connectivity in behavioral variant frontotemporal dementia and Alzheimer's disease

Anne Hafkemeijer, Christiane Möller, Elise Dopper, Lize Jiskoot,
Annette van den Berg-Huysmans, John van Swieten, Wiesje van der Flier,
Hugo Vrenken, Yolande Pijnenburg, Frederik Barkhof,
Philip Scheltens, Jeroen van der Grond, and Serge Rombouts



5.1. ABSTRACT

Alzheimer's disease (AD) and behavioral variant frontotemporal dementia (bvFTD) are the most common types of early-onset dementia. We applied longitudinal resting state functional magnetic resonance imaging to delineate functional brain connections relevant for disease progression and diagnostic accuracy.

We used two-center resting state functional magnetic resonance imaging (fMRI) data of 20 AD patients (65.1 ± 8.0 years), 12 bvFTD patients (64.7 ± 5.4 years), and 22 control subjects (63.8 ± 5.0 years) at baseline and 1.8-year follow-up measurement. We used whole-network and voxel-based network-to-region analyses to study group differences in functional connectivity at baseline and at follow-up, and longitudinal *changes* in connectivity within and between groups. A general linear model approach, controlling for physiological noise, age, gender, and study center, was used.

At baseline, connectivity differs between AD and controls (cuneal cortex, paracingulate gyrus, lingual gyrus, dorsal visual stream network). These differences were also present after 1.8 years. At follow-up, connectivity was lower in bvFTD compared with controls (angular gyrus, paracingulate gyrus), and compared with AD (anterior cingulate gyrus, lateral occipital cortex). Over time, connectivity decreased in AD (precuneus) and in bvFTD (inferior frontal gyrus). Longitudinal changes in supramarginal gyrus connectivity differ between both patient groups and controls.

We found disease-specific brain regions with longitudinal connectivity changes. This suggests the potential of longitudinal resting state fMRI to delineate regions relevant for disease progression and for diagnostic accuracy, although no group differences in longitudinal changes in the direct comparison of AD and bvFTD were found.

5.2. INTRODUCTION

Alzheimer's disease (AD) and behavioral variant frontotemporal dementia (bvFTD) are the most common types of early-onset dementia (Ratnavalli et al. 2002). AD is mainly characterized by deficits in episodic and working memory (McKhann 2011), whereas patients with bvFTD typically present with changes in behavior (Rascovsky et al. 2011).

A substantial amount of dementia research used neuroimaging to elucidate the pathophysiology of bvFTD and AD (McMillan et al. 2014; Raamana et al. 2014). Imaging of brain structure shows typical AD atrophy in the hippocampus, precuneus, posterior cingulate cortex, parietal, and occipital brain regions (Buckner et al. 2005; Seeley et al. 2009; Krueger et al. 2010). In bvFTD, atrophy is most often found in the anterior cingulate cortex, frontoinsula, and frontal brain regions (Seeley et al. 2009; Krueger et al. 2010).

Longitudinal studies have shown to be useful to elucidate changes in gray matter volume over time, showing that in AD atrophy progresses faster in the hippocampus and posterior cingulate cortex, while atrophy progresses faster in the orbitofrontal gyrus and frontal lobe in bvFTD (Barnes et al. 2007; Whitwell et al. 2007; Krueger et al. 2010; Frings et al. 2014). These studies show the importance of longitudinal designs to delineate regions relevant for disease progression.

The disease-specific patterns of gray matter atrophy show spatial overlap with functional brain networks (Seeley et al. 2009). Imaging of these functional networks offers the opportunity to study brain function and dysfunction in AD and bvFTD (Seeley et al. 2009; Pievani et al. 2011). AD patients show abnormalities in functional network connectivity in the posterior hippocampal-cingulo-temporal-parietal network known as the default mode network (Greicius et al. 2004; Zhou et al. 2010; Hafkemeijer, van der Grond, and Rombouts 2012; Balthazar et al. 2014). Patients with bvFTD show functional connectivity abnormalities in the anterior frontoinsular-cingulo-orbitofrontal network often called the salience network (Zhou et al. 2010; Borroni et al. 2012; Agosta et al. 2013; Farb et al. 2013; Filippi et al. 2013; Rytty et al. 2013).

Despite evidence from cross-sectional studies that functional network connectivity gives the opportunity to study brain dysfunction in dementia and therefore has

potential to study disease progression, little is known about how functional connections change over time in AD and bvFTD. Studying longitudinal functional connectivity is important to monitor disease progression and may have utility to improve differential diagnosis of both types of dementia.

The aim of the present study was to delineate functional connections relevant for disease progression and diagnostic accuracy. We used longitudinal resting state functional magnetic imaging (fMRI) data of AD and bvFTD patients to investigate, in addition to cross-sectional group differences, longitudinal changes in functional connectivity within and between groups.

5.3. MATERIALS AND METHODS

Participants

We included 20 patients with probable AD, 12 patients with probable bvFTD, and 22 control participants (*Table 5.1*). All subjects were recruited from two Dutch centers specialized in dementia: the Alzheimer Center of the VU University Medical Center Amsterdam, and the Alzheimer Center of the Erasmus University Medical Center Rotterdam, as described previously (Hafkemeijer et al. 2015).

TABLE 5.1 Characteristics of the study population

Characteristic	AD (n=20)		bvFTD (n=12)		HC (n=22)	
Age (years)	65.1 (8.0)		64.7 (5.4)		63.8 (5.0)	
Follow-up time (years)	1.79 (0.43)		1.76 (0.43)		1.77 (0.59)	
Gender (male/female)	16/4		9/3		14/8	
Study center^a (VUMC/LUMC)	16/4		8/4		12/10	
Level of education^b	4.9 (1.1)		5.0 (1.3)		5.6 (0.7)	
Duration of symptoms (months)	43.2 (26.8)		67.0 (58.2)		n/a	
	BL	FU	BL	FU	BL	FU
MMSE (max score: 30)	23.2 (2.9)	19.8* (5.2)	24.3 (3.9)	20.9 (6.7)	29.1 (0.9)	29.0 (1.5)
FAB (max score: 18)	14.1 (2.7)	11.7* (3.7)	13.3 (2.7)	10.5 (6.3)	17.4 (1.2)	17.2 (1.1)
CDR (max score: 3)	1.1 (0.8)	1.2 (0.5)	1.3 (0.8)	1.7 (0.8)	0.0 (0.0)	0.0 (0.0)
GDS (max score: 15)	2.7 (3.4)	1.9 (2.0)	1.4 (0.8)	2.7 (3.5)	1.2 (1.2)	0.8 (1.4)

Abbreviations: AD = Alzheimer's disease; bvFTD = behavioral variant of frontotemporal dementia; HC = healthy controls; BL = baseline; FU = Follow-up; MMSE = Mini Mental State Examination; FAB = Frontal Assessment Battery; CDR = Clinical Dementia Rating Scale; GDS = Geriatric Depression Scale. Values are means (standard deviation) for continuous variables or numbers for dichotomous variables. Scores on FAB and GDS were missing in 5 patients.

^aImaging was performed either in the Alzheimer Center of the VU University Medical center (VUMC) or in the Leiden University Medical Center (LUMC) in the Netherlands. ^bLevel of education was determined on a Dutch 7-point scale ranging from 1 (less than elementary school) to 7 (university or technical college). * Significant differences between baseline and follow-up

All patients underwent a standardized dementia screening including medical history, informant-based history, physical and neurological examination, blood tests, extensive neuropsychological assessment, and magnetic resonance imaging (MRI) of the brain. Diagnoses were established in a multidisciplinary consensus meeting according to the core clinical criteria of the National Institute on Aging and the Alzheimer's Association workgroup for probable AD (McKhann et al. 1984; McKhann 2011) and according to the clinical diagnostic criteria for bvFTD (Rascovsky et al. 2011). To minimize center effects, all diagnoses were re-evaluated in a panel including clinicians from both Alzheimer centers.

The control participants were screened to exclude memory complaints, drug or alcohol abuse, major psychiatric disorders, and neurological or cerebrovascular diseases. They underwent an assessment including medical history, physical examination, extensive neuropsychological assessment, and an MRI of the brain, comparable to the work-up of patients. All study participants underwent extensive neuropsychological assessment and MRI scanning at baseline and follow-up. Mean interval between the first visit (baseline measurement) and second visit (follow-up measurement) was 1.8 years (1.79 years for AD patients, 1.76 years for bvFTD patients, and 1.77 years for controls).

This study was performed in compliance with the Code of Ethics of the World Medical Association (Declaration of Helsinki). Ethical approval was obtained from the local ethics committees. Written informed consent from all participants was obtained.

Data acquisition

All participants underwent an MRI of the brain, on a 3 Tesla scanner using a standard 8-channel head coil, either in the VU University Medical Center (Signa HDxt, GE Healthcare, Milwaukee, WI, USA), or in the Leiden University Medical Center (Achieva, Philips Medical Systems, Best, the Netherlands) at baseline and follow-up.

Resting state fMRI T2*-weighted scans were acquired using whole-brain multislice gradient echo planar imaging. Imaging parameters in the VU University Medical Center were: TR = 1.8 sec, TE = 35 msec, flip angle = 80°, 34 slices, resulting in a voxel size of 3.30 x 3.30 x 3.30 mm, including 10% interslice gap, 200 volumes, scan duration 6 minutes. Imaging parameters in the Leiden University Medical Center were: TR = 2.2 sec, TE = 30 msec, flip angle = 80°, 38 slices, resulting in a voxel size of 2.75 x 2.75 x 2.99 mm, including 10% interslice gap, 200 volumes, scan duration 7 minutes

and 33 seconds. Participants were instructed to lie still with their eyes closed and not to fall asleep during the resting state scan.

For registration purposes, three-dimensional T1-weighted anatomical images were acquired. Imaging parameters in the VU University Medical Center were: TR = 7.8 msec, TE = 3 msec, flip angle = 12°, 180 slices, resulting in a voxel size of 0.98 x 0.98 x 1.00 mm. Imaging parameters in the Leiden University Medical Center were: TR = 9.8 msec, TE = 4.6 msec, flip angle = 8°, 140 slices, resulting in a voxel size of 0.88 x 0.88 x 1.20 mm. In the Leiden University Medical Center an additional high-resolution echo planar imaging scan was acquired for registration purposes (TR = 2.2 sec, TE = 30 msec, flip angle = 80°, 84 slices, resulting in a voxel size of 1.96 x 1.96 x 2.00 mm, including 10% interslice gap).

Data analysis

Before analysis, all MRI scans were submitted to a visual quality control check to ensure that no gross artifacts were present in the data. Data analysis was performed with Functional Magnetic Resonance Imaging of the Brain Software Library (FSL 5.0.1, Oxford, United Kingdom) (Smith et al. 2004). Anatomical regions were determined using the Harvard-Oxford cortical and subcortical structures atlas integrated in FSL.

Preprocessing

The preprocessing of the resting state data consisted of motion correction (Jenkinson et al. 2002), brain extraction (Smith 2002), spatial smoothing using a Gaussian kernel with a full width at half maximum of 3 mm, and high-pass temporal filtering (cutoff frequency of 0.01 Hz). After preprocessing, the functional images were registered to the corresponding T1-weighted images using Boundary-Based Registration (Greve and Fischl 2009). T1-weighted images were registered to the 2 mm isotropic MNI standard space image (Montreal Neurological Institute, Montreal, QC, Canada) using nonlinear registration (Andersson et al. 2007b) with a warp resolution of 10 mm. High-resolution echo planar images (only available for subjects scanned in the Leiden University Medical Center) were used for an additional registration step between functional images and T1-weighted images.

In order to achieve better comparison across voxels, subjects, time points, and centers, standardization on a voxel-by-voxel basis has been recommended (Yan et al.

2013). We used the Z-standardization approach in which individual resting state fMRI time series were normalised (standardized to z-scores) on a voxel-by-voxel basis using the mean and standard deviation of each individual resting state signal across time (previously described in (Yan et al. 2013)).

Single-session independent component analysis (ICA) was performed on the preprocessed resting state data to decompose the data into distinct components for denoising purposes (Beckmann and Smith 2004). FMRIB's ICA-based Xnoiseifier 1.05 (FIX) was used to auto-classify ICA components into "good" (i.e., functional signal) and "bad" (i.e., noise) components (Salimi-Khorshidi et al. 2014). FIX removed unique variance related to "noise" components and motion confounds from the preprocessed fMRI data to denoise the resting state data and to increase the signal-to-noise ratio.

Resting state networks of interest

Group differences and longitudinal changes in functional connectivity were studied using the dual regression method of FSL (previously described in (Filippini et al. 2009)). We used eight standard resting state networks as a reference to study functional connectivity in a standardized way (Khalili-Mahani et al. 2012; Hafkemeijer et al. 2013). Resting state functional connectivity was determined in terms of similarity of the blood oxygenation level dependent (BOLD) fluctuations in the brain in relation to characteristic fluctuations in the eight predefined resting state networks (Beckmann et al. 2005; Damoiseaux et al. 2006).

These standardized resting state networks parcellate the brain into eight templates that represent over 80% of the total brain volume (Khalili-Mahani et al. 2012): network I) calcarine sulcus, precuneal cortex, and primary visual cortex (medial visual network); network II) superior and fusiform areas of lateral occipital cortex (lateral visual network); network III) superior temporal cortex, insular cortex, anterior cingulate cortex, auditory cortex, operculum, somatosensory cortices, thalamus (auditory system network); network IV) precentral and postcentral somatosensory somatomotor areas (sensorimotor system network); network V) rostral medial prefrontal cortex, precuneal cortex, posterior cingulate cortex (default mode network); network VI) medial and inferior prefrontal cortex, anterior cingulate and paracingulate gyri, prefrontal cortex (executive control network); networks VII and VIII) frontal pole, dorsolateral prefrontal cortex, parietal lobule, paracingulate gyrus, posterior cingulate

cortex (dorsal visual stream networks) (for further details, see (Beckmann et al. 2005; Khalili-Mahani et al. 2014), *Fig. 5.2A*). To account for noise, even after FIX, white matter and cerebrospinal fluid templates were included in the analysis (Fox et al. 2005; Cole et al. 2010; Birn 2012).

In the dual regression, individual time series were first extracted for each template, using the eight resting state networks (Beckmann et al. 2005) and the two additional white matter and cerebrospinal fluid maps (Fox et al. 2005; Cole et al. 2010; Birn 2012), in a spatial regression against the individual fMRI data set (regression 1). The resulting matrices described temporal dynamics for each template and individual. Next, the ten temporal regressors were used to fit a linear model to the individual fMRI data set (regression 2), to estimate the spatial maps for each individual. This results in ten 3D images per individual, with voxel-wise z-scores representing the functional connectivity to each of the templates. The higher the absolute value of the z-score, the stronger the connectivity to a network. Here, we studied 1) mean network connectivity (z-score) within the eight resting state networks of interest, and 2) network-to-region connectivity using a more detailed voxel-based analysis.

Mean network connectivity

First, we performed a whole-network analysis to study mean functional connectivity within each network of interest. For each participant, mean functional connectivity (z-score) per network was calculated. *Figure 5.1* shows the statistical analyses that were performed. We studied 1) cross-sectional group differences at baseline (*Fig. 5.1.1*), 2) cross-sectional group differences at follow-up (*Fig. 5.1.2*), 3) longitudinal *changes* in connectivity within groups (i.e., is, within each group, the functional connectivity at follow-up different from that at baseline (delta)?) (*Fig. 5.1.3*), 4) group differences in longitudinal *changes* in connectivity (i.e., are the deltas different between groups?) (*Fig. 5.1.4*).

We used analysis of covariance (ANCOVA; general linear model (GLM) procedure), adjusted for age, gender, and study center, with post hoc Bonferroni adjusted t-tests (IBM SPSS Statistics Version 20, IBM Corp. Somers, NY, USA), to study cross-sectional group differences in mean network connectivity at baseline and at follow-up. To study longitudinal *changes* in mean network connectivity, individual mean z-score per network from the second visit (follow-up) were subtracted from the corresponding

mean z-score from the first visit (baseline). This results in a delta score between the two time points per network for each subject. These delta scores were tested using an ANCOVA, adjusted for age, gender, study center, and network connectivity at baseline, with post hoc Bonferroni adjusted t-tests, to study longitudinal changes in network connectivity within and between groups. Statistical threshold was set at $p < 0.05$ for all statistical tests.

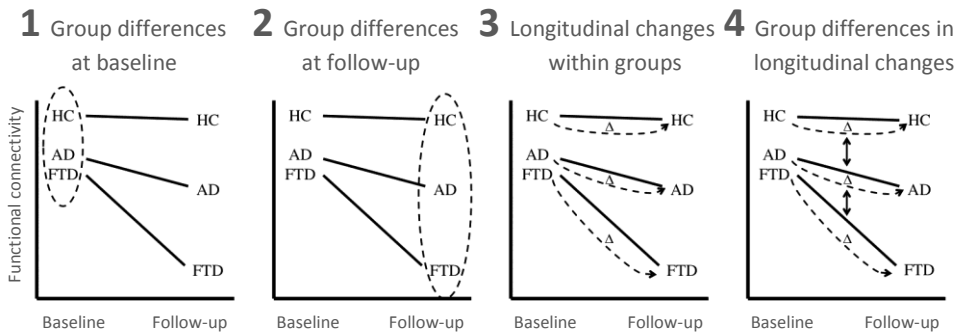


FIGURE 5.1 The four main analyses of this study

This hypothetical model is intended to show the four main analyses performed in the current study. Data points reflect examples of functional connectivity in patients with Alzheimer's disease (AD), patients with behavioral variant frontotemporal dementia (FTD), and healthy controls (HC) at two time points (baseline and follow-up). We have studied 1) cross-sectional group differences at baseline, 2) cross-sectional group differences at follow-up, 3) longitudinal changes within groups (i.e., is functional connectivity at follow-up different from that at baseline (delta)?), 4) group differences in longitudinal changes (i.e., are the deltas different between groups?).

Network-to-region connectivity

In a second, more detailed voxel-based analysis, we studied functional connectivity between resting state networks and localized brain regions. We used a GLM approach, as implemented in FSL, with the same statistical model as used in the mean network connectivity analyses, using F-tests, adjusted for age, gender, and study center, with post hoc t-tests, to study cross-sectional group differences at baseline (*Fig. 5.1.1*) and at follow-up (*Fig. 5.1.2*). To study longitudinal *changes* in network-to-region connectivity, individual functional connectivity maps (parameter estimates) from the second visit (follow-up) were subtracted from the corresponding functional connectivity maps from the first visit (baseline). This results for each subject in a map containing, per network, the differences in functional connectivity between the two time points (delta). These maps were concatenated across subjects into single 4D maps (one per predefined network) and were submitted to voxel-based statistical

testing (F-tests, adjusted for age, gender, and study center, with post hoc t-tests) to study longitudinal changes in network-to-region connectivity within (*Fig. 5.1.3*) and between groups (*Fig. 5.1.4*). Per network, the statistical analyses were masked by the baseline one-sample map from the control group for that network. Voxel-wise non-parametric permutation testing (Nichols and Holmes 2001) with 5000 permutations was performed using FSL-randomise correcting for multiple comparisons across voxels (statistical threshold set at $p < 0.05$, Family-Wise Error (FWE) corrected), using the Threshold-Free Cluster Enhancement (TFCE) technique (Smith and Nichols 2009).

Associations with cognitive performance

In a final analysis, the possible associations between longitudinal changes in cognitive performance (i.e., Mini Mental State Examination (MMSE) score (Folstein et al. 1975) and Frontal Assessment Battery (FAB) scores (Dubois et al. 2000)) and changes in network-to-region connectivity within groups were investigated, using linear regression analyses (IBM SPSS Statistics Version 20, IBM Corp. Somers, NY, USA), adjusted for age, gender, and study center (statistical threshold was set at $p < 0.05$).

5.4. RESULTS

Demographic characteristics

Demographic data for all participants are summarized in *Table 5.1*. There were no differences between patient groups with regard to age at baseline, follow-up time, gender, study center distribution, level of education, and duration of symptoms. As expected, both dementia groups performed worse on cognitive tests compared with controls (all $p < 0.05$). Patients with AD performed worse at follow-up compared with baseline on MMSE ($p = 0.016$) and FAB ($p = 0.049$). In the bvFTD and control group, no significant longitudinal changes in neuropsychological scores were found.

Mean network connectivity

First, we performed a whole-network analysis to study mean network functional connectivity in the eight resting state networks of interest (*Fig. 5.2A*).

At baseline (*Fig. 5.1.1*), we found significant group differences in network VII and VIII. The results of post hoc testing showed lower mean connectivity in these dorsal visual stream networks (which include parietal lobule, paracingulate and posterior cingulate gyrus, and frontal pole) in the AD group compared with the control group ($p = 0.045$ and $p = 0.008$) (*Fig. 5.2B*). No baseline differences in mean network connectivity were found in the bvFTD group.

At follow-up (*Fig. 5.1.2*), significant group differences were found in mean network connectivity in network VII. Post hoc testing showed lower connectivity in this network in AD compared with controls ($p = 0.010$) and in bvFTD compared with controls ($p = 0.012$) (*Fig. 5.2B*).

When longitudinal *changes* in mean network connectivity were studied (*Fig. 5.1.3*), we found decreased mean connectivity in network VIII after the 1.8-year follow-up period in the bvFTD group ($p = 0.021$) (*Fig. 5.2B*). No longitudinal changes in mean network connectivity were found in the AD and control group. When group differences in longitudinal *changes* were studied (*Fig. 5.1.4*), we found with post hoc tests group differences in longitudinal changes in mean network connectivity in network VII between AD and controls ($p = 0.041$), and between bvFTD and controls ($p = 0.043$). The mean connectivity in this network decreased more in AD and bvFTD patients than in controls.

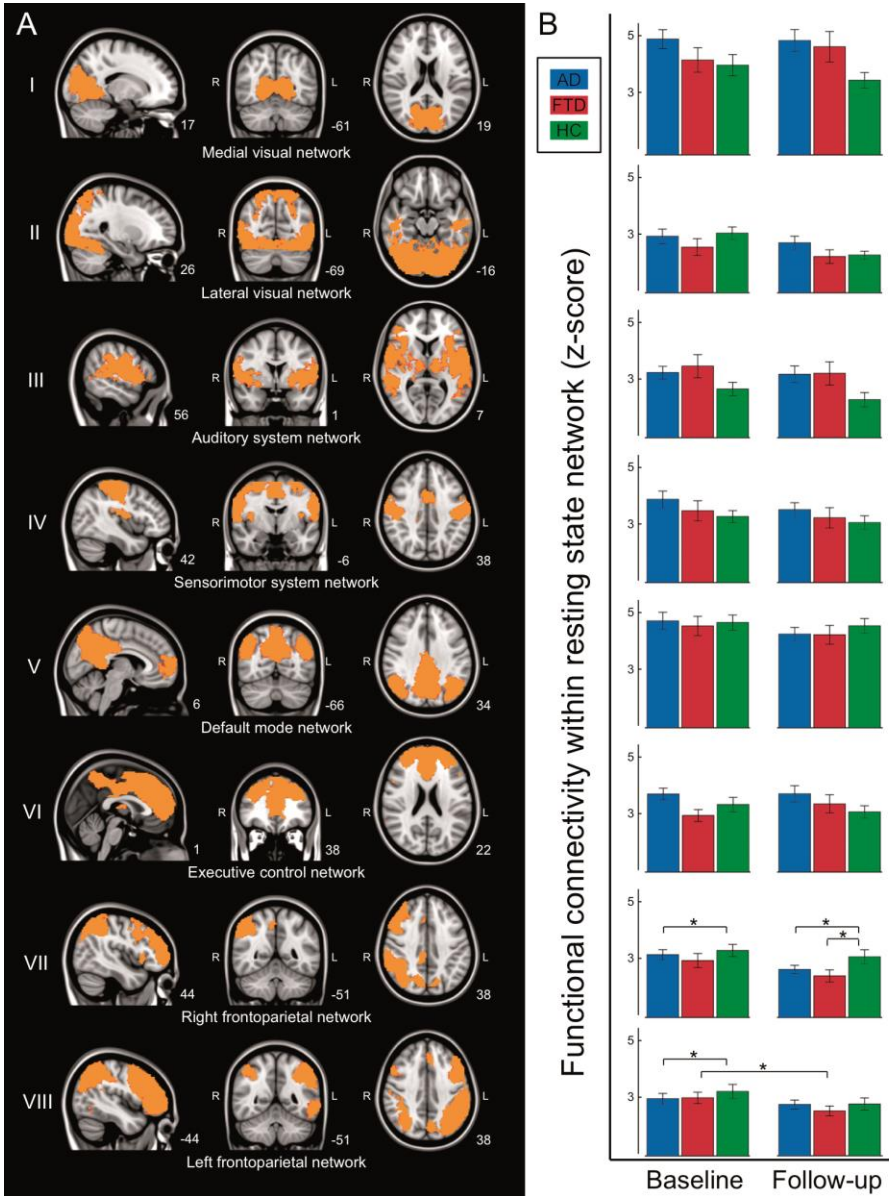


FIGURE 5.2 Mean network connectivity in resting state networks of interest

A) Spatial maps of eight predefined resting state networks of interest. Images are overlaid on the most informative sagittal, coronal, and axial slices of the MNI standard anatomical image (x, y, and z coordinates of each slice are given). Images are displayed following the radiological convention, which means that the left side of the image corresponds to the right hemisphere and vice versa. B) Bar graphs show mean (\pm standard error) functional connectivity within each resting state network for patients with Alzheimer's disease (AD, blue), patients with behavioral variant frontotemporal dementia (FTD, red), and healthy controls (HC, green) both at baseline and follow-up. Asterisks indicate significant group differences or longitudinal changes (post hoc t-tests, adjusted for age, gender, and study center, Bonferroni corrected).

Network-to-region connectivity

In a second, more detailed voxel-based analysis, we studied functional connectivity between the eight resting state networks of interest (*Fig. 5.2A*) and localized brain regions.

At baseline (*Fig. 5.1.1*), we found significant group differences in network-to-region connectivity within three resting state networks: networks I, III, VI (*Fig 5.3A*). The results of post hoc testing showed higher functional connectivity in AD compared with controls between the lingual gyrus and network I (medial visual network), between the central opercular gyrus and network III (somatosensory network), and between the paracingulate gyrus and network VI (executive control network) (*Fig. 5.3A*, AD versus HC, *Table 5.2*). No baseline differences in network-to-region connectivity were found in the bvFTD group.

At follow-up (*Fig. 5.1.2*), significant group differences in network-to-region connectivity were found in five resting state networks: networks I, III, V, VI, VII (*Fig. 5.3B*). Post hoc testing showed that the baseline differences in functional connectivity between AD patients and controls were also present at the 1.8-year follow-up measurement (*Fig. 5.3B*, AD versus HC). Note that the lateralization of the effect in network III at follow-up. This lateralization was not visible in the images that were not corrected for FWE (uncorrected images not shown). The results of post hoc testing showed also group differences that were only present at follow-up: functional connectivity was lower in AD compared with controls between the angular gyrus and network VII (dorsal visual stream network) (*Fig. 5.3B*, AD versus HC), and in bvFTD between the paracingulate gyrus and network V (default mode network), and between the angular gyrus and network VII (dorsal visual stream network) (*Fig. 5.3B*, FTD versus HC, *Table 5.2*). Functional connectivity in bvFTD was lower compared with AD patients between the lateral occipital cortex and network I (medial visual network), and between the anterior cingulate gyrus and network VI (executive control network) (*Fig. 5.3B*, FTD versus AD, *Table 5.2*).

When longitudinal *changes* in network-to-region connectivity were studied (*Fig. 5.1.3*), we found decreased connectivity over time within two networks: network VII and VIII (*Fig. 5.4*). In the AD group, functional connectivity between the precuneus and network VII (dorsal visual stream network) decreased over time (*Fig. 5.4A, and D*). In

the bvFTD group, functional connectivity between the supramarginal gyrus and network VII (dorsal visual stream network), and between the inferior frontal gyrus and network VIII (dorsal visual stream network) decreased over time (*Fig. 5.4B-D*). No longitudinal changes in network-to-region connectivity were found in the control group.

When group differences in longitudinal *changes* were studied (*Fig. 5.1.4*), we found group differences in longitudinal changes in network-to-region connectivity in network VII (*Fig. 5.5*). The results of post hoc testing showed group differences in longitudinal changes in connectivity between the supramarginal gyrus and network VII (dorsal visual stream network) in AD (*Fig. 5.5A*, AD versus HC), and in bvFTD (*Fig. 5.5B*, FTD versus HC) when compared with controls. These small brain clusters show a decrease in functional connectivity over time in both patients groups, and an (insignificant) increase in the control group (*Fig. 5.5C*).

Associations with cognitive performance

Finally, we studied whether the changes in network-to-region connectivity within groups (i.e., decreased connectivity with the precuneus in AD (*Fig. 5.4A*), and with the supramarginal (*Fig. 5.4B*) and inferior frontal gyrus (*Fig. 5.4C*) in bvFTD) were associated with changes in cognitive performance. In AD, no associations between changes in MMSE scores and changes in precuneal connectivity were found ($p = 0.818$). Changes in FAB scores were not associated with changes in supramarginal ($p = 0.565$) and inferior frontal gyrus ($p = 0.821$) connectivity in bvFTD.

Figure legend figure 5.3, page 100

FIGURE 5.3 Group differences in network-to-region connectivity

Cross-sectional group differences in functional connectivity between resting state networks and localized brain regions (full list of structures in Table 5.2). Roman numerals show in which predefined resting state network (*Fig. 5.2A*) group differences were found. A) Post hoc testing showed at baseline higher connectivity in Alzheimer's disease compared with controls (AD versus HC). B) The results of post hoc testing showed that the baseline differences were also present at 1.8-year follow-up measurement (AD versus HC). At follow-up, functional connectivity was lower in behavioral variant frontotemporal dementia compared with controls (FTD versus HC), and compared with AD patients (FTD versus AD). F-tests did not show at baseline group differences in networks I, V, VI, VII, which is for illustration purposes illustrated by brains without colored voxels. P values are color coded from 0.05 FWE corrected (red) to < 0.0001 FWE corrected (yellow). Images are overlaid on the sagittal, coronal, and transverse slices of the MNI standard anatomical image (x , y , and z coordinates of each slice are given). Images are displayed following the radiological convention, which means that the left side of the image corresponds to the right hemisphere and vice versa.

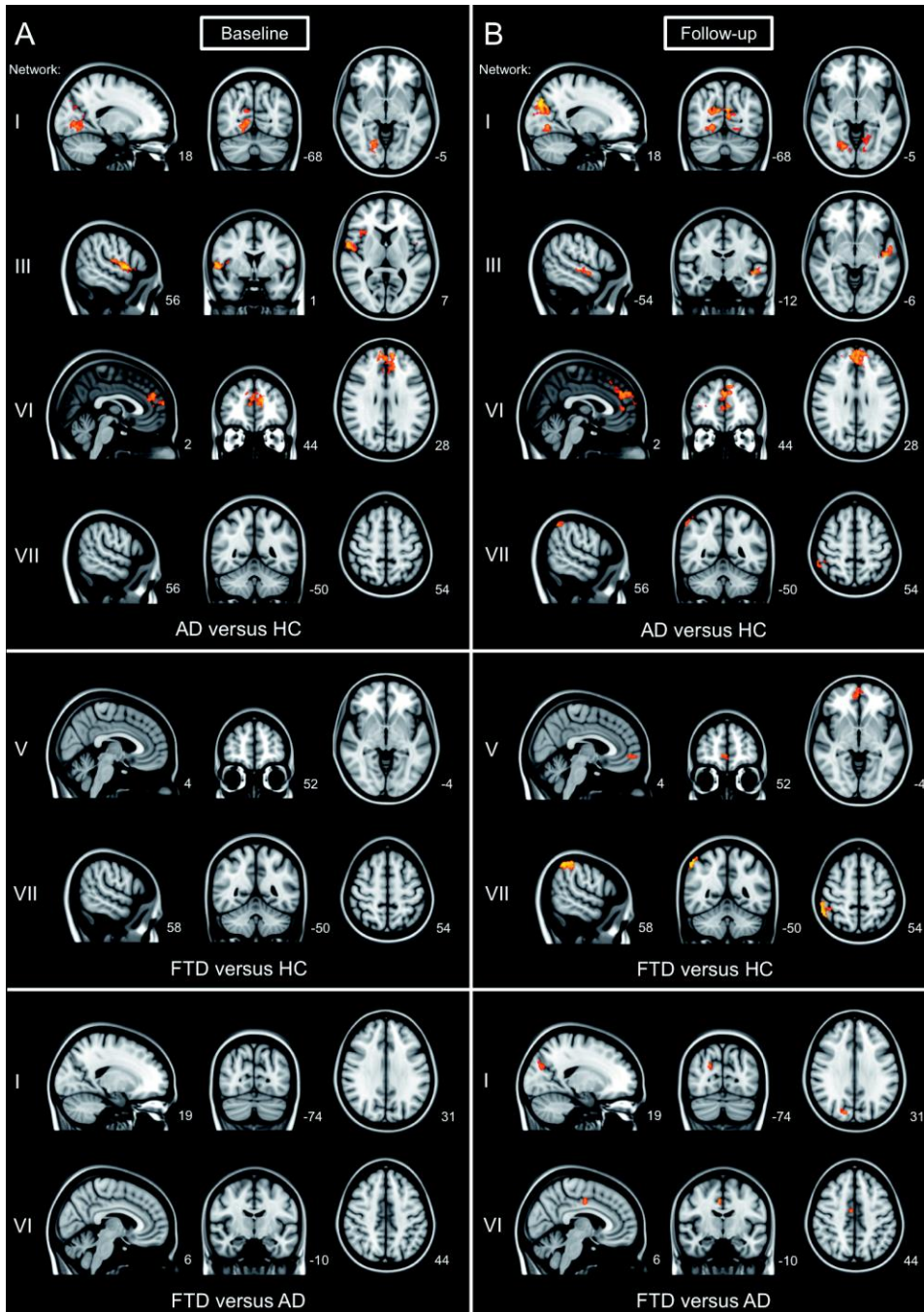


FIGURE 5.3 Group differences in network-to-region connectivity

Cross-sectional group differences in functional connectivity between resting state networks and localized brain regions (full list of structures in Table 5.2). See bottom of page 99 for complete figure legend.

TABLE 5.2 Group differences in network-to-region connectivity

Network and contrast	Brain structure ^a	Side	Peak voxel coordinates (MNI)			Peak T score
			x	y	z	
Group differences at baseline						
Medial visual network (I) AD > HC	Lingual gyrus	R	10	-74	0	4.32
Auditory system network (III) AD > HC	Central opercular cortex	R	56	4	2	4.51
Executive control network (VI) AD > HC	Paracingulate gyrus	L	-12	44	18	4.23
Group differences at follow-up						
Medial visual network (I) AD > HC	Lingual gyrus	R	18	-70	-4	4.82
	Cuneal cortex	R	18	-80	28	3.87
Auditory system network (III) AD > HC	Planum polare	L	-48	-14	-4	5.24
Executive control network (VI) AD > HC	Paracingulate gyrus	R	6	50	26	4.08
Dorsal visual stream right (VII) AD < HC	Angular gyrus	R	58	-52	50	4.54
Default mode network (V) bvFTD < HC	Paracingulate gyrus	R	10	52	-4	4.48
Dorsal visual stream right (VII) bvFTD < HC	Angular gyrus	R	56	-52	48	4.47
Medial visual network (I) bvFTD < AD	Lateral occipital cortex	R	24	-72	28	4.50
	Lateral occipital cortex	L	-18	-82	26	3.72
Executive control network (VI) bvFTD < AD	Anterior cingulate gyrus	R	6	-10	38	4.61
	Anterior cingulate gyrus	L	-12	-2	38	3.97

Abbreviations: MNI = Montreal Neurological Institute standard space image; AD = Alzheimer's disease; HC = healthy controls; bvFTD = behavioral variant frontotemporal dementia; R = right; L = left.

^aFull list of structures with group differences in network-to-region connectivity (Fig. 5.3). Between group effects are independent of physiological noise, age, gender, and study center. Thresholding using $p < 0.05$, FWE corrected, based on the TFCE statistic image. For each peak voxel x-, y-, and z-coordinates in the MNI standard space image are given.

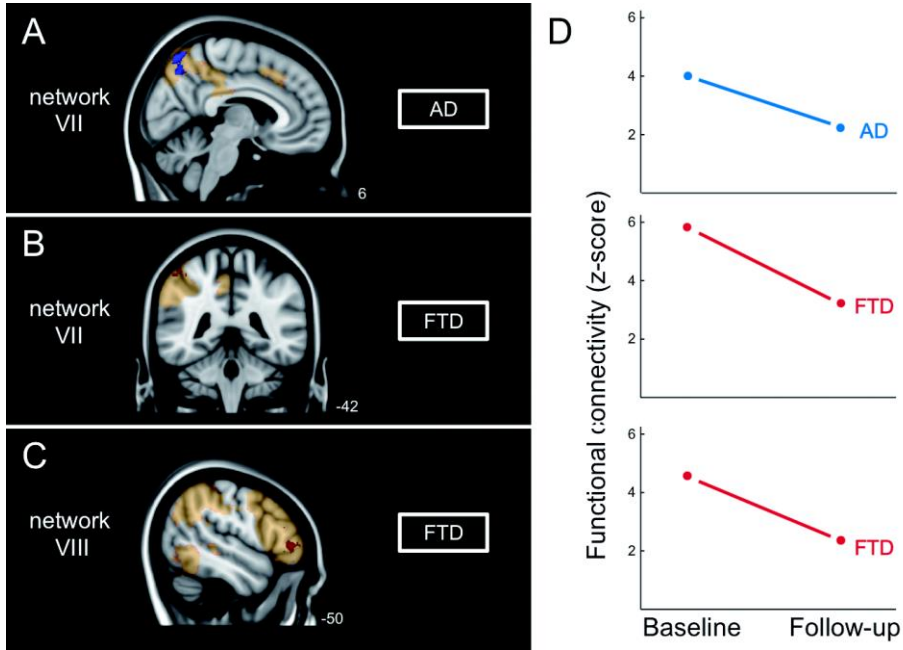


FIGURE 5.4 Longitudinal changes in network-to-region connectivity within a group

Longitudinal changes in functional connectivity between dorsal visual stream networks (indicated in light orange and by roman numerals) and A) precuneus in Alzheimer’s disease (AD, blue), B) supramarginal gyrus, and C) inferior frontal gyrus in behavioral variant frontotemporal dementia (FTD, red). Images are overlaid on the MNI standard anatomical image (coordinates of each slice are given). Images are displayed following the radiological convention, which means that the left side of the image corresponds to the right hemisphere and vice versa. D) Graphs are included to show the directionality of the effects. This shows decreased longitudinal functional connectivity in AD (blue) and FTD (red).

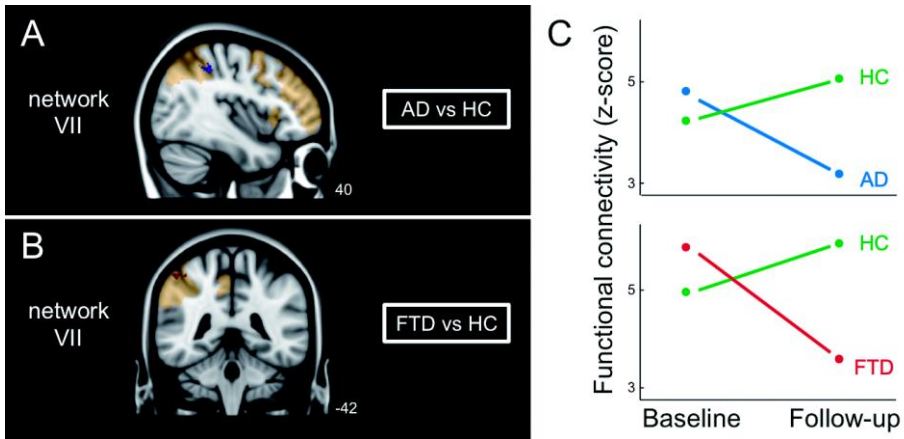


FIGURE 5.5 Group differences in longitudinal changes in network-to-region connectivity

Group differences in longitudinal changes in functional connectivity between the right dorsal visual stream network (indicated in light orange and by roman numerals) and A) the supramarginal gyrus in patients with Alzheimer’s disease (AD, blue), and B) the supramarginal gyrus in patients with behavioral variant frontotemporal dementia (FTD, red) compared with healthy controls (HC). Images are overlaid on the MNI standard anatomical image (coordinates of each slice are given). Images are displayed following the radiological convention, which means that the left side of the image corresponds to the right hemisphere and vice versa. C) Graphs are included to show the directionality of the effects. This shows group differences in changes in functional connectivity in patients with AD (blue) and in patients with FTD (red) compared with healthy controls (HC, green). The increase in functional connectivity over time in the healthy control group was not significant.

5.5. DISCUSSION

In this longitudinal study on resting state fMRI data in AD and bvFTD, we used whole-network and network-to-region analyses to study group differences in functional connectivity at baseline and at 1.8-year follow-up measurement, and *changes* in functional connectivity over time. We found disease-specific brain regions with longitudinal changes in functional connectivity in AD and bvFTD. Over time, precuneal connectivity decreased in AD, whereas in bvFTD inferior frontal gyrus connectivity decreased.

Our results suggest the potential of longitudinal resting state fMRI to delineate regions relevant for disease progression and for diagnostic accuracy, although the direct comparison between our relatively small AD and bvFTD groups did not yield significant group differences in longitudinal changes. Further studies, with larger patient groups, a longer follow-up time, and with more disease progression and neuropsychological decline, may give additional valuable information for disease progression and differential diagnosis.

This is the first study that investigates longitudinal *changes* in functional connectivity in both bvFTD and AD. In bvFTD, we found with the whole-network analysis decreasing longitudinal functional connectivity in the dorsal visual stream network that encompassed frontal pole, dorsolateral prefrontal cortex, parietal lobe, paracingulate gyrus, and posterior cingulate cortex. In more detail, the network-to-region analysis showed decreased longitudinal connectivity between this network and the inferior frontal gyrus. Cross-sectional differences in functional connectivity of the inferior frontal gyrus have been found between bvFTD and controls (Rytty et al. 2013).

Furthermore, longitudinal connectivity between the supramarginal gyrus and the dorsal visual stream network was decreased over time in bvFTD. The exact role of the supramarginal gyrus in the behavior of bvFTD is not clear. It has been shown that this brain area plays a crucial role in empathy (Silani et al. 2013), and gray matter atrophy in the supramarginal gyrus has been reported in bvFTD (Lillo et al. 2012), but is also common in AD (Seeley et al. 2009). In the present study, we found that the longitudinal changes in the supramarginal gyrus in both bvFTD and AD were significantly different from those in control participants.

In AD, we found decreased longitudinal functional connectivity between the precuneus and the dorsal visual stream network. The precuneus is particularly vulnerable for AD pathology, including gray matter atrophy and amyloid pathology (Buckner et al. 2005; Jack et al. 2010). Our finding is in line with the observation of decreasing longitudinal connectivity in the precuneus in AD (Damoiseaux et al. 2012).

In addition to longitudinal changes, we reported cross-sectional group differences at two time points. At baseline, we found higher functional connectivity in AD compared with controls, with the most prominent group differences in the lingual gyrus, cuneal cortex, and paracingulate gyrus. These findings are in line with the observation of higher functional connectivity in the lingual gyrus and cuneal cortex in AD (He et al. 2007; Wang et al. 2007), although not consistently observed (Greicius et al. 2004; Zhou et al. 2010). In the present study, we were able to replicate our baseline findings 1.8 years later at the follow-up measurement. Visual inspection shows more extended group differences at the follow-up measurement, suggesting longitudinal changes in functional connectivity, however, these were not significant.

In bvFTD, we observed lower functional connectivity compared with controls in the paracingulate and angular gyrus. These findings were comparable with a study that found differences in these functional connections when comparing patients with bvFTD and controls (Rytty et al. 2013). In our study, we found these group differences only at follow-up, not at baseline. The inability to find baseline group differences in bvFTD is most likely related to less statistical power due to the relatively small number of subjects that was included in the bvFTD group. Another potential explanation is that we included less severely affected bvFTD patients, since we only included patients with scans available at both time points (baseline and follow-up). As a consequence, no data were available for the more severely affected subjects that dropped out of the study prematurely.

The most prominent finding in the direct cross-sectional comparison of AD and bvFTD is the lower functional connectivity in the anterior cingulate cortex in bvFTD compared with AD at the follow-up measurement. The anterior cingulate cortex is identified as a region that is among the first affected brain regions in bvFTD (Seeley et al. 2008; Dopper et al. 2014). The deficits in social-emotional functions, which are common in bvFTD, rely on structures including the anterior cingulate cortex and frontoinsula

(Rosen et al. 2002; Broe et al. 2003). Gray matter atrophy in these structures has shown to be more severe in bvFTD than in AD (Rabinovici et al. 2008). Cross-sectional group differences in the anterior cingulate cortex are observed as well in the two other resting state fMRI studies that performed the direct comparison of functional connectivity between patients with bvFTD and AD (Zhou et al. 2010; Filippi et al. 2013).

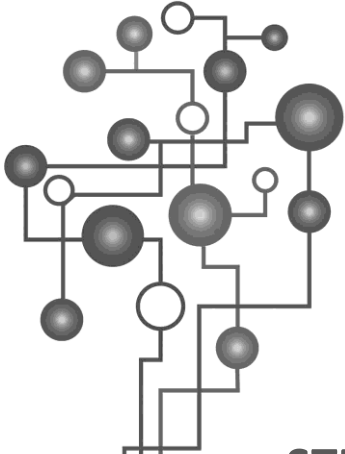
As expected, both dementia groups performed worse on cognitive functioning compared with controls. Patients with AD showed lowest scores on MMSE, which is a general measurement of cognitive performance (Folstein et al. 1975), with, as expected, a decline in MMSE score over time. Lowest FAB scores, a general measurement of executive functioning, were found in the bvFTD group. We found a decline in FAB scores in the AD group; however, we expected this decline in the bvFTD group. Overall, the AD patients showed low scores in all cognitive domains, not only in the memory domain, but also in executive functioning. Although executive functioning could be useful to differentiate AD from bvFTD (Iavarone et al. 2004; Slachevsky et al. 2004), some studies reported that executive functioning, measured with FAB, does not discriminate AD from bvFTD patients (Lipton et al. 2005; Castiglioni et al. 2006). It has been suggested that testing multiple cognitive domains is required to differentiate both types of dementia rather than focus on one cognitive test (Lipton et al. 2005). In the current study, all patients underwent extensive neuropsychological assessment. Diagnoses were established according to the core clinical criteria for probable AD (McKhann 2011) and for bvFTD (Rascovsky et al. 2011) and therefore were not based on one single neuropsychological test score.

The diagnosis FTD or AD can only be confirmed by postmortem brain autopsy after death. A limitation of our study is that postmortem data were not available, therefore the possibility of misdiagnosis of the patients cannot be excluded. Nevertheless, all patients underwent an extensive dementia screening and were evaluated in a multidisciplinary panel including clinicians from different centers specialized in dementia. Only dementia patients that fulfilled the most recent clinical criteria for probable AD (McKhann 2011) and bvFTD (Rascovsky et al. 2011) were included in the present study. Another limitation of our study is the relatively small number of subjects that was included in the bvFTD group. Further studies, with larger patient groups and more disease progression and neuropsychological decline, may give additional valuable information.

This longitudinal study showed data that were collected in two centers. The main strength of multicenter studies is the increased generalizability of the study findings. However, multicenter studies have also its limitations, since the data will be less homogeneous than in single center studies. To increase homogeneity between centers in the current study, we evaluated all patients in a multidisciplinary panel including clinicians from different centers specialized in dementia, we used a standardization approach in order to achieve better comparison across voxels, subjects, and centers (Yan et al. 2013), and we added center as covariate in all statistical models, following previous approaches (Kim et al. 2009; Zhou et al. 2010).

5.5.1. CONCLUSION

To conclude, we used longitudinal resting state fMRI data of patients with AD and patients with bvFTD and found disease-specific brain regions with longitudinal connectivity changes. Over time, precuneal functional connectivity decreased in AD, and inferior frontal gyrus connectivity decreased in bvFTD. This suggests the potential of longitudinal resting state fMRI to delineate regions relevant for disease progression and for diagnostic accuracy, although we did not find group differences in longitudinal changes in the direct comparison of AD and bvFTD patients.



SECTION 2

STRUCTURAL BRAIN NETWORKS

Chapter 6

Associations between age and gray matter volume in anatomical brain networks in middle-aged to older adults

Anne Hafkemeijer, Irmhild Altmann-Schneider, Ton de Craen,
Eline Slagboom, Jeroen van der Grond, and Serge Rombouts



6.1. ABSTRACT

Aging is associated with cognitive decline, diminished brain function, regional brain atrophy, and disrupted structural and functional brain connectivity. Understanding brain networks in aging is essential, as brain function depends on large-scale distributed networks. Little is known of structural covariance networks to study inter-regional gray matter anatomical associations in aging.

Here, we investigate anatomical brain networks based on structural covariance of gray matter volume among 370 middle-aged to older adults of 45-85 years. For each of the 370 subjects, we acquired a T1-weighted anatomical magnetic resonance imaging (MRI) scan. After segmentation of structural MRI scans, nine anatomical networks were defined based on structural covariance of gray matter volume among subjects. We analyzed associations between age and gray matter volume in anatomical networks using linear regression analyses.

Age was negatively associated with gray matter volume in four anatomical networks ($p < 0.001$, corrected): a subcortical network, sensorimotor network, posterior cingulate network, and an anterior cingulate network. Age was not significantly associated with gray matter volume in five networks: temporal network, auditory network, and three cerebellar networks. These results were independent of gender and white matter hyperintensities.

Gray matter volume decreases with age in networks containing subcortical structures, sensorimotor structures, posterior, and anterior cingulate cortices. Gray matter volume in temporal, auditory, and cerebellar networks remain relatively unaffected with advancing age.

6.2. INTRODUCTION

It is well recognized that the process of aging is associated with cognitive decline and diminished brain function (Grady 2012). In addition, numerous neuroimaging studies have unequivocally shown that aging is associated with loss of brain tissue, in which process especially the gray matter seems affected. Volumetric and morphometric neuroimaging studies have demonstrated a consistent age-dependent decrease in regional gray matter volume, mainly expressed in the temporal lobe and hippocampus, the cingulate cortex, and prefrontal regions (Good et al. 2001; Jernigan et al. 2001; Resnick et al. 2003; Raz et al. 2005).

There is increasing evidence that, in addition to brain atrophy, aging and loss of cognitive function at high ages is associated with disrupted structural and functional brain connectivity. It has been shown that functional connectivity decreases with age, especially connectivity in the default mode network between the medial prefrontal cortex, anterior and posterior cingulate cortex, precuneus, parietal cortex, and hippocampus (Damoiseaux et al. 2008; Hafkemeijer, van der Grond, and Rombouts 2012; Ferreira and Busatto 2013). Furthermore, aging is associated with disrupted white matter anatomical connections, specifically in the frontal white matter, anterior cingulum, and the genu of the corpus callosum (Salat et al. 2005; Madden et al. 2012).

In addition to functional brain networks and white matter anatomical connectivity, population (intersubject) covariance of gray matter volume can be used to study inter-regional anatomical associations (Alexander-Bloch et al. 2013). The integrity of these gray matter structural covariance networks change throughout lifespan (Wu et al. 2012, 2013). Here, we will investigate the integrity of gray matter anatomical networks in the aging brain. In this respect, mainly the structural covariance of the default mode network has been studied, showing a breakdown with increasing age (Spreng and Turner 2013). While most studies focused on the default mode network, there is evidence for age-dependent decreases in other anatomical networks (Montembeault et al. 2012; Segall et al. 2012; Li et al. 2013).

Currently, anatomical networks are mostly studied using a model-driven seed-based approach with a priori hypotheses of manually selected regions of interest and their connected networks (Montembeault et al. 2012; Zielinski et al. 2012; Li et al. 2013; Soriano-Mas et al. 2013). The manual selection of regions of interest might introduce a

selection bias (Damoiseaux and Greicius 2009). To avoid this, we will use a model-free method to investigate whole-brain anatomical networks in an unrestricted exploratory way. This method has proven to be a powerful tool to characterize structural networks in schizophrenia (Xu et al. 2009). Here, we will apply this method to study gray matter anatomical networks in middle-aged to older adults.

In the present study, we explored anatomical networks in a large group of middle-aged to older adults (45 - 85 years, $n = 370$). Our aim was to investigate whole-brain anatomical networks to explore which networks are associated with the process of healthy aging and which networks do not show an age association.

6.3. RESULTS

Demographic characteristics

We analyzed structural magnetic resonance imaging (MRI) scans of in total 370 middle-aged to older participants aged between 45.5 and 84.3 years (mean age 65.7 ± 6.7 years). The cohort was nearly balanced on gender (192 women, 51.9 %), with similar age distributions across genders. The study population has been described in more detail elsewhere (Altmann-Schneider et al. 2013).

The total study population was divided in four age subgroups: 1) 45-55 years, mean age = 51.4 ± 2.3 years, $n = 26$, 18 women, 2) 55-65 years, mean age = 61.5 ± 2.4 years, $n = 145$, 83 women, 3) 65-75 years, mean age = 69.3 ± 2.7 years, $n = 171$, 83 women, and 4) 75-85 years, mean age = 78.0 ± 2.6 years, $n = 28$, 8 women. White matter hyperintensities (WMHs) were defined as areas within the cerebral white matter with increased signal intensity. Mean volume of WMHs was 1.93 mL for the total study population (0.81 mL (45-55 years), 1.25 mL (55-65 years), 1.93 mL (65-75 years), 5.99 mL (75-85 years)).

Gray matter anatomical brain networks

After segmentation of structural MRI scans, gray matter images were used to define nine anatomical brain networks based on the covariation of gray matter volumes among the middle-aged to older adults (*Fig. 6.1A*). Brain structures of the networks were identified using the Harvard-Oxford atlas integrated in Functional Magnetic Resonance Imaging of the Brain Software Library (FSL) (*Table 6.1*).

Aging

To analyze the possible association between age and gray matter volume in anatomical networks, we used a linear regression analysis based on four age subgroups (45-55, 55-65, 65-75, 75-85 years). To statistically account for the possible influences of gender, family characteristics (i.e., offspring of long-lived parents or nonoffspring), and volumes of WMHs, these factors were used as independent factors in the linear regression model. The age association of gray matter volume in anatomical networks is illustrated in *Figure 6.1B* (this figure shows the networks in order of age association, with the first network showing the strongest association with age).

Age showed a negative association with gray matter volume in four networks (*Fig. 6.1a-d*). These networks included 1) thalamus, nucleus accumbens, caudate nucleus, hippocampus, and lingual gyrus (network a in *Fig. 6.1* and *Table 6.1*, $p < 0.0001$, $R^2 = 0.291$, Beta = -0.510), 2) lateral occipital cortex and precuneus (network b in *Fig. 6.1* and *Table 6.1*, $p < 0.0001$, $R^2 = 0.257$, Beta = -0.255), 3) posterior cingulate cortex, paracingulate gyrus, subcallosal cortex, and operculum cortex (network c in *Fig. 6.1* and *Table 6.1*, $p < 0.0001$, $R^2 = 0.158$, Beta = -0.347), and 4) anterior cingulate cortex, middle frontal gyrus, and frontal medial cortex (network d in *Fig. 6.1* and *Table 6.1*, $p = 0.0004$, $R^2 = 0.150$, Beta = -0.186).

Age was not significantly associated with gray matter volume in five networks (*Fig. 6.1e-i*). These networks included 1) temporal pole and temporal fusiform cortex (network e in *Fig. 6.1* and *Table 6.1*, $p = 0.0038$, $R^2 = 0.085$, Beta = -0.157), 2) putamen, caudate nucleus, and superior parietal lobule (network f in *Fig. 6.1* and *Table 6.1*, $p = 0.0137$, $R^2 = 0.083$, Beta = -0.134), and 3-5) three cerebellar networks (network g in *Fig. 6.1* and *Table 6.1*, $p = 0.1709$, $R^2 = 0.078$, Beta = -0.074; network h in *Fig. 6.1* and *Table 6.1*, $p = 0.3496$, $R^2 = 0.020$, Beta = -0.052; network i in *Fig. 6.1* and *Table 6.1*, $p = 0.1233$, $R^2 = 0.030$, Beta = 0.086).

Longevity

All subjects were included from the Leiden Longevity Study, which was set up to identify genetic and phenotypic markers related to longevity (Altmann-Schneider et al. 2013). The study cohort consists of offspring of long-lived siblings and their partners (194 offspring and 176 partners). The offspring was characterized by having long-lived parents (with male parents aged ≥ 89 years and female parents aged ≥ 91 years). No significant differences in association between age and the gray matter volume in the anatomical networks were found between offspring of long-lived parents and nonoffspring participants.

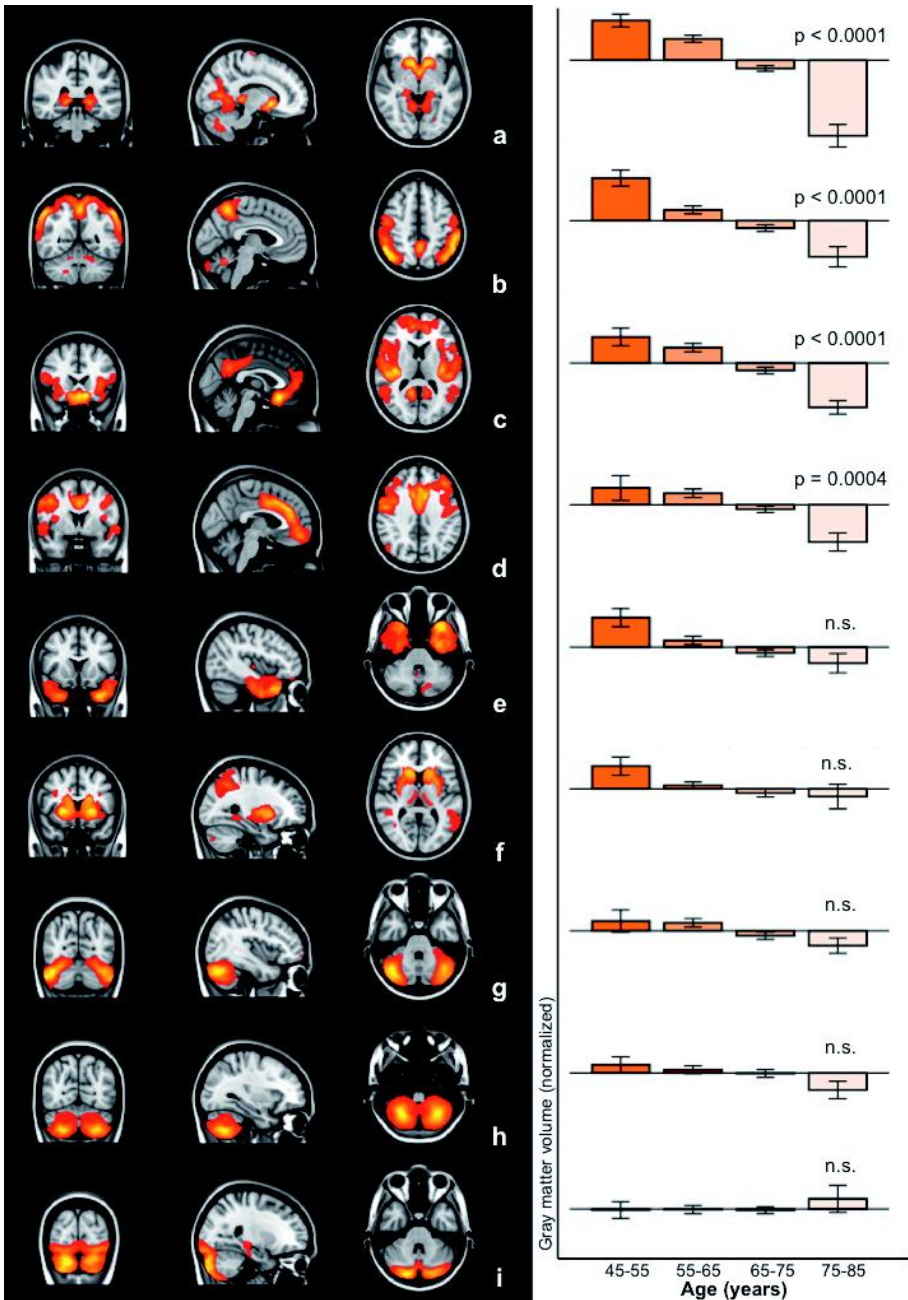


FIGURE 6.1 Gray matter structural networks and associations with age

A) Overview of the nine anatomical networks based on the covariation of gray matter volumes among middle-aged to older adults. Networks are overlaid on the most informative coronal, sagittal, and transverse slices of the MNI standard anatomical image. B) The association between age and gray matter volume in the anatomical networks is illustrated by bar graphs (\pm standard error of the mean). Age was negatively associated with anatomical networks a-d, and was not significantly associated with networks e-i.

TABLE 6.1 Brain clusters of anatomical brain networks

	Brain cluster ^a	Cluster volume (cm ³)	MNI coordinates		
			x	y	z
Network a	Thalamus cluster also contains nucleus accumbens, caudate nucleus, hippocampus, lingual gyrus, and cerebellum	17.90	-2	-2	-8
	(Postcentral gyrus)	1.03	52	-8	32
	(Precentral gyrus)	0.89	-20	-18	70
	(Heschl's gyrus)	0.41	-50	-26	10
Network b	Lateral occipital cortex cluster also contains precuneus, and supramarginal gyrus	36.76	50	-62	44
	Cerebellum	3.17	-18	-72	-34
Network c	Posterior cingulate cortex cluster also contains paracingulate gyrus subcallosal cortex, operculum cortex, and precuneus	56.75	-8	22	-16
	Middle temporal gyrus	6.32	56	-48	8
	(Occipital fusiform gyrus)	0.42	26	-74	-14
	Lateral occipital cortex	0.28	-40	-72	26
Network d	Anterior cingulate cortex cluster also contains middle frontal gyrus precentral gyrus, and frontal medial cortex	36.81	-2	32	28
	(Cerebellum)	3.06	-20	-80	-44
	(Lateral occipital cortex)	2.47	50	-74	26
	(Temporal pole)	1.56	-58	6	-2
	(Cuneus)	0.84	12	-68	24
	(Precuneus)	0.68	-14	-62	22
Network e	Temporal pole cluster also contains temporal fusiform cortex	29.04	-32	22	-38
	(Cerebellum)	2.59	-12	-74	-30
	(Anterior cingulate cortex)	1.57	10	-12	44

TABLE 6.1 continued

Brain cluster ^a		Cluster volume (cm ³)	MNI coordinates x y z		
Network f	Putamen	18.74	24	14	0
	cluster also contains caudate nucleus, and insular cortex				
	Superior parietal lobule	10.40	34	-48	38
	cluster also contains lateral occipital cortex, and (precuneus)				
	(Cerebellum)	5.37	-6	-66	-16
	Angular gyrus	5.35	-44	-58	20
Network g	Cerebellum	24.35	42	-68	-32
	(Frontal pole)	0.41	52	34	-6
Network h	Cerebellum	30.43	26	-64	-52
	(Middle frontal gyrus)	0.57	-50	28	24
	(Precuneus)	0.90	20	-58	20
Network i	Cerebellum	25.18	18	-86	-36
	Hippocampus	0.49	24	-24	-8
	(Postcentral gyrus)	0.49	-40	-30	40
	(Frontal pole)	0.28	8	64	12

Abbreviation: MNI = Montreal Neurological Institute standard space image

^aEach gray matter anatomical network is divided in brain clusters using the cluster tool integrated in FSL. Cluster size and MNI x-, y-, and z-coordinates of each cluster are given. Brain structures are anatomically identified using the Harvard-Oxford atlas integrated in FSL. Figure 6.1 shows the most informative coronal, sagittal, and transverse slices. Structures in parentheses in the table are not visible in Figure 6.1.

6.4. DISCUSSION

We identified anatomical brain networks based on structural covariance of gray matter volume in a large sample of healthy participants aged between 45 and 85 years. Our aim was to investigate whole-brain anatomical networks to explore which networks are associated with the process of healthy aging and which networks do not show an age association. In summary, by doing a cross-sectional analysis, we found gray matter volume decreases with age in four networks containing predominantly subcortical structures, lateral occipital, posterior, and anterior cingulate cortices. The gray matter in five networks containing the temporal pole, putamen, and cerebellum remained relatively unaffected with advancing age.

The greatest associations with age were found in an anatomical network containing among other structures the thalamus, nucleus accumbens, caudate nucleus, and hippocampus (network a). It is well recognized that subcortical structures are vulnerable to atrophy with advancing age (Jernigan et al. 2001; Raz et al. 2005). Additionally, network studies have shown age-dependent relationships between these structures (Brickman et al. 2007; Bergfield et al. 2010; Soriano-Mas et al. 2013).

We found associations between age and the gray matter volume in the lateral occipital network (network b). Evidence for age associations of gray matter volume in this anatomical network is supported by others (Montembeault et al. 2012; Li et al. 2013). Montembeault and colleagues found reduced structural associations between occipital regions and the temporal pole (Montembeault et al. 2012). That finding is consistent with disrupted white matter anatomical connections between occipital and temporal areas in elderly (Kantarci et al. 2011). It has been suggested that these age-related reduced structural associations may explain the decline in language-related semantics in elderly (Montembeault et al. 2012).

In general, gray matter anatomical networks and resting state functional connectivity networks spatially overlap (Seeley et al. 2009; Segall et al. 2012) and reflect regions that co-degenerate in several neurodegenerative syndromes (Seeley et al. 2009). Our study also shows spatial overlap between the structures of anatomical networks and resting state functional connectivity networks found in other studies (Beckmann et al. 2005; Damoiseaux et al. 2006; Laird et al. 2011). Visual inspection shows spatial overlap between network a and the medial visual cortical functional connectivity

network, network b and sensorimotor functional connectivity network, network c and default mode network, network d and executive control network, network e and medial temporal functional connectivity network, and network f and the auditory functional connectivity network. The cerebellum (network g, h, and i) is less frequently studied with functional connectivity.

The association with age we found in the posterior cingulate anatomical network (network c) is consistent with a recent study that showed that this anatomical network changes with age in healthy and pathological aging (Spreng and Turner 2013). Visual inspection of our data showed spatial overlap between the structures of this anatomical network and the default mode functional connectivity network found in other studies (Beckmann et al. 2005; Damoiseaux et al. 2006; Laird et al. 2011). The default mode network is affected by age-related atrophy (Buckner et al. 2008) and age-related decreases in functional connectivity (Damoiseaux et al. 2008; Hafkemeijer, van der Grond, and Rombouts 2012; Ferreira and Busatto 2013).

The anatomical network containing predominantly the anterior cingulate cortex (network d) shows spatial overlap with a functional connectivity network associated with executive control functions (Beckmann et al. 2005; Damoiseaux et al. 2006; Laird et al. 2011). The associations between age and gray matter volume in this network is supported by other anatomical network studies (Bergfield et al. 2010; Montembeault et al. 2012). It has been suggested that the age-dependent breakdown of this network may explain the difficulties in cognitively demanding tasks generally observed in elderly (Montembeault et al. 2012).

Prior studies mostly focused on age-related differences in the aging brain. Relatively few studies have sought to identify anatomical networks that were not associated with age. Functional connectivity in somatosensory and cerebellar networks, do not show an association with advancing age (Tomasi and Volkow 2012). Here, we showed that gray matter volume in five anatomical networks, predominantly containing the temporal pole (network e), putamen (network f), and cerebellum (networks g, h, and i), was not associated with age. The lack of age associations in these five networks is in line with an anatomical network study in healthy elderly (Bergfield et al. 2010). Others have shown that the temporal areas, putamen, and cerebellum are less susceptible to age-related differences in both gray matter volume and metabolism (Kalpouzos et al.

2009). However, age-related differences in the temporal anatomical network are frequently reported (Alexander et al. 2006; Brickman et al. 2007; Montembeault et al. 2012), which makes preservation of this network more unlikely. In this study, we found a nonsignificant trend towards age-related gray matter volume loss in the temporal network (network e). Further research is highly recommended to investigate the association between age and the gray matter volume in the temporal anatomical network.

Here, we studied whole-brain anatomical networks. The method used in the current study examines the inter-regional anatomical relationship among spatially distributed brain structures as networks of connected regions. This approach showed associations between age and gray matter networks containing brain areas that were found earlier in several other studies exploring regional (non-network) gray matter differences. This suggests a high sensitivity of the network approach used in our study. However, this interpretation should be taken with caution, given the lack of direct comparisons between non-network and network studies and given the differences in statistical correction for multiple comparisons (i.e., network studies should correct for multiple networks, whereas regional non-network studies are forced to use a more stringent voxelwise correction for multiple comparisons).

In this study, we used the ICA method to determine anatomical networks based on the covariation of gray matter volumes among all 370 middle-aged to older adults. The age associations reported in our study might be influenced by the fact that the anatomical networks are based on the total study population of middle-aged to older adults. Although much can be learned from the age associations found in our study, a limitation of this cross-sectional study is that the participants were not followed over time. A longitudinal design is required to study changes in individual brain structure as aging occurs.

Another limitation is that the number of components to estimate (i.e., anatomical networks) is arbitrarily chosen. The topic of choosing the number of components and the effect of the dimensionality on the statistical results is currently an active area of research. There is no consensus on the optimal number of components (Cole et al. 2010), which may vary depending on the data and the research question. In the current study, we decided to use a dimensionality within the range of the most often

applied dimensionality in studies of brain networks, that is use eight to ten components (Beckmann et al. 2005; Damoiseaux et al. 2006; Smith et al. 2009; Segall et al. 2012; Zielinski et al. 2012). However, it is important to note that varying the dimensionality may affect the sensitivity to detect regional effects and may impact the findings of this study.

6.4.1. CONCLUSION

Overall, we showed that regionally separate gray matter regions are organized in anatomical networks. We gave an overview of associations between age and the gray matter volume in these networks. Elderly show a decline in gray matter volume in networks containing subcortical structures, lateral occipital, posterior, and anterior cingulate cortices. Anatomical networks containing the temporal pole, putamen, and cerebellum remain relatively unaffected with advancing age. The current work supports the application of gray matter structural network analysis to evaluate inter-regional anatomical relationships among spatially distributed brain structures in the aging brain. Additionally, this approach may also be useful in distinguishing the effects of age-related neurodegenerative disease from healthy aging.

6.5. MATERIALS AND METHODS

Participants

In total, 370 subjects aged between 45 and 85 years were included from the Leiden Longevity Study, which was set up to identify genetic and phenotypic markers related to longevity (Altmann-Schneider et al. 2013). For the current study, the offspring of long-lived siblings and their partners were included (194 offspring and 176 partners). The offspring is characterized by having long-lived parents (with male parents aged ≥ 89 years and female parents aged ≥ 91 years). The cohort is nearly balanced on gender (192 females, 51.9 %), with similar age distributions across genders.

All subjects underwent an extensive medical screening. Cognitive functioning was assessed by a neuropsychological protocol. The participants did not demonstrate any abnormalities on neuropsychological evaluation (Mini Mental State Examination score > 28 , Geriatric Depression Scale-15 score < 6) and did not have a history of psychiatric or neurodegenerative disorders. In accordance with the Declaration of Helsinki, written informed consent from all participants was obtained. The Medical Ethical Committee of the Leiden University Medical Center approved the study.

Data acquisition

All participants underwent an MRI of the brain in the Leiden University Medical Center. Imaging was performed on a Philips 3 Tesla Achieva MRI scanner using a standard whole-head coil for radiofrequency transmission (Philips Medical Systems, Best, the Netherlands).

Three-dimensional T1-weighted anatomical images were acquired with the following parameters: TR = 9.7 ms, TE = 4.6 ms, flip angle = 8° , FOV = 224 x 177 x 168 mm, resulting in a nominal voxel size of 1.17 x 1.17 x 1.40 mm, covering the entire brain with no gap between slices. To determine WMHs, we acquired fluid attenuated inversion recovery (FLAIR) images (TR = 11000 ms, TE = 125 ms, flip angle = 90° , FOV = 220 x 176 x 137 mm, matrix size 320 x 240, 25 transverse slices to cover the entire brain with a slice thickness of 5 mm with no gap between slices).

Gray matter anatomical brain networks

Before analysis, all MRI scans were submitted to a visual quality control check to ensure that no gross artifacts were present in the data. Data analysis was performed

with FSL (FSL 4.1.9, Oxford, United Kingdom, www.fmrib.ox.ac.uk/fsl) (Smith et al. 2004).

First, nonbrain tissue (e.g., scalp) was removed from T1-weighted images using a semi-automated brain extraction tool as implemented in FSL (Smith 2002). Next, tissue-type segmentation was performed using voxel-based morphometric analysis (Ashburner and Friston 2000). We performed a control check after each processing step to ensure appropriate brain extraction and tissue-type segmentation. To correct for the partial volume effect (i.e., voxels 'containing' more than one tissue-type), the tissue-type segmentation was carried out with partial volume estimation. For each partial volume voxel, the proportion of each tissue-type was estimated, that is, a partial volume vector was formed, with each element being a 'fraction' of a specific tissue type and having a sum of one (Zhang et al. 2001a). The segmented images have values that indicate the probability of a given tissue-type (i.e., they are not binary).

The resulting gray matter partial volume images were aligned to the gray matter MNI standard space image (Montreal Neurological Institute, Montreal, QC, Canada) (Jenkinson et al. 2002), followed by nonlinear registration (Andersson et al. 2007b). The resulting images were averaged to create a study-specific gray matter template, to which the native gray matter segmented images were nonlinearly re-registered (Ashburner and Friston 2000; Good et al. 2001). As a result of nonlinear spatial registration, the volume of some brain structures may grow, whereas others may shrink. To correct for these enlargements and contractions, a further processing step (modulation) is recommended (Ashburner and Friston 2000; Good et al. 2001). In this additional step, each voxel of each registered gray matter image was multiplied by the Jacobian of the warp field, which defines the direction (larger or smaller) and the amount of modulation. The modulated segmented images were finally spatially smoothed with an isotropic Gaussian kernel with a sigma of 3 mm.

The modulated gray matter images in MNI space of all 370 subjects were used as a four-dimensional data set on which an independent component analysis (ICA) was applied using multivariate exploratory linear optimised decomposition into independent components (Beckmann et al. 2005). ICA is a statistical technique that decomposes a set of signals into spatial component maps of maximal statistical independence (Beckmann and Smith 2004). When applied on gray matter images of

different subjects, this method defines fully automatically spatial components based on the covariation of gray matter volumes among subjects (i.e., structural covariance networks), without a priori selected regions of interest. A limitation of this technique is that the number of components to estimate is arbitrarily chosen and that there is no consensus on how to choose the optimal number of components (Cole et al. 2010). There even exists no single ‘best’ dimensionality. Structural covariance and resting state functional networks are in general investigated using eight to ten components (Beckmann et al. 2005; Damoiseaux et al. 2006; Smith et al. 2009; Segall et al. 2012; Zielinski et al. 2012). Therefore, in this study the ICA output was restricted to nine components.

A mixture model was used to assign significance to individual voxels within a spatial map, using a standard threshold level of 0.5 (Beckmann and Smith 2004). This indicates that a voxel ‘survives’ thresholding as soon as the probability of being in the ‘nonbackground’ class exceeds the probability of being in the ‘background’ noise class. A threshold of 0.5 indicates that an equal loss is placed on false positives and false negatives. Anatomical locations were determined using the Harvard-Oxford atlas integrated in FSL.

White matter hyperintensities

We statistically accounted for the possible influence of WMHs, as the prevalence of WMHs increases with age (Galluzzi et al. 2008). Furthermore, the degree of white matter damage is associated with a decrease in gray matter volume in healthy elderly (Wen et al. 2006). The anatomical locations of the networks were identified based on covariance of gray matter, the presence of WMHs do not affect the identification of the networks. However, WMHs could be associated with the amount of gray matter within each individual network. Therefore, we added the volumes of WMHs as independent factor to the linear regression model (see section ‘Statistical analysis’).

WMHs were defined as areas within the cerebral white matter with increased signal intensity on the FLAIR images. Volumes of WMHs were automatically determined using a previously validated method (King et al. 2013). In short, after tissue segmentation of the T1-weighted images, white matter masks generated by FSL were spatially transformed to the FLAIR images using FMRIB’s linear image registration tool (Jenkinson et al. 2002). WMHs in the mask were automatically identified by using a

threshold of three standard deviations above the mean FLAIR signal intensity (King et al. 2013).

Statistical analysis

To analyze the possible association between age and gray matter volume in anatomical networks, we used a linear regression analysis (IBM SPSS Statistics Version 20, IBM Corp., Somers, NY, USA). We divided the total age span four age subgroups (45-55, 55-65, 65-75, 75-85 years) and used these four age subgroups as a categorical variable in the linear regression model. To statistically account for the possible influences of gender, family characteristics (i.e., offspring of long-lived parents or nonoffspring), and volumes of WMHs, these factors were used as independent factors in the model. The statistical threshold was corrected for multiple comparisons using the Bonferroni correction based on $2 \times 9 = 18$ comparisons (two-tailed, nine networks) yielding a corrected p value threshold of $0.05 / 18 = 0.003$.

Chapter 7

Differences in structural covariance brain networks between behavioral variant frontotemporal dementia and Alzheimer's disease

Anne Hafkemeijer, Christiane Möller, Elise Dopper, Lize Jiskoot,
Annette van den Berg-Huysmans, John van Swieten, Wiesje van der Flier,
Hugo Vrenken, Yolande Pijnenburg, Frederik Barkhof,
Philip Scheltens, Jeroen van der Grond, and Serge Rombouts



7.1. ABSTRACT

Disease-specific patterns of gray matter atrophy in Alzheimer's disease (AD) and behavioral variant frontotemporal dementia (bvFTD) overlap with distinct structural covariance networks (SCNs) in cognitively healthy controls. This suggests that both types of dementia target specific structural networks.

Here, we study SCNs in AD and bvFTD. We used structural magnetic resonance imaging data of 31 AD patients, 24 bvFTD patients, and 30 controls from two centers specialized in dementia. Ten SCNs were defined based on structural covariance of gray matter density using independent component analysis. We studied group differences in SCNs using F-tests, with Bonferroni corrected t-tests, adjusted for age, gender, and study center. Associations with cognitive performance were studied using linear regression analyses.

Cross-sectional group differences were found in three SCNs (all $p < 0.0025$). In bvFTD, we observed decreased anterior cingulate network integrity compared with AD and controls. Patients with AD showed decreased precuneal network integrity compared with bvFTD and controls, and decreased hippocampal network and anterior cingulate network integrity compared with controls. In AD, we found an association between precuneal network integrity and global cognitive performance ($p = 0.0043$). Our findings show that AD and bvFTD target different SCNs.

The comparison of both types of dementia showed decreased precuneal (i.e., default mode) network integrity in AD and decreased anterior cingulate (i.e., salience) network integrity in bvFTD. This confirms the hypothesis that AD and bvFTD have distinct anatomical networks of degeneration and shows that structural covariance gives valuable insights in the understanding of network pathology in dementia.

7.2. INTRODUCTION

The most common types of early-onset dementia are Alzheimer's disease (AD) and behavioral variant frontotemporal dementia (bvFTD) (Ratnavalli et al. 2002). Patients with AD typically present with deficits in episodic and working memory (McKhann 2011), whereas bvFTD is mainly characterized by changes in behavior (Rascovsky et al. 2011).

Both types of dementia are associated with gray matter loss (Krueger et al. 2010). In AD, gray matter atrophy is most often found in the hippocampus, precuneus, posterior cingulate cortex, parietal, and occipital brain regions (Buckner et al. 2005; Seeley et al. 2009; Krueger et al. 2010). Patients with bvFTD show atrophy most prominent in the anterior cingulate cortex, frontoinsula, and frontal brain regions (Seeley et al. 2009; Krueger et al. 2010).

These disease-specific patterns of gray matter atrophy spatially overlap with distinct structural covariance networks (SCNs) based on covariance of gray matter density (Seeley et al. 2009). Studying anatomical networks allows us to investigate inter-regional dependencies, which might provide additional valuable information to the common analyses that consider voxels separately. Network approaches have the potential to give more insights in dementia pathology than voxel-based approaches that focus on local gray matter atrophy, since brain disorders appear not to be localized in one specific brain area, but rather in networks of a multitude of brain regions (Evans 2013; Fornito et al. 2015).

Here, we used structural magnetic resonance imaging (MRI) to study whether SCNs differ between AD and bvFTD. The typical atrophy pattern in AD shows overlap with the default mode SCN in cognitively healthy controls and gray matter atrophy in bvFTD shows overlap with the salience SCN in controls (Seeley et al. 2009). This spatial colocalization of atrophy and anatomical brain networks suggests that both types of dementia target specific anatomical networks. The aim of this study was to test this hypothesis that both types of dementia have distinct anatomical networks of degeneration (i.e., the default mode anatomical network in AD and the salience anatomical network in bvFTD).

7.3. MATERIALS AND METHODS

Participants

We included 31 patients with probable AD, 24 patients with probable bvFTD, and 30 control participants (*Table 7.3*). All subjects were recruited from two Dutch centers specialized in dementia: the Alzheimer Center of the VU University Medical Center Amsterdam, and the Alzheimer Center of the Erasmus University Medical Center Rotterdam, as described previously (Hafkemeijer et al. 2015).

All patients underwent a standardized dementia screening including medical history, informant-based history, physical and neurological examination, blood tests, extensive neuropsychological assessment, and an MRI of the brain. Diagnoses were established in a multidisciplinary consensus meeting according to the core clinical criteria of the National Institute on Aging and the Alzheimer's Association workgroup for probable AD (McKhann 2011) and according to the clinical diagnostic criteria for bvFTD (Rascovsky et al. 2011). Cerebral spinal fluid measures of amyloid beta, total tau, and

TABLE 7.1 Characteristics of the study population

Characteristic	bvFTD (n=24)	AD (n=31)	HC (n=30)
Age (years)	61.5 (7.3)	65.3 (7.0)	62.8 (5.0)
Gender (male/female)	18/6	19/12	18/12
Study center (VUMC/LUMC)^a	16/8	20/11	17/13
Level of education^b	5.1 (1.6)	4.9 (1.3)	5.4 (1.2)
Duration of symptoms (months)	50.2 (49.2)	41.9 (30.7)	n/a
CSF Total Tau (ng/L)	321.1 (125.5)	668.1 (385.3)	n/a
CSF Phospho Tau (ng/L)	41.3 (14.2)	84.7 (35.7)	n/a
CSF Amyloid Beta (ng/L)	1019.9 (231.9)	478.7 (121.2)	n/a
MMSE (max score: 30)	24.6 (3.6)	22.7 (2.8)	28.7 (1.6)
FAB (max score: 18)	14.1 (2.5)	13.3 (3.4)	17.4 (1.0)
CDR (max score: 3)	0.7 (0.4)	0.8 (0.3)	0.0 (0.0)
GDS (max score: 15)	3.8 (3.3)	2.8 (2.9)	1.2 (1.4)

Abbreviations: bvFTD = behavioral variant frontotemporal dementia; AD = Alzheimer's disease; HC = healthy controls; CSF = Cerebrospinal Fluid; MMSE = Mini Mental State Examination; FAB = Frontal Assessment Battery; CDR = Clinical Dementia Rating Scale; GDS = Geriatric Depression Scale. Values are means (standard deviation) for continuous variables or numbers for dichotomous variables.

^aImaging was performed either in the Alzheimer Center of the VU University Medical center (VUMC) or in the Leiden University Medical Center (LUMC) in the Netherlands. ^bLevel of education was determined on a Dutch 7-point scale ranging from 1 (less than elementary school) to 7 (university or technical college).

phosphorylated tau were available to gain diagnostic certainty. To minimize center effects, all diagnoses were re-evaluated in a panel including clinicians from both Alzheimer centers. The control participants were screened to exclude memory complaints, drugs- or alcohol abuse, major psychiatric disorder, and neurological or cerebrovascular diseases. They underwent an assessment including medical history, physical examination, extensive neuropsychological assessment, and an MRI of the brain, comparable to the work-up of the patients.

This study was performed in compliance with the Code of Ethics of the World Medical Association (Declaration of Helsinki). Ethical approval was obtained from the local ethics committees (VU University Medical Center Amsterdam (CWO-nr 11-04, METC-nr 2011/55) and Leiden University Medical Center (2011/55 P11.146)). Written informed consent from all participants was obtained.

Data acquisition

All participants underwent an MRI of the brain on a 3 Tesla scanner either in the VU University Medical Center (Signa HDxt, GE Healthcare, Milwaukee, WI, USA), or in the Leiden University Medical Center (Achieva, Philips Medical Systems, Best, the Netherlands), using a standard 8-channel head coil. For each participant, a three-dimensional T1-weighted anatomical image was acquired. Imaging parameters in the VU University Medical Center were: TR = 7.8 msec, TE = 3 msec, flip angle = 12°, 180 slices, resulting in a voxel size of 0.98 x 0.98 x 1.00 mm. Imaging parameters in the Leiden University Medical Center were: TR = 9.8 msec, TE = 4.6 msec, flip angle = 8°, 140 slices, resulting in a voxel size of 0.88 x 0.88 x 1.20 mm.

Data analysis

Before analysis, all MRI scans were submitted to a visual quality control check to ensure that no gross artifacts were present in the data. Data analysis was performed with Functional Magnetic Resonance Imaging of the Brain Software Library (FSL 5.0.1, Oxford, United Kingdom) (Smith et al. 2004).

Preprocessing

The SCNs analyses were performed as described in our previous work (Hafkemeijer et al. 2014). First, nonbrain tissue (e.g. scalp) was removed from the T1-weighted images using the brain extraction tool as implemented in FSL (Smith 2002). Next, tissue-type

segmentation was performed using the voxel-based morphometry tool (Ashburner and Friston 2000). We performed a control check after each preprocessing step to ensure appropriate brain extraction and tissue-type segmentation. To correct for the partial volume effect (i.e., voxels “containing” more than one tissue type), the tissue-type segmentation was carried out with partial volume estimation. For each partial volume voxel, the proportion of each tissue type is estimated, that is, a partial volume vector is formed, with each element being a “fraction” of a specific tissue type and having a sum of one (Zhang et al. 2001a). The segmented images have values that indicate the probability of a given tissue type.

The gray matter partial volume images were aligned to the gray matter MNI standard space image (Montreal Neurological Institute, Montreal, QC, Canada) (Jenkinson et al. 2002), followed by nonlinear registration (Andersson et al. 2007b). The resulting images were averaged to create a study-specific gray matter template, to which the native gray matter segmented images were nonlinearly re-registered (Ashburner and Friston 2000; Good et al. 2001). As a result of nonlinear spatial registration, the volume of some brain structures may grow, whereas others may shrink. To correct for these enlargements and contractions, a further processing step (modulation) was applied, as recommended (Ashburner and Friston 2000; Good et al. 2001). In this additional step, each voxel of each registered gray matter image was multiplied by the Jacobian of the warp field, which defines the direction (larger or smaller) and the amount of modulation. The modulated segmented images were finally spatially smoothed with an isotropic Gaussian kernel with a sigma of 3 mm.

Gray matter volume

To study group differences in local voxel-based gray matter volume between patient groups, a general linear model approach using two-sample t-tests was applied, including age, gender, and study center as covariate in the statistical model. Voxel-wise non-parametric permutation testing (Nichols and Holmes 2001) with 5000 permutations was performed using FSL randomise correcting for multiple comparisons across space (statistical threshold was set at $p < 0.05$, Family-Wise Error (FWE) corrected), using the Threshold-Free Cluster Enhancement (TFCE) technique (Smith and Nichols 2009).

Structural covariance networks

The modulated gray matter images in MNI space were concatenated into a four dimensional data set on which an independent component analysis (ICA) was applied using the multivariate exploratory linear optimised decomposition into independent components tool (Beckmann et al. 2005). To avoid bias towards any particular group, networks were defined on gray matter images of three groups of equal size (i.e., 24 bvFTD patients, 24 AD patients (randomly selected), and 24 controls (randomly selected)), balanced between centers. ICA is a statistical technique that decomposes a set of signals into spatial component maps of maximal statistical independence (Beckmann and Smith 2004). When applied on gray matter images of different subjects, this method defines spatial components based on the structural covariance of gray matter density among subjects (i.e. SCNs) (Douaud et al. 2014; Hafkemeijer et al. 2014), without *a priori* selected regions of interest. Structural covariance and resting state functional networks are in general investigated using eight to ten components (Beckmann et al. 2005; Damoiseaux et al. 2006; Smith et al. 2009; Segall et al. 2012; Zielinski et al. 2012). Therefore, in this study the ICA output was restricted to ten components.

A mixture model was used to assign significance to individual voxels within a spatial map, using a standard threshold level of 0.5 (Beckmann and Smith 2004). This indicates that a voxel “survives” thresholding as soon as the probability of being in the “nonbackground” class exceeds the probability of being in the “background” noise class. A threshold of 0.5 indicates that an equal loss is placed on false positives and false negatives. Anatomical regions of the SCNs were determined using the Harvard-Oxford cortical and subcortical structures atlas integrated in FSL.

Statistical analysis

The ICA approach provides for the 24 bvFTD patients, 24 AD patients, and 24 controls an index that reflects the degree to which each subject expresses the identified network pattern (i.e., SCN integrity score) (Segall et al. 2012). We want to study cross-sectional group differences in SCN integrity using data of all participants (i.e., 31 AD patients, 24 bvFTD patients, and 30 controls). Therefore, an additional step was performed to obtain the SCN integrity scores of these participants. Individual SCN integrity was calculated using the four-dimensional data set of gray matter images in a spatial regression against the ten SCN probability maps (general linear model approach

integrated in FSL) (Filippini et al. 2009). This procedure gives for all subjects the SCN integrity scores, i.e., the beta weights of the regression analysis, which can be negative or positive. The higher the score, the stronger the expression of the identified SCN. Group differences in SCN integrity were studied using analysis of covariance (ANCOVA), adjusted for age, gender, and study center, with post hoc Bonferroni corrected t-tests (IBM SPSS Statistics Version 20, IBM Corp., Somers, NY, USA). To further correct for multiple network testing, the statistical threshold was set at $p < 0.0025$ ($= 0.05 / 20$, based on $10 \times 2 = 20$ comparisons (ten networks, two-tailed)).

Associations with cognitive performance

We investigated the possible associations between SCN integrity and global cognitive performance, Mini Mental State Examination (MMSE) score (Folstein et al. 1975) in AD and Frontal Assessment Battery (FAB) score (Dubois et al. 2000) in bvFTD, using linear regression analyses (IBM SPSS Statistics Version 20, IBM Corp. Somers, NY, USA), adjusted for age, gender, and study center (statistical threshold was set at $p < 0.05$).

7.4. RESULTS

Demographic characteristics

Demographic data for all participants are summarized in *Table 7.1*. There were no significant differences between the groups with regard to age, gender, study center distribution, level of education, or duration of symptoms (all $p > 0.05$).

As expected, both dementia groups performed worse on cognitive tests compared with controls (all $p < 0.05$). Patients with AD performed worse on MMSE compared with bvFTD patients ($p = 0.037$). FAB ($p = 0.367$), Clinical Dementia Rating Scale (CDR, $p = 0.455$), and Geriatric Depression Scale (GDS, $p = 0.279$) scores did not differ significantly between AD and bvFTD.

Regional gray matter volume

The regional voxel-based gray matter analysis revealed group differences in gray matter volume (*Fig. 7.1*). Patients with AD showed less gray matter compared with bvFTD in precuneal and posterior cingulate cortex (*Fig. 7.1A*). Patients with bvFTD had less gray matter compared with AD in insular cortex (*Fig. 7.1B*).

Structural covariance networks

Ten SCNs were defined based on gray matter structural covariance (*Fig. 7.2A*, *Table 7.2*): (a) anterior cingulate network, (b) precuneal network, (c) parahippocampal network, (d) hippocampal network, (e) subcortical network, (f) lateral occipital network, (g) precentral network, (h-j) cerebellar networks.

SCN group differences

Cross-sectional group differences were found in three SCNs: the anterior cingulate network (SCN a), the precuneal network (SCN b), and the hippocampal network (SCN d) (*Fig. 7.2B*). The results of post hoc testing showed decreased anterior cingulate network (SCN a) integrity in bvFTD compared with AD ($p = 0.0002$) and compared with controls ($p < 0.0001$). Patients with AD showed decreased precuneal network (SCN b) integrity compared with bvFTD ($p = 0.0002$) and compared with controls ($p < 0.0001$), and decreased anterior cingulate network (SCN a) and hippocampal network (SCN d) integrity compared with controls ($p = 0.0006$, $p = 0.0022$). No cross-sectional group differences were found in the other seven networks (SCNs c, e-j).

Associations with global cognitive performance

We found a positive association between SCN integrity and MMSE score in the precuneal network (SCN b) in AD ($p = 0.0043$, $R^2 = 0.316$, $\text{Beta} = 0.508$). No associations between SCN integrity and FAB scores were found ($p > 0.05$).

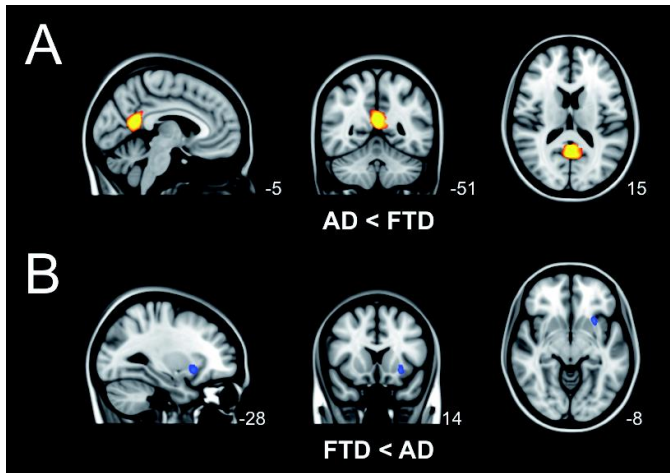


FIGURE 7.1 Group differences in regional voxel-based gray matter volume

Differences in gray matter volume between behavioral variant frontotemporal dementia (FTD) and Alzheimer's disease (AD) (TFCE, FWE corrected). A) Local gray matter was decreased in patients with AD compared with patients with bvFTD in precuneal and posterior cingulate cortex (yellow). B) Local gray matter was decreased in patients with bvFTD compared with AD in insular cortex (blue).

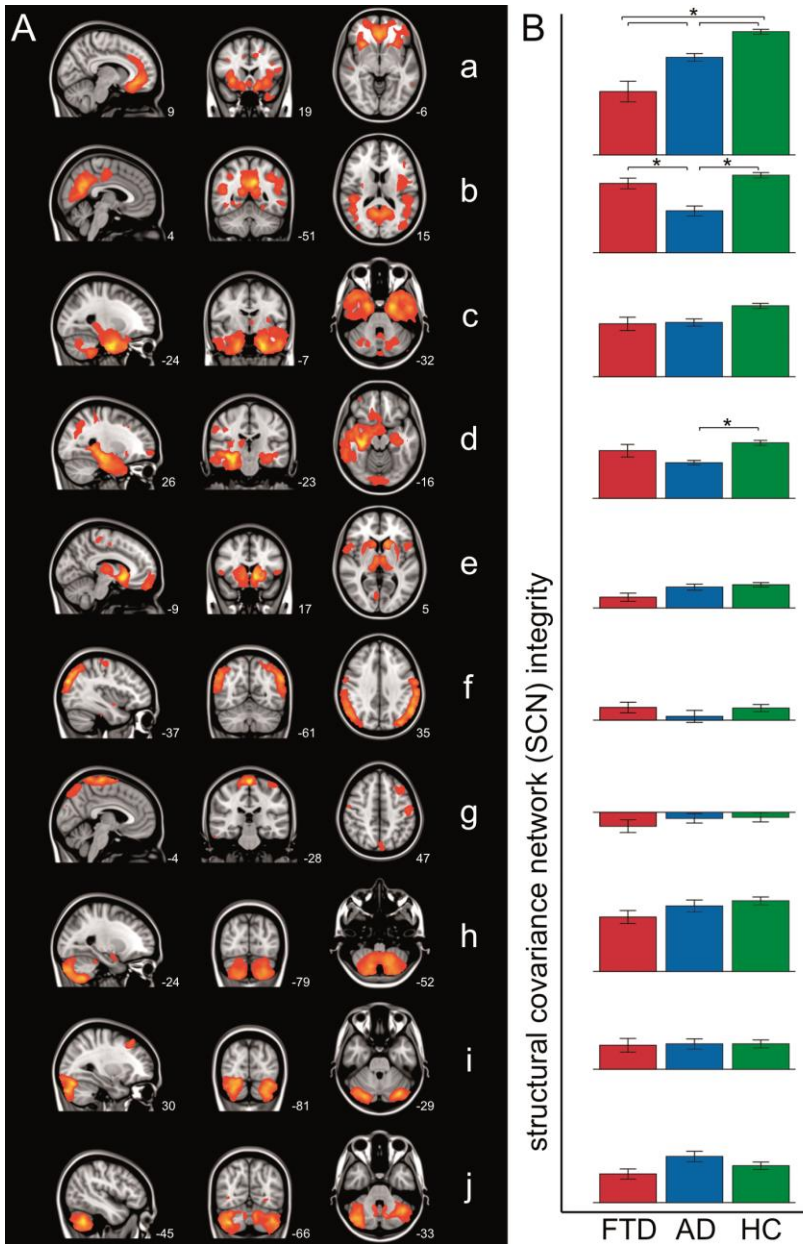


FIGURE 7.2 Group differences in structural covariance networks

A) Overview of structural covariance networks (SCNs) defined on gray matter structural covariance. Networks are overlaid on the most informative sagittal, coronal, and transverse slices of the MNI standard anatomical image (x, y, and z coordinates of each slice are given). B) Bar graphs show SCN integrity in patients with behavioral variant frontotemporal dementia (FTD, red), patients with Alzheimer's disease (AD, blue), and healthy controls (HC, green) (\pm standard error). Group differences were found in anterior cingulate network (a), precuneal network (b), and hippocampal network (d) (indicated with asterisks, Bonferroni corrected, adjusted for age, gender, and study center).

TABLE 7.2 Brain clusters of the structural covariance networks

Brain cluster ^a		MNI coordinates		
		x	y	z
Network a	Anterior cingulate cortex cluster also contains insular cortex, paracingulate gyrus, and frontal medial cortex	-2	34	-14
	(Inferior temporal gyrus)	46	-6	-50
	Paracingulate gyrus	-6	8	46
	(Middle frontal gyrus)	-24	-2	48
	(Superior frontal gyrus)	20	32	36
Network b	Precuneal cortex cluster also contains posterior cingulate cortex	-8	-52	34
	Lateral occipital cortex	52	-74	-2
	Lingual gyrus	-22	-60	-10
	(Inferior temporal gyrus)	48	-22	-18
	(Middle frontal gyrus)	-36	20	24
Network c	Parahippocampal gyrus cluster also contains hippocampus, temporal fusiform cortex, inferior temporal gyrus, and temporal pole	-24	-8	-38
	(Cuneal cortex)	2	-88	30
	Cerebellum	0	-86	-34
Network d	Hippocampus cluster also contains temporal fusiform cortex and temporal pole	36	-26	-14
	Occipital pole	0	-92	-10
	(Middle frontal gyrus)	42	14	56
	(Frontal pole)	26	60	-6
	Lateral occipital cortex	-30	-74	20
Network e	Nucleus accumbens cluster also contains caudate nucleus, putamen, and thalamus	-10	14	-8
	Frontal pole	4	62	-12
	Precentral gyrus	-4	-10	54
	(Intracalcarine cortex)	8	-74	4
	Inferior frontal gyrus	56	10	4

TABLE 7.2 continued

Brain cluster ^a		MNI coordinates		
		x	y	z
Network f	Lateral occipital cortex	-36	-84	28
	Supramarginal gyrus	56	-30	46
	(Superior parietal lobule)	-18	-54	74
Network g	Precentral gyrus	0	-28	72
	cluster also contains precuneal cortex and middle frontal gyrus			
	(Middle temporal gyrus)	-58	-4	-32
	(Cerebellum)	-14	-74	-38
	(Frontal pole)	-18	42	34
Network h	Cerebellum	-18	-62	-56
	Amygdala	-20	-6	-18
	(Putamen)	34	-14	-10
Network i	Cerebellum	34	-74	-22
	cluster also contains lateral occipital cortex			
	Middle frontal gyrus	32	28	46
	(Frontal pole)	-32	52	22
Network j	Cerebellum	36	-68	-44
	(Pallidum)	24	-4	-6
	(Precentral gyrus)	40	-16	56
	(Insular cortex)	-34	-24	-2

Abbreviation: MNI = Montreal Neurological Institute standard space image

^aEach SCN is divided in brain clusters using the cluster tool integrated in FSL. MNI x-, y-, and z-coordinates of each cluster are given. Brain structures are anatomically identified using the Harvard-Oxford atlas integrated in FSL. Figure 7.1 shows the most informative sagittal, coronal, and transverse slices. Structures in parentheses in the table are not visible in Figure 7.1.

7.5. DISCUSSION

This is the first study that compares networks of structural covariance between patients with AD and patients with bvFTD. Our results show that AD and bvFTD are associated with different networks of degeneration. The comparison of both types of dementia showed decreased anterior cingulate network integrity in bvFTD and decreased precuneal network integrity in AD. We used structural MRI data to study anatomical networks based on structural covariance of gray matter density. Until now structural covariance had not been compared between patients with AD and patients with bvFTD. However, the spatial colocalization of local gray matter atrophy in AD and bvFTD with the topography of SCNs in cognitively healthy elderly (Seeley et al. 2009), suggests that both types of dementia target different SCNs (i.e., the default mode network in AD and the salience network in bvFTD).

In bvFTD, we found decreased anterior cingulate network integrity compared with AD and controls. This SCN includes the anterior cingulate cortex, insular cortex, paracingulate gyrus, and frontal medial cortex. These brain areas show typical bvFTD pathology (Seeley et al. 2009; Krueger et al. 2010; Dopfer et al. 2014), with more severe gray matter atrophy in the anterior cingulate cortex and insula in bvFTD compared with AD (Rabinovici et al. 2008). Deficits in social-emotional functioning, which are common in bvFTD, rely on structures including the anterior cingulate cortex and insula (Rosen et al. 2002; Broe et al. 2003). In general, SCNs show spatial overlap with functional connectivity networks (Segall et al. 2012). Visual inspection of our data shows overlap between the anterior cingulate SCN and the salience functional connectivity network, which is related to social-emotional processing (Seeley, Menon, et al. 2007). Decreased functional connectivity within the salience network has been observed in bvFTD (Zhou et al. 2010; Borroni et al. 2012; Agosta et al. 2013; Farb et al. 2013; Filippi et al. 2013; Rytty et al. 2013).

In AD, we found decreased precuneal network integrity compared with bvFTD and controls. This SCN includes the precuneal cortex, posterior cingulate cortex, lateral occipital cortex, and lingual gyrus, which are brain areas that typically show AD pathology (Buckner et al. 2005; Seeley et al. 2009; Krueger et al. 2010). Our findings are in line with the observations of decreased network integrity (Spreng and Turner 2013; Tijms et al. 2013; Montembeault et al. 2015) and cortical shrinking (He et al. 2008; Reid and Evans 2013) in this network in AD compared with controls. Visual

inspection shows overlap between the precuneal SCN and the default mode functional connectivity network, which is related to episodic memory (Buckner et al. 2005; Seeley et al. 2009). Decreased functional connectivity within the default mode network has been found in AD (Greicius et al. 2004; Zhou et al. 2010; Hafkemeijer, van der Grond, and Rombouts 2012; Balthazar et al. 2014). In addition to decreased precuneal network integrity, we found decreased hippocampal network integrity in AD compared with controls. This network includes the hippocampus, temporal fusiform cortex, occipital, and temporal pole, brain areas that show typical AD pathology (Buckner et al. 2005; Seeley et al. 2009; Krueger et al. 2010).

SCNs show spatial overlap with functional connectivity networks (Segall et al. 2012). In addition to structural covariance, functional connections were studied using resting state functional magnetic resonance imaging fMRI data of the patients included in the current study (Hafkemeijer et al. 2015). We showed that functional connections are different between AD and bvFTD, but less abundant than in the current SCN study. This suggests that SCNs are more sensitive to detect average dementia network pathology in the mild to moderate stage.

We investigated whether SCN integrity is related with cognitive performance. The MMSE score (Folstein et al. 1975), which is a general measurement of cognitive performance, and the integrity of the precuneal SCN are positively associated in AD, which is in line with our expectations. This relationship between SCN integrity and global cognitive performance, suggest the potential of SCNs to monitor disease severity. However, MMSE is a general screening tool and should not be regarded as an extensive neuropsychological assessment. We expected to find an association between FAB score (Dubois et al. 2000), which is a general screening tool for bvFTD, and the integrity of the anterior cingulate network. The inability to find this association might be related to the relatively small number of subjects that was included in the bvFTD group and the more limited range in FAB scores. Further research is recommended to study whether SCN integrity is related to dysfunction in specific cognitive domains and to investigate its potential to monitor disease progression.

The whole-brain gray matter networks were based on structural covariance of gray matter density, using the ICA method (Beckmann et al. 2005). This multivariate approach takes into account inter-regional dependencies rather than the common

analyses that consider voxels separately. Multivariate approaches have the potential to give more insights in dementia pathology than univariate approaches that focused on local gray matter atrophy, since brain disorders appear not to be localized in one specific brain area, but rather in networks of a multitude of brain regions (Evans 2013; Fornito et al. 2015). Cognitive dysfunction might not just be the consequence of localized brain damage, but of a damaged brain network as well. Therefore, studying the brain as a network of connected regions might give valuable information. Analyzing networks in dementia increases sensitivity compared with regional voxel-based methods (Rombouts et al. 2009). The current study also suggests a higher sensitivity of multivariate SCNs to detect disease specific patterns.

An advantage of the ICA approach is that it defines fully automatically spatial components without *a priori* selected region of interest. However, a limitation of this technique is that the number of components to estimate (i.e. the number of SCNs) is arbitrarily chosen. The topic of choosing the number of components and the effect of the dimensionality on the statistical results is currently an active area of research. There is no consensus on the optimal number of components (Cole et al. 2010), which may vary depending on the data and the research question. In the current study, we decided to use a dimensionality within the range of the most often applied dimensionality in studies of brain networks, that is use eight to ten components (Beckmann et al. 2005; Damoiseaux et al. 2006; Smith et al. 2009; Segall et al. 2012; Zielinski et al. 2012). However, varying the dimensionality may impact the spatial organization of the networks. For example, increasing the dimensionality will split networks into several subnetworks.

In the current study, we decided to use all available data to define the SCNs, i.e., we used three equal-sized groups including both patients and controls for the ICA approach. Although network approaches are widely applied, the way to define networks has not been standardized (Griffanti, Rolinski, et al. 2015). Brain networks can be defined in subjects from all groups or on the control subjects only (Jafri et al. 2008), with both approaches having their own advantages. Using all groups and therefore more data may increase the robustness of the defined networks. However, a potential disadvantage is its decreased sensitivity for group differences (Rytty et al. 2013; Griffanti, Rolinski, et al. 2015).

A limitation of our study is the possibility of misdiagnosis of the patients. The diagnosis FTD or AD can only be confirmed by brain autopsy after death. In this study, postmortem data were not available. Nevertheless, all patients underwent an extensive dementia screening and were evaluated in a multidisciplinary panel including clinicians from different centers specialized in dementia. Only dementia patients that fulfilled the most recent clinical criteria for probable bvFTD (Rascovsky et al. 2011) and probable AD (McKhann 2011) were included in the present study.

7.5.1. CONCLUSION

This is the first study that used structural MRI data to compare whole-brain networks of gray matter structural covariance between patients with AD and patients with bvFTD. Our findings show that AD and bvFTD target different SCNs. The comparison of both types of dementia showed bvFTD pathology in the anterior cingulate network (i.e., salience network) and AD pathology in the precuneal network (i.e., default mode network). This confirms the hypothesis that AD and bvFTD have specific anatomical networks of degeneration and shows that structural covariance gives valuable insights in the understanding of network pathology in dementia.

Chapter 8

General discussion

In this thesis, we studied brain networks in aging and dementia. A number of cross-sectional and longitudinal magnetic resonance imaging (MRI) studies were conducted to examine functional brain networks (*section 1*) and structural brain networks (*section 2*) in healthy aging (*chapters 2 and 6*), subjective memory complainers (*chapter 3*), and in Alzheimer's disease (AD) and behavioral variant frontotemporal dementia (bvFTD) (*chapters 2, 4, 5, and 7*). The main finding of this thesis is that brain networks change with healthy and pathological aging, with differences in network degeneration between different types of dementia.

This disease-specific network degeneration suggests the potential of brain networks to improve diagnostic accuracy and early differential diagnosis. However, the findings presented in this thesis are based on group differences, not on individual subjects. Therefore, although functional and structural networks do contribute to our understanding of dementia pathology, brain networks are not yet suitable as biomarker for individual classification of dementia patients. In this chapter, the main findings of the studies described in this thesis are summarized and integrated, followed by critical considerations and recommendations for future research.

8.1. SUMMARY OF THE FINDINGS

Functional brain networks in aging and dementia

In *chapter 2*, a literature overview of studies focusing on the default mode functional brain network in aging and dementia was given. This network is particularly relevant for aging and dementia, since its structures are vulnerable to dementia pathology. The majority of studies described in *chapter 2* showed decreased default mode functional connectivity along a continuum from healthy aging to mild cognitive impairment and to dementia. Decreased default mode functional connectivity was further observed in subjects at risk for developing dementia, either in terms of having amyloid plaques, which is a major pathological feature of AD, or in having a genetic risk for dementia.

While most studies showed decreased functional connectivity, some studies showed evidence for increased functional connectivity as well. Increased connectivity might be explained by a compensatory-recruitment mechanism in which additional neural resources are used to compensate for losses of cognitive function and to maintain task performance (Bondi et al. 2005). *Chapter 2* concluded that resting state functional magnetic resonance imaging (fMRI) is a useful tool for detecting changes in default

mode functional connectivity in aging and dementia, however, more work needs to be conducted to conclude whether these measures will become useful as a clinical diagnostic tool in dementia.

Functional brain networks in elderly with subjective memory complaints

In *chapter 3*, resting state fMRI was applied to investigate functional brain networks in elderly with self-reported subjective memory complaints. These elderly are characterized by a subjectively noticeable decline in memory functioning, which can hardly be confirmed by neuropsychological tests (Hejl et al. 2002). Elderly with subjective memory complaints do not meet the criteria for mild cognitive impairment or dementia. *Chapter 3* showed, in addition to gray matter volume reductions, increased functional connectivity in the default mode network and medial visual network, even when was account for the potential effects of local structural differences within and between groups. The results of this study suggested that memory complaints are a reflection of objective alterations in the brain. This indicates that functional brain networks might be useful to objectively determine differences in brain integrity.

Functional brain network differences between AD and bvFTD

Two chapters of this thesis focused on resting state fMRI in dementia. The main aim of these chapters was to investigate whether functional connections differ between AD and bvFTD. In *chapter 4*, the potential of resting state fMRI to distinguish both types of dementia in an early stage of the disease was studied. This baseline study showed that the pathophysiology of functional brain connectivity is different between AD and bvFTD, which supported the hypothesis that resting state fMRI shows disease-specific functional connectivity differences and can be used to elucidate the pathology of both types of dementia.

Functional brain network changes in AD and bvFTD

Chapter 5 described a follow-up study that explored the potential of longitudinal resting state fMRI to delineate regions relevant for disease progression and diagnostic accuracy in dementia. This was the first study that investigated longitudinal resting state fMRI data in AD and bvFTD, with the aim to show group differences in functional connectivity at baseline, at follow-up, and changes in functional connectivity over time. *Chapter 5* showed disease-specific brain regions with longitudinal changes in

functional connectivity in AD and bvFTD. Over time, precuneal connectivity decreased in AD, whereas in bvFTD inferior frontal gyrus connectivity decreased longitudinally. These findings suggest the potential of longitudinal resting state fMRI to delineate regions relevant for disease progression and for diagnostic accuracy, although the direct comparison between the AD and bvFTD groups did not yield significant group differences in longitudinal changes.

Structural brain networks in healthy aging

In the second section of this thesis, a relatively new approach was applied to examine structural brain networks based on covariance of gray matter intensity. In *chapter 6*, structural covariance networks were studied in a large group of cognitively healthy middle-aged to older adults. Studying these anatomical networks allowed us to investigate inter-regional dependencies, which may provide additional valuable information to the common structural MRI analyses that consider voxels separately. *Chapter 6* showed that subcortical, cingulate cortex, and sensorimotor networks degenerate with age, while temporal, auditory, and cerebellar structural networks remain relatively unaffected with advancing age.

Structural brain network differences between AD and bvFTD

In *chapter 7*, structural covariance networks were studied in dementia. This study showed that the pathophysiology of bvFTD and AD was associated with disease-specific structural brain networks. The comparison of both types of dementia showed decreased anterior cingulate or salience network integrity in bvFTD and decreased precuneal or default mode network integrity in AD. This confirmed the hypothesis that both types of dementia have distinct anatomical networks of degeneration and implied that structural covariance gives additional valuable insight in the understanding of network pathology in dementia.

8.2. INTEGRATION OF THE FINDINGS

The main goal of this thesis was to improve our insights in functional and structural brain networks in healthy and pathological aging. Cognitive dysfunctioning is understood not to be localized in one brain area, but rather in networks of a multitude of brain regions (Evans 2013; Fornito et al. 2015). In the network degeneration or disconnection hypothesis it has been suggested that dementia starts in one part of the brain and progressively spreads to connected brain areas (Seeley et al. 2009). It has

been hypothesized that each neurodegenerative disease has its specific network of degeneration, with abnormalities in a posterior hippocampal-cingulo-temporal-parietal network known as the default mode network in AD and in an anterior frontoinsula-cingulo-orbitofrontal network often called the salience network in bvFTD (Seeley et al. 2009; Zhou et al. 2010; Dopper et al. 2014).

In this thesis, we reported that brain networks change with healthy and pathological aging. Healthy aging is mostly associated with decreased functional connections in the default mode network, while increased functional connectivity was reported as well (*chapter 2*). Elderly with subjective memory complaints, who do not meet the criteria for dementia, showed increased functional connections in the default mode network and medial visual network (*chapter 3*). This increased connectivity between hippocampus, posterior cingulate cortex, cuneal, and precuneal cortex might be the result of a compensatory mechanism to compensate for losses of cognitive function (Bondi et al. 2005). Studying brain networks in these elderly with subjective cognitive decline is relevant for dementia since there is evidence that subjective cognitive complaints may represent the earliest symptomatic manifestation of dementia (Jessen et al. 2014).

In dementia mostly decreased, not increased, functional connectivity was found (*chapters 4-5*), suggesting a further breakdown of functional connections. We showed that, given the gray matter atrophy, functional connections differ between AD and bvFTD. Over time, we found decreased precuneal connectivity in AD and inferior frontal gyrus connectivity in bvFTD (*chapter 5*). This indicates, in line with our expectations, that posterior regions of the brain are involved in AD, while network pathology of bvFTD may progress more anterior (Seeley et al. 2009; Zhou et al. 2010; Dopper et al. 2014).

In addition to functional brain networks, inter-regional dependencies were studied based on structural covariance of gray matter intensity. Healthy aging affects subcortical, cingulate cortex, and sensorimotor structural brain networks, while auditory, temporal, and cerebellar structural networks remain relatively unaffected with advancing age (*chapter 6*). Consistent with the hypothesis that both types of dementia have distinct networks of degeneration (Seeley et al. 2009), the comparison of AD and bvFTD showed decreased anterior cingulate or salience structural network

integrity in bvFTD and decreased precuneal or default mode structural network integrity in AD (*chapter 7*).

Together, the studies that were conducted for this thesis showed that in addition to the commonly studied functional networks (*section 1*), structural networks provide valuable insights in brain networks in aging and underlying pathological mechanisms in dementia (*section 2*). Although we did not compare structural and functional brain networks directly, the findings described in this thesis might suggest that structural brain networks are more sensitive compared with functional brain networks to detect network pathology.

8.3. CRITICAL CONSIDERATIONS

We used innovative neuroimaging analyses to study functional and structural brain networks in aging and dementia. In the following paragraphs, methodological considerations will be critically discussed.

Networks of interest

In this thesis, functional brain networks (*chapters 3-5*) were studied in a standardized way using eight predefined functional networks as a reference (Beckmann et al. 2005). This model-free approach was applied to investigate whole-brain functional connections between networks and all voxels throughout the entire brain without any bias towards specific brain regions. These standardized resting state networks parcellate the brain into eight templates that represent over 80% of the total brain volume (Khalili-Mahani et al. 2012), and include brain areas relevant for aging and dementia.

The main advantage of standardized networks is that it will improve comparability between studies (Khalili-Mahani et al. 2012; Klumpers et al. 2012; Niesters et al. 2012). However, in the field of network imaging, no “gold standard networks” were defined. In addition to the standard reference networks used in this thesis, other reference networks could be used as well in network analyses (for example (Smith et al. 2009; Laird et al. 2011)). Although brain networks are relatively consistent across studies (Damoiseaux et al. 2006), there may exhibit small differences in the spatial organisation of the networks, which might impact the findings.

In addition to predefined networks as a reference, functional connections can be studied using so-called seed-based analyses. This is a suitable approach to address hypothesis-driven questions, since it investigates the connections between a specific brain region (the seed) and other regions throughout the brain. Especially for bvFTD the connectivity analyses could have been reduced to specific brain areas (e.g., seeds in the frontoinsula and cingulate cortex). Choosing the right seed in AD, and more especially in subjective memory complaints and healthy aging, is more difficult since less is known about which connections are affected. As the focus on specific connections is the main advantage of the seed-based approach, certain essential connections may be missed. In the functional connectivity studies in this thesis (*chapter 3-5*), we have chosen to study connections throughout the entire brain and not be restricted to a priori defined connections. Furthermore, choosing standardized networks as 'seeds' allows us to compare results presented in this thesis.

Another often applied approach to study brain networks is the data-driven independent component analysis (ICA). This statistical technique decomposes a set of signals into spatial component maps of maximal statistical independence (Beckmann and Smith 2004). In this thesis, the data-driven method was used to define the structural brain networks (*chapter 6 and 7*), since no standardized structural networks were available. Although this approach is commonly applied, it has its limitations since the number of networks to estimate is arbitrarily chosen. The topic of choosing the number of networks and the effect of the dimensionality on the findings is currently an active area of research. At this moment, there is no consensus on the optimal number of components (Cole et al. 2010), which may vary depending on the data and the research question. In this thesis, we decided to use a dimensionality within the range of the most often applied dimensionality in brain network studies, that is eight to ten (Beckmann et al. 2005; Damoiseaux et al. 2006; Smith et al. 2009; Segall et al. 2012; Zielinski et al. 2012). However, varying the dimensionality may impact the spatial organization of the networks. For example, increasing the dimensionality will split networks into several subnetworks.

Noise reduction

A critical consideration related to the resting state fMRI analyses (*chapters 3-5*) is that the spontaneous blood oxygen level dependent (BOLD) signal might contain noise related to head motion, cardiac pulsation, respiration, or other nuisance sources. This

noise could be especially problematic if it differs between groups (Van Dijk et al. 2012). The studies described in this thesis used multiple approaches to remove the unique variance related to noise. First, all data were submitted to a quality control check to exclude subjects with motion artifacts. Second, standard motion correction was performed during the preprocessing of the data (Jenkinson et al. 2002). Third, a relatively new approach was applied to remove spatial components related to noise (Salimi-Khorshidi et al. 2014). This powerful technique used independent component analysis (ICA) to decompose the resting state fMRI data into spatial maps and removed the components related to non-neural noise, which provides an effective cleanup of the data (Griffanti, Dipasquale, et al. 2015). Although we found very similar values of movement across groups, special attention was paid to this denoising approach in which additional motion regressors were added to regress out motion related signal. Fourth, it has been shown that BOLD signal fluctuations measured in the white matter and cerebrospinal fluid are reliable representations of noise (Birn 2012). Therefore, white matter and cerebrospinal fluid templates were included in the analyses to further account for noise, even after the motion correction and noise reduction steps.

Patient selection

A limitation of studies that included data of patients (*chapters 4, 5, and 7*) is the possibility of misdiagnosis. Due to the heterogeneity of the symptoms, clinical differentiation between AD and bvFTD can be challenging. All patients that were included for this thesis, underwent an extensive dementia screening and were evaluated in a multidisciplinary panel including clinicians from different centers specialized in dementia. For two patients in our study population, the diagnosis could be further strengthened since mutations in progranulin (GRN) or microtubule associated protein tau (MAPT) were found. These genetic mutations have been identified as the major genetic causes of FTD (Seelaar et al. 2008; Rohrer et al. 2009). Only dementia patients that fulfilled the most recent clinical criteria for probable AD (McKhann 2011) and bvFTD (Rascovsky et al. 2011) were included. However, the diagnosis FTD or AD can only be diagnosed with certainty by brain autopsy after death. Postmortem data were not available, therefore the possibility of misdiagnosis cannot be excluded.

Cognitive functioning of all participants was assessed using an extensive neuropsychological protocol. As expected, both dementia groups performed worse on

cognitive functioning compared with controls. Patients with AD showed lowest scores a general measurement of cognitive performance (Folstein et al. 1975), and showed, in line with our expectations, a decline in cognitive performance over time. We expected lower executive functioning scores in bvFTD compared with AD, however, AD patients did not differ from bvFTD patients in most executive functioning tests. Overall, the AD patients showed low scores in all cognitive domains, not only in the memory domain, but also in executive functioning. Although executive functioning could be useful to differentiate AD from bvFTD (Iavarone et al. 2004; Slachevsky et al. 2004), some studies reported that executive functioning does not discriminate AD from bvFTD (Lipton et al. 2005; Castiglioni et al. 2006). It has been suggested that testing multiple cognitive domains is required to differentiate both types of dementia rather than focus on one cognitive test (Lipton et al. 2005). All patients underwent extensive neuropsychological assessment and diagnoses were established according to the core clinical criteria for probable AD (McKhann 2011) and bvFTD (Rascovsky et al. 2011), and therefore were not based on one single neuropsychological test score.

Multicenter studies

Most of the studies described in this thesis (*chapters 4, 5, and 7*) are based on multicenter data, which is a result of the collaboration between the Leiden University Medical Center, the Alzheimer Center of the VU University Medical Center Amsterdam, and the Alzheimer Center of the Erasmus University Medical Center Rotterdam. Although the distribution of participants between centers did not differ significantly between groups, we followed previous approaches to account for the potential effects of center (Kim et al. 2009; Zhou et al. 2010). The strengths of multicenter studies are the larger number of participants that can be included and the increased generalizability of the study findings. However, multicenter studies have also its limitations, since the data will be less homogenous than in single center studies. To increase homogeneity between centers, all patients were evaluated in a multidisciplinary panel including clinicians from the different centers. Furthermore, MRI scans were collected using comparable acquisition protocols, although this was not always possible since some sequences were already included in the routine diagnostic protocols. In addition, a standardization approach was applied in order to achieve better comparison across voxels, subjects, and centers (Yan et al. 2013). To further minimize possible center effects, center was used as covariate in all statistical models (Kim et al. 2009; Zhou et al. 2010).

8.4. FUTURE RESEARCH

The disease-specific network differences and longitudinal changes reported in this thesis show the potential of functional and structural networks to improve diagnostic accuracy, early differential diagnosis, and monitor disease progression. Although brain networks contribute to the understanding of dementia pathology, these are not yet suitable as biomarker for individual classification of dementia patients, since the results in this thesis are based on group differences, not on individual subjects. This thesis concludes with some recommendations for future research.

Individual classification

More work needs to be conducted to conclude whether brain networks will become useful as a clinical diagnostic tool for different types of dementia. Our research group recently extended the work described in this thesis and investigated the potential of a machine learning classification approach to improve individual classification of dementia patients. In addition to structural and functional network changes, valuable information for individual classification come from diffusion weighted MRI (Schouten et al. 2016) and cortical thickness (De Vos et al. 2016). Moreover, combining multiple MRI modalities might further improve diagnostic classification (Mesrob 2012; Sui et al. 2013). Furthermore, other imaging techniques than MRI could also provide promising biomarker information, which could include positron emission tomography (PET) and electroencephalography.

Preclinical stage

An early diagnosis is essential, since it gives clarity for patients and caregivers, more efficient health care, and most important, interventional studies are most promising at an early stage of the disease. Since dementia pathophysiology is present in the brain years before the first symptoms appear, studies in healthy persons carrying a genetic mutation that causes dementia are important for early detection and differentiation of dementia disorders.

Our research group in collaboration with the Alzheimer Center of the Erasmus University Medical Center Rotterdam used longitudinal resting-state fMRI, diffusion weighted MRI, and arterial spin labeling data to investigate brain changes in presymptomatic carriers with a mutation that causes FTD ((Dopper et al. 2014) and (Dopper et al. n.d.) submitted for publication). The promising findings from these

studies suggest that these various MRI methods provide sensitive biomarkers for presymptomatic carriers. Diffusion weighted MRI in particular might provide a predictor for conversion into the symptomatic disease stage.

Brain structure

For the multicenter project of this thesis, “Functional markers for cognitive disorders: dementia”, longitudinal structural MRI data were collected to study voxel-based structural brain differences between bvFTD and AD as well. Promising group differences in brain structure (Möller et al. 2015) and differences in gray matter loss over time (Möller, Hafkemeijer, et al. 2016) were found between the two types of dementia. Machine learning classification approach showed that brain structure might give reliable information that could improve the diagnostic process (Möller, Pijnenburg, et al. 2016). Further research is needed before changes in brain structure are useful as a clinical diagnostic tool in daily practice. Another challenge for future studies lies in the understanding of the relation between changes in brain structure and function, since the relationship between structure and function is very complex and is not yet completely understood.

Disease severity

Future studies might investigate the relationship between network changes and disease severity, which can be done by comparing groups of patients at different stages of the disease. Another approach might be studying possible associations between brain changes and changes in cognitive performance. In this thesis, associations with general measurements of cognitive performance were investigated. A relationship between brain changes and cognitive performance suggests the potential of brain networks to monitor disease severity. However, general screening tools should not be regarded as an extensive neuropsychological assessment. Future research is needed to investigate whether brain changes are related to dysfunction in specific cognitive domains and to investigate the relationship between network changes and disease severity.

8.5. CONCLUSION

Brain networks have the potential to give insight in cognitive dysfunctioning in dementia, since cognitive functions, including memory and behavior, are understood not to be localized in one specific brain area, but rather in networks of a multitude of brain regions (Evans 2013; Fornito et al. 2015). The network degeneration hypothesis implies that dementia starts in one part of the brain and progressively spreads to connected areas (Seeley et al. 2009).

The disease-specific network differences reported in this thesis suggest that studying brain networks can detect and discriminate different underlying pathophysiological mechanisms and show the opportunity to improve diagnostic accuracy and monitor disease progression. Functional and structural networks do contribute to our understanding of pathology in dementia and have the potential of serving as diagnostic tool since they allow reliable discrimination of groups. However, at this moment, these results are only applicable for groups of patients and not for individual subjects.

Chapter 9

Nederlandse samenvatting

Mensen leven langer dan ooit en de levensverwachting neemt steeds verder toe (Mathers et al. 2015). Een gevorderde leeftijd is één van de belangrijkste risicofactoren voor het ontwikkelen van dementie. De komende jaren zal daarom het aantal dementie patiënten toenemen. De ziekte van Alzheimer (Engelse afkorting AD) is de meest voorkomende vorm van dementie en wordt voornamelijk gekarakteriseerd door geheugenverlies (McKhann 2011). Een ander veelvoorkomend type dementie is de gedragsvariant van frontotemporale dementie (Engelse afkorting bvFTD) (Ratnavalli et al. 2002). Patiënten met bvFTD presenteren zich met veranderingen in gedrag en persoonlijkheid (Rascovsky et al. 2011). Echter, de symptomen variëren sterk, met overlap tussen de verschillende vormen van dementie. Hierdoor kan het lastig zijn klinisch onderscheid te maken tussen AD en bvFTD. Dit leidt voornamelijk vroeg in het ziekteproces tot problemen.

Een vroege en juiste diagnose is van groot belang omdat het duidelijkheid geeft voor de patiënt en diens verzorgers, het zal leiden tot efficiëntere gezondheidszorg en interventionele studies hebben de meeste kans op succes als ze op een vroeg moment in het ziekteproces worden uitgevoerd. Om vroegtijdige diagnostiek te verbeteren is er een grote behoefte aan meetbare kenmerken die geassocieerd zijn met de verschillende vormen van dementie (Raamana et al. 2014).

9.1. ONDERZOEKSDOEL VAN DIT PROEFSCHRIFT

In dit proefschrift bestuderen we de hersenen bij veroudering en dementie. Cognitief functioneren, zoals geheugen en gedrag, is naar alle waarschijnlijkheid niet gelokaliseerd in één specifiek gebied in de hersenen, maar in een netwerk bestaande uit verschillende hersengebieden. Daarom hebben hersennetwerken de potentie om meer inzicht te geven in cognitief disfunctioneren bij dementerenden vergeleken met methodes die zich richten op één bepaald hersengebied (Evans 2013; Fornito et al. 2015). De netwerkdegeneratie hypothese gaat ervan uit dat dementie begint in een bepaald gebied in de hersenen en zich verder uitbreidt naar gebieden die hiermee verbonden zijn (Seeley et al. 2009). Men vermoedt dat elke neurodegeneratieve ziekte, en dus ook elke vorm van dementie, een specifiek netwerk van degeneratie heeft (Seeley et al. 2009).

Het doel van de studies beschreven in dit proefschrift was meer inzicht te krijgen in hersennetwerken bij gezonde veroudering (*hoofdstukken 2 en 6*) en hoe deze afwijken

bij mensen met subjectieve geheugenklachten (*hoofdstuk 3*) en bij patiënten met dementie (*hoofdstukken 2, 4, 5 en 7*). Hierbij gebruikte we magnetische resonantie imaging (MRI) om zowel de functie (*sectie 1*) als de structuur (*sectie 2*) van de hersennetwerken te onderzoeken.

9.2. FUNCTIONELE HERSENNETWERKEN

De eerste sectie van dit proefschrift beschrijft de bevindingen in functionele netwerken (*sectie 1*). Deze netwerken zijn opgebouwd uit hersengebieden die overeenkomsten in functie vertonen.

Hoofdstuk 2 geeft een literatuur overzicht van studies die het zogenaamde ‘default mode’ netwerk bestuderen bij veroudering en dementie. Dit netwerk is specifiek van belang voor gezonde veroudering en dementie omdat de structuren hiervan vatbaar zijn voor dementie pathologie (Buckner et al. 2005). Dit hoofdstuk geeft relevante achtergrond informatie voor het verdere werk dat in dit proefschrift wordt gepresenteerd. Een Nederlandse versie van dit hoofdstuk is terug te vinden in het themanummer ‘Neuro fMRI’ van het radiologen tijdschrift ‘MemoRad’ (Hafkemeijer, van der Grond, van Buchem, et al. 2012).

Hoofdstuk 3 beschrijft de bevindingen van een studie naar functionele netwerken bij ouderen met zelf-gerapporteerde subjectieve geheugenklachten die niet voldoen aan de criteria voor milde cognitieve achteruitgang of dementie. Deze ouderen hebben dus wel geheugenklachten maar zijn niet dement. Deze studie laat veranderingen zien in zowel de hersenstructuur als in functionele hersennetwerken. Dit toont vermoedelijk aan dat deze subjectieve geheugenklachten een weerspiegeling zijn van objectieve veranderingen in het brein.

Hoofdstukken 4 en 5 zijn het resultaat van een samenwerking tussen het Leids Universitair Medisch Centrum, het Alzheimer centrum van de Vrije Universiteit Universitair Medisch Centrum Amsterdam en het Alzheimer centrum van het Erasmus Universitair Medisch Centrum Rotterdam. Beide hoofdstukken hebben als doel om te onderzoeken of functionele netwerken nuttig zijn bij het onderscheiden van verschillende vormen van dementie. In *hoofdstuk 4* laten we zien dat al in een vroeg stadium van de ziekte de functionele netwerken verschillend zijn tussen patiënten met AD en patiënten met bvFTD. We hebben deze patiënten in de loop van hun ziekte

gevolgd. *Hoofdstuk 5* beschrijft de longitudinale studie waarin we vonden dat elke vorm van dementie veranderingen over de tijd liet zien in een ziekte specifiek netwerk. Dit toont het belang van longitudinale studies aan om inzicht te krijgen in hersengebieden die relevant zijn voor ziekteprogressie en differentiaal diagnose.

9.3. STRUCTURELE HERSENNETWERKEN

Naast de functionele netwerken zijn in dit proefschrift ook structurele netwerken bestudeerd (*sectie 2*). Deze netwerken zijn opgebouwd uit hersengebieden die overeenkomsten in structuur vertonen. Om deze netwerken te kunnen bestuderen is een relatief nieuwe methode toegepast.

Hoofdstuk 6 beschrijft de invloed van gezonde veroudering op deze structurele netwerken. Bepaalde netwerken gaan achteruit met het ouder worden, terwijl andere netwerken juist relatief onaangetast blijven. In *hoofdstuk 7* beschrijven we hoe deze netwerken eruitzien bij dementerenden. De resultaten bevestigen ons vermoeden dat de verschillende vormen van dementie verschillende netwerken aantasten, wat laat zien dat structurele netwerken ons waardevolle informatie geven over de ziekte en een goede aanvulling kunnen zijn op de vaker bestudeerde functionele netwerken.

9.4. CONCLUSIE

Samenvattend laten de studies beschreven in dit proefschrift zien dat hersennetwerken ons meer inzicht geven in het proces dat zich afspeelt in het brein van gezonde ouderen, mensen met subjectieve geheugenklachten en van patiënten met dementie. Bovendien geeft het in de toekomst mogelijkheden om vroeg diagnostiek te verbeteren en ziekteprogressie te monitoren. Eén kanttekening echter: hoewel de bevindingen gepresenteerd in dit proefschrift ons veel leren over verschillen op groepsniveau, zijn ze op dit moment nog niet direct toepasbaar in de praktijk. Verder onderzoek in de toekomst zal uitwijzen of hersennetwerken van belang zijn bij het stellen van de diagnose van een individuele patiënt.

Appendix

Abbreviations

References

Dankwoord

Curriculum vitae

List of publications

Abbreviations

ACC	Anterior Cingulate Cortex
AD	Alzheimer's Disease
APOE4	Apolipoprotein E4
BOLD	Blood Oxygenation Level Dependent
bvFTD	Behavioral variant Frontotemporal Dementia
CDR	Clinical Dementia Rating
DLB	Dementia with Lewy Bodies
DMN	Default Mode Network
FAB	Frontal Assessment Battery
FIX	FMRIB's ICA-based Xnoiseifier
FLAIR	Fluid-Attenuated Inversion Recovery
fMRI	Functional Magnetic Resonance Imaging
FSL	Functional magnetic resonance imaging of the brain Software Library
FWE	Family-Wise Error
GDS	Geriatric Depression Scale
GLM	General Linear Model
GRN	Progranulin
ICA	Independent Component Analysis
MAPT	Microtubule Associated Protein Tau
MCI	Mild Cognitive Impairment
MMSE	Mini Mental State Examination
MNI	Montreal Neurological Institute standard space image
mPFC	Medial Prefrontal Cortex
MRI	Magnetic Resonance Imaging
PCC	Posterior Cingulate Cortex
PET	Positron Emission Tomography
RSNs	Resting State Networks
SCNs	Structural Covariance Networks
SMC	Subjective Memory Complaints
TFCE	Threshold-Free Cluster Enhancement
VBM	Voxel-Based Morphometric
WMHs	White Matter Hyperintensities
3D	Three-Dimensional

References

- Agosta F, Sala S, Valsasina P, Meani A, Canu E, Magnani G, Cappa SF, Scola E, Quatto P, Horsfield MA, Falini A, Comi G, Filippi M. 2013. Brain network connectivity assessed using graph theory in frontotemporal dementia. *Neurology* 81:134–143.
- Alexander GE, Chen K, Merkle TL, Reiman EM, Caselli RJ, Aschenbrenner M, Santerre-Lemmon L, Lewis DJ, Pietrini P, Teipel SJ, Hampel H, Rapoport SI, Moeller JR. 2006. Regional network of magnetic resonance imaging gray matter volume in healthy aging. *Neuroreport* 17:951–956.
- Alexander-Bloch A, Raznahan A, Bullmore E, Giedd J. 2013. The convergence of maturational change and structural covariance in human cortical networks. *J Neurosci* 33:2889–2899.
- Allen G, Barnard H, McColl R, Hester AL, Fields JA, Weiner MF, Ringe WK, Lipton AM, Brooker M, McDonald E, Rubin CD, Cullum CM. 2007. Reduced hippocampal functional connectivity in Alzheimer disease. *Arch Neurol* 64:1482–1487.
- Altmann-Schneider I, van der Grond J, Slagboom PE, Westendorp RGJ, Maier AB, van Buchem MA, de Craen AJM. 2013. Lower susceptibility to cerebral small vessel disease in human familial longevity: the leiden longevity study. *Stroke* 44:9–14.
- American Psychiatric Association A. 1994. Diagnostic and statistical manual of mental disorders, 4th Edn. Washington DC, Am Psychiatric Assoc 4:1–886.
- Andersson JLR, Jenkinson M, Smith S. 2007a. Non-linear optimisation. FMRIB Tech Rep TR07JA1 from www.fmrib.ox.ac.uk/analysis/techrep Last accessed June 26, 2015.
- Andersson JLR, Jenkinson M, Smith S. 2007b. Non-linear registration aka Spatial normalisation. FMRIB Tech Rep TR07JA2 from www.fmrib.ox.ac.uk/analysis/techrep Last accessed June 26, 2015.
- Andrews-Hanna JR, Snyder AZ, Vincent JL, Lustig C, Head D, Raichle ME, Buckner RL. 2007. Disruption of large-scale brain systems in advanced aging. *Neuron* 56:924–935.
- Army Test Battery. 1994. Army Individual Test Battery. Manual of directions and scoring. War Dep Adjut Gen Off Washington, DC.
- Ashburner J, Friston KJ. 2000. Voxel-based morphometry - the methods. *Neuroimage* 11:805–821.
- Bai F, Zhang Z, Yu H, Shi Y, Yuan Y, Zhu W, Zhang X, Qian Y. 2008. Default-mode network activity distinguishes amnesic type mild cognitive impairment from healthy aging: a combined structural and resting-state functional MRI study. *Neurosci Lett* 438:111–115.
- Bajo R, Castellanos NP, López ME, Ruiz JM, Montejo P, Montenegro M, Llanero M, Gil

- P, Yubero R, Baykova E, Paul N, Aurtenetxe S, Del Pozo F, Maestu F. 2011. Early dysfunction of functional connectivity in healthy elderly with subjective memory complaints. *Age (Omaha)* 34:497–506.
- Balthazar MLF, de Campos BM, Franco AR, Damasceno BP, Cendes F. 2014. Whole cortical and default mode network mean functional connectivity as potential biomarkers for mild Alzheimer's disease. *Psychiatry Res* 221:37–42.
- Barnes J, Godbolt AK, Frost C, Boyes RG, Jones BF, Scahill RI, Rossor MN, Fox NC. 2007. Atrophy rates of the cingulate gyrus and hippocampus in AD and FTLD. *Neurobiol Aging* 28:20–28.
- Beckmann CF, Deluca M, Devlin JT, Smith SM. 2005. Investigations into resting-state connectivity using independent component analysis. *Phil Trans R Soc B* 360:1001–1013.
- Beckmann CF, Smith SM. 2004. Probabilistic independent component analysis for functional magnetic resonance imaging. *IEEE Trans Med Imaging* 23:137–152.
- Benson DF, Kuhl DE, Hawkins RA, Phelps ME, Cummings JL, Tsai SY. 1983. The fluorodeoxyglucose 18F scan in Alzheimer's disease and multi-infarct dementia. *Arch Neurol* 40:711–714.
- Bergfield KL, Hanson KD, Chen K, Teipel SJ, Hampel H, Rapoport SI, Moeller JR, Alexander GE. 2010. Age-related networks of regional covariance in MRI gray matter: reproducible multivariate patterns in healthy aging. *Neuroimage* 49:1750–1759.
- Binnewijzend MAA, Schoonheim MM, Sanz-Arigita E, Wink AM, van der Flier WM, Tolboom N, Adriaanse SM, Damoiseaux JS, Scheltens P, van Berckel BNM, Barkhof F. 2012. Resting-state fMRI changes in Alzheimer's disease and mild cognitive impairment. *Neurobiol Aging* 33:2018–2028.
- Birn RM. 2012. The role of physiological noise in resting-state functional connectivity. *Neuroimage* 62:864–870.
- Biswal BB, Mennes M, Zuo X, Gohel S, Kelly C, Smith SM, Beckmann CF, Adelstein JS, Buckner RL, Colcombe S, Dogonowski A, Ernst M, Fair D, Hampson M, Hoptman MJ, Hyde JS, Kiviniemi VJ, Kötter R, Li S, Lin C, Lowe MJ, Mackay C, Madden DJ, Madsen KH, Margulies DS, Mayberg HS, McMahon K, Monk CS, Mostofsky SH, Nagel BJ, Pekar JJ, Peltier SJ, Petersen SE, Riedl V, Rombouts SARB, Rypma B, Schlaggar BL, Schmidt S, Seidler RD, Siegle GJ, Sorg C, Teng G, Veijola J, Villringer A, Walter M, Wang L, Weng X, Whitfield-gabrieli S, Williamson P, Windischberger C, Zang Y, Zhang H, Castellanos FX, Milham MP. 2010. Toward discovery science of human brain function. *Proc Natl Acad Sci USA* 107:4734–4739.
- Bokde ALW, Lopez-Bayo P, Born C, Dong W, Meindl T, Leinsinger G, Teipel SJ, Faltraco F, Reiser M, Möller H-J, Hampel H. 2008. Functional abnormalities of the visual processing system in subjects with mild cognitive impairment: An fMRI study. *Psychiatry Res* 163:248–259.

- Bokde ALW, Lopez-Bayo P, Born C, Ewers M, Meindl T, Teipel SJ, Faltraco F, Reiser MF, Moller H-J, Hampel H. 2010. Alzheimer disease: functional abnormalities in the dorsal visual pathway. *Radiology* 254:219–226.
- Bondi MW, Houston WS, Eyster LT, Brown GG. 2005. fMRI evidence of compensatory mechanisms in older adults at genetic risk for Alzheimer disease. *Neurology* 64:501–508.
- Bookheimer SY, Strojwas MH, Cohen MS, Saunders AM, Pericak-Vance MA, Mazziotta JC, Small GW. 2000. Patterns of brain activation in people at risk for Alzheimer's disease. *N Engl J Med* 343:450–456.
- Borroni B, Alberici A, Cercignani M, Premi E, Serra L, Cerini C, Cosseddu M, Pettenati C, Turla M, Archetti S, Gasparotti R, Caltagirone C, Padovani A, Bozzali M. 2012. Granulin mutation drives brain damage and reorganization from preclinical to symptomatic FTL. *Neurobiol Aging* 33:2506–2520.
- Bosch B, Bartrés-Faz D, Rami L, Arenaza-Urquijo EM, Fernández-Espejo D, Junqué C, Solé-Padullés C, Sánchez-Valle R, Bargalló N, Falcón C, Molinuevo JL. 2010. Cognitive reserve modulates task-induced activations and deactivations in healthy elders, amnesic mild cognitive impairment and mild Alzheimer's disease. *Cortex* 46:451–461.
- Braak H, Braak E. 1991. Neuropathological staging of Alzheimer-related changes. *Acta Neuropathol* 82:239–259.
- Brickman AM, Habeck C, Zarahn E, Flynn J, Stern Y. 2007. Structural MRI covariance patterns associated with normal aging and neuropsychological functioning. *Neurobiol Aging* 28:284–295.
- Brier MR, Thomas JB, Fagan AM, Hassenstab J, Holtzman DM, Benzinger TL, Morris JC, Ances BM. 2014. Functional connectivity and graph theory in preclinical Alzheimer's disease. *Neurobiol Aging* 35:757–768.
- Broe M, Hodges JR, Schofield E, Shepherd CE, Kril JJ, Halliday GM. 2003. Staging disease severity in pathologically confirmed cases of frontotemporal dementia. *Neurology* 60:1005–1011.
- Broyd SJ, Demanuele C, Debener S, Helps SK, James CJ, Sonuga-Barke EJS. 2009. Default-mode brain dysfunction in mental disorders: a systematic review. *Neurosci Biobehav Rev* 33:279–296.
- Buckner RL, Andrews-Hanna JR, Schacter DL. 2008. The brain's default network: anatomy, function, and relevance to disease. *Ann N Y Acad Sci* 1124:1–38.
- Buckner RL, Sepulcre J, Talukdar T, Krienen FM, Liu H, Hedden T, Andrews-Hanna JR, Sperling R a, Johnson K a. 2009. Cortical hubs revealed by intrinsic functional connectivity: mapping, assessment of stability, and relation to Alzheimer's disease. *J Neurosci* 29:1860–1873.
- Buckner RL, Snyder AZ, Sanders AL, Raichle ME, Morris JC. 2000. Functional brain

- imaging of young, nondemented, and demented older adults. *J Cogn Neurosci* 12:24–34.
- Buckner RL, Snyder AZ, Shannon BJ, LaRossa G, Sachs R, Fotenos AF, Sheline YI, Klunk WE, Mathis CA, Morris JC, Mintun MA. 2005. Molecular, structural, and functional characterization of Alzheimer's disease: evidence for a relationship between default activity, amyloid, and memory. *J Neurosci* 25:7709–7717.
- Castiglioni S, Pelati O, Zuffi M, Somalvico F, Marino L, Tentorio T, Franceschi M. 2006. The frontal assessment battery does not differentiate frontotemporal dementia from Alzheimer's disease. *Dement Geriatr Cogn Disord* 22:125–131.
- Celone KA, Calhoun VD, Dickerson BC, Atri A, Chua EF, Miller SL, DePeau K, Rentz DM, Selkoe DJ, Blacker D, Albert MS, Sperling RA. 2006. Alterations in memory networks in mild cognitive impairment and Alzheimer's disease: an independent component analysis. *J Neurosci* 26:10222–10231.
- Chai XJ, Castañón AN, Ongür D, Whitfield-Gabrieli S. 2012. Anticorrelations in resting state networks without global signal regression. *Neuroimage* 59:1420–1428.
- Chen G, Ward D, Xie C, Li W, Wu Z, Jones J, Franczak M, Antuono P, Li S-J. 2011. Classification of Alzheimer Disease, mild cognitive impairment, and normal cognitive status with large-scale network analysis based on resting-state functional MR imaging. *Radiology* 259:213–221.
- Chhatwal JP, Schultz AP, Johnson K, Jack C, Ances BM, Sullivan CA, Salloway SP, Ringman JM, Koeppe RA, Marcus DS, Thompson P, Correia S, Rowe CC, Buckles VD, Morris JC, Sperling RA. 2013. Impaired default network functional connectivity in autosomal dominant Alzheimer disease. *Neurology* 81:736–744.
- Cole DM, Smith SM, Beckmann CF. 2010. Advances and pitfalls in the analysis and interpretation of resting-state fMRI data. *Front Syst Neurosci* 4:1–15.
- Couto B, Sedeño L, Sposato LA, Sigman M, Riccio PM, Salles A, Lopez V, Schroeder J, Manes F, Ibanez A. 2013. Insular networks for emotional processing and social cognition: comparison of two case reports with either cortical or subcortical involvement. *Cortex* 49:1420–1434.
- Damoiseaux JS, Beckmann CF, Arigita EJS, Barkhof F, Scheltens P, Stam CJ, Smith SM, Rombouts SARB. 2008. Reduced resting-state brain activity in the “default network” in normal aging. *Cereb Cortex* 18:1856–1864.
- Damoiseaux JS, Greicius MD. 2009. Greater than the sum of its parts: a review of studies combining structural connectivity and resting-state functional connectivity. *Brain Struct Funct* 213:525–533.
- Damoiseaux JS, Prater KE, Miller BL, Greicius MD. 2012. Functional connectivity tracks clinical deterioration in Alzheimer's disease. *Neurobiol Aging* 33:19–30.
- Damoiseaux JS, Rombouts SARB, Barkhof F, Scheltens P, Stam CJ, Smith SM, Beckmann CF. 2006. Consistent resting-state networks across healthy subjects. *Proc Natl*

- Acad Sci USA 103:13848–13853.
- Day GS, Farb NAS, Tang-Wai DF, Masellis M, Black SE, Freedman M, Pollock BG, Chow TW. 2013. Saliency network resting-state activity: prediction of frontotemporal dementia progression. *JAMA Neurol* 70:1249–1253.
- De Rover M, Pironti VA, McCabe JA, Acosta-Cabronero J, Arana FS, Morein-Zamir S, Hodges JR, Robbins TW, Fletcher PC, Nestor PJ, Sahakian BJ. 2011. Hippocampal dysfunction in patients with mild cognitive impairment: a functional neuroimaging study of a visuospatial paired associates learning task. *Neuropsychologia* 49:2060–2070.
- De Vos F, Schouten T, Hafkemeijer A, Dopper E, van Swieten J, de Rooij M, van der Grond J, Rombouts S. 2016. Combining multiple anatomical MRI measures improves Alzheimer's classification. In press. *Hum Brain Mapp*.
- Delaère P, He Y, Fayet G, Duyckaerts C, Hauw JJ. 1993. Beta A4 deposits are constant in the brain of the oldest old: an immunocytochemical study of 20 French centenarians. *Neurobiol Aging* 14:191–194.
- Dennis NA, Browndyke JN, Stokes J, Need A, Burke JR, Welsh-Bohmer KA, Cabeza R. 2010. Temporal lobe functional activity and connectivity in young adult APOE varepsilon4 carriers. *Alzheimers Dement* 6:303–311.
- Dik MG, Jonker C, Comijs HC, Bouter LM, Twisk JW, van Kamp GJ, Deeg DJ. 2001. Memory complaints and APOE-epsilon4 accelerate cognitive decline in cognitively normal elderly. *Neurology* 57:2217–2222.
- Dopper E, Jiskoot L, den Heijer T, Hafkemeijer A, de Koning I, Seelaar H, Veer I, van Buchem M, van Minkelen R, Rombouts S, van Swieten J. n.d. Longitudinal brain changes in presymptomatic familial frontotemporal dementia. Submitted for publication.
- Dopper EGP, Rombouts SAR, Jiskoot LC, den Heijer T, de Graaf JRA, de Koning I, Hammerschlag AR, Seelaar H, Seeley WW, Veer IM, van Buchem MA, Rizzu P, van Swieten JC. 2014. Structural and functional brain connectivity in presymptomatic familial frontotemporal dementia. *Neurology* 83:e19–e26.
- Douaud G, Groves AR, Tamnes CK, Westlye LT, Duff EP, Engvig A, Walhovd KB, James A, Gass A, Monsch AU, Matthews PM, Fjell AM, Smith SM, Johansen-Berg H. 2014. A common brain network links development, aging, and vulnerability to disease. *Proc Natl Acad Sci USA* 111:17648–17653.
- Drzezga A, Becker JA, Van Dijk KRA, Sreenivasan A, Talukdar T, Sullivan C, Schultz AP, Sepulcre J, Putcha D, Greve D, Johnson KA, Sperling RA. 2011. Neuronal dysfunction and disconnection of cortical hubs in non-demented subjects with elevated amyloid burdens. *Brain* 134:1635–1646.
- Dubois B, Slachevsky A, Litvan I, Pillon B. 2000. The FAB: A frontal assessment battery at bedside. *Neurology* 55:1621–1626.

- Evans AC. 2013. Networks of anatomical covariance. *Neuroimage* 80:489–504.
- Farb NAS, Grady CL, Strother S, Tang-Wai DF, Masellis M, Black S, Freedman M, Pollock BG, Campbell KL, Hasher L, Chow TW. 2013. Abnormal network connectivity in frontotemporal dementia: evidence for prefrontal isolation. *Cortex* 49:1856–1873.
- Ferreira LK, Busatto GF. 2013. Resting-state functional connectivity in normal brain aging. *Neurosci Biobehav Rev* 37:384–400.
- Filippi M, Agosta F. 2011. Structural and functional network connectivity breakdown in Alzheimer’s disease studied with magnetic resonance imaging techniques. *J Alzheimers Dis* 24:455–474.
- Filippi M, Agosta F, Scola E, Canu E, Magnani G, Marcone A, Valsasina P, Caso F, Copetti M, Comi G, Cappa SF, Falini A. 2013. Functional network connectivity in the behavioral variant of frontotemporal dementia. *Cortex* 49:2389–2401.
- Filippini N, MacIntosh BJ, Hough MG, Goodwin GM, Frisoni GB, Smith SM, Matthews PM, Beckmann CF, Mackay CE. 2009. Distinct patterns of brain activity in young carriers of the APOE-epsilon4 allele. *Proc Natl Acad Sci USA* 106:7209–7214.
- Fleisher AS, Houston WS, Eyler LT, Frye S, Jenkins C, Thal LJ, Bondi MW. 2005. Identification of Alzheimer Disease risk by functional magnetic resonance imaging. *Arch Neurol* 62:1881–1888.
- Fleisher AS, Sherzai A, Taylor C, Langbaum JBS, Chen K, Buxton RB. 2009. Resting-state BOLD networks versus task-associated functional MRI for distinguishing Alzheimer’s disease risk groups. *Neuroimage* 47:1678–1690.
- Folstein MF, Folstein SE, McHugh PR. 1975. Mini-mental state: a practical method for grading the cognitive state of patients for the clinician. *J Psychiat Res* 12:189–198.
- Fornito A, Zalesky A, Breakspear M. 2015. The connectomics of brain disorders. *Nat Rev Neurosci* 16:159–172.
- Fox MD, Raichle ME. 2007. Spontaneous fluctuations in brain activity observed with functional magnetic resonance imaging. *Nat Rev Neurol* 8:700–711.
- Fox MD, Snyder AZ, Vincent JL, Corbetta M, Van Essen DC, Raichle ME. 2005. The human brain is intrinsically organized into dynamic, anticorrelated functional networks. *Proc Natl Acad Sci USA* 102:9673–9678.
- Fox MD, Zhang D, Snyder AZ, Raichle ME. 2009. The global signal and observed anticorrelated resting state brain networks. *J Neurophysiol* 101:3270–3283.
- Fox NC, Schott JM. 2004. Imaging cerebral atrophy: normal ageing to Alzheimer’s disease. *Lancet* 363:392–394.
- Frings L, Yew B, Flanagan E, Lam BYK, Hüll M, Huppertz H-J, Hodges JR, Hornberger M. 2014. Longitudinal grey and white matter changes in frontotemporal dementia

- and Alzheimer's disease. *PLoS One* 9:1–8.
- Gallagher M, Bakker A, Yassa M, Stark C. 2010. Bridging neurocognitive aging and disease modification: targeting functional mechanisms of impairment. *Curr Alzheimer Res* 7:197–199.
- Galluzzi S, Lanni C, Pantoni L, Filippi M, Frisoni GB. 2008. White matter lesions in the elderly: pathophysiological hypothesis on the effect on brain plasticity and reserve. *J Neurol Sci* 273:3–9.
- Galvin JE, Price JL, Yan Z, Morris JC, Sheline YI. 2011. Resting bold fMRI differentiates dementia with Lewy bodies vs Alzheimer disease. *Neurology* 76:1797–1803.
- Genovese CR, Lazar NA, Nichols T. 2002. Thresholding of statistical maps in functional neuroimaging using the false discovery rate. *Neuroimage* 15:870–878.
- Gili T, Cercignani M, Serra L, Perri R, Giove F, Maraviglia B, Caltagirone C, Bozzali M. 2011. Regional brain atrophy and functional disconnection across Alzheimer's disease evolution. *J Neurol Neurosurg Psychiatry* 82:58–66.
- Glodzik-Sobanska L, Reisberg B, De Santi S, Babb JS, Pirraglia E, Rich KE, Brys M, de Leon MJ. 2007. Subjective memory complaints: presence, severity and future outcome in normal older subjects. *Dement Geriatr Cogn Disord* 24:177–184.
- Gomez-Ramirez J, Wu J. 2014. Network-based biomarkers in Alzheimer's disease: review and future directions. *Front Aging Neurosci* 6:1–9.
- Good CD, Johnsrude IS, Ashburner J, Henson RN, Friston KJ, Frackowiak RS. 2001. A voxel-based morphometric study of ageing in 465 normal adult human brains. *Neuroimage* 14:21–36.
- Grady C. 2012. The cognitive neuroscience of ageing. *Nat Rev Neurosci* 13:491–505.
- Grady CL, McIntosh AR, Beig S, Keightley ML, Burian H, Black SE. 2003. Evidence from functional neuroimaging of a compensatory prefrontal network in Alzheimer's disease. *J Neurosci* 23:986–993.
- Grady CL, Springer M V, Hongwanishkul D, McIntosh AR, Winocur G. 2006. Age-related changes in brain activity across the adult lifespan. *J Cogn Neurosci* 18:227–241.
- Greicius MD, Srivastava G, Reiss AL, Menon V. 2004. Default-mode network activity distinguishes Alzheimer's disease from healthy aging: evidence from functional MRI. *Proc Natl Acad Sci USA* 101:4637–4642.
- Greve DN, Fischl B. 2009. Accurate and robust brain image alignment using boundary-based registration. *Neuroimage* 48:63–72.
- Griffanti L, Dipasquale O, Laganà MM, Nemni R, Clerici M, Smith SM, Baselli G, Baglio F. 2015. Effective artifact removal in resting state fMRI data improves detection of DMN functional connectivity alteration in Alzheimer's disease. *Front Hum Neurosci* 9:1–11.

- Griffanti L, Rolinski M, Szewczyk-Krolikowski K, Menke RA, Filippini N, Zamboni G, Jenkinson M, Hu MTM, Mackay CE. 2015. Challenges in the reproducibility of clinical studies with resting state fMRI: An example in early Parkinson's disease. *Neuroimage* 16:704–713.
- Gusnard DA, Raichle ME. 2001. Searching for a baseline: functional imaging and the resting human brain. *Nat Rev Neurosci* 2:685–694.
- Hafkemeijer A, Altmann-Schneider I, de Craen AJM, Slagboom PE, van der Grond J, Rombouts SA. 2014. Associations between age and gray matter volume in anatomical brain networks in middle-aged to older adults. *Aging Cell* 13:1068–1074.
- Hafkemeijer A, Altmann-Schneider I, Oleksik AM, van de Wiel L, Middelkoop HA, van Buchem MA, van der Grond J, Rombouts SA. 2013. Increased functional connectivity and brain atrophy in elderly with subjective memory complaints. *Brain Connect* 3:353–362.
- Hafkemeijer A, Möller C, Dopfer EG, Jiskoot LC, van Swieten JC, van der Flier WM, Vrenken H, Pijnenburg YA, Barkhof F, Scheltens P, van der Grond J, Rombouts SA. 2015. Resting state functional connectivity differences between behavioral variant frontotemporal dementia and Alzheimer's disease. *Front Hum Neurosci* 9:1–12.
- Hafkemeijer A, van der Grond J, Rombouts SA. 2012. Imaging the default mode network in aging and dementia. *Biochim Biophys Acta* 1822:431–441.
- Hafkemeijer A, van der Grond J, van Buchem MA, Rombouts SAR. 2012. fMRI bij veroudering en dementie: het default-mode netwerk. *MemoRad Neuro-fMRI* 17:40–44.
- Hampson M, Driesen N, Roth JK, Gore JC, Constable RT. 2010. Functional connectivity between task-positive and task-negative brain areas and its relation to working memory performance. *Magn Reson Imaging* 28:1051–1057.
- Han Y, Wang J, Zhao Z, Min B, Lu J, Li K, He Y, Jia J. 2011. Frequency-dependent changes in the amplitude of low-frequency fluctuations in amnesic mild cognitive impairment: a resting-state fMRI study. *Neuroimage* 55:287–295.
- He X, Qin W, Liu Y, Zhang X, Duan Y, Song J, Li K, Jiang T, Yu C. 2014. Abnormal salience network in normal aging and in amnesic mild cognitive impairment and Alzheimer's disease. *Hum Brain Mapp* 35:3446–3464.
- He Y, Chen Z, Evans A. 2008. Structural insights into aberrant topological patterns of large-scale cortical networks in Alzheimer's disease. *J Neurosci* 28:4756–4766.
- He Y, Wang L, Zang Y, Tian L, Zhang X, Li K, Jiang T. 2007. Regional coherence changes in the early stages of Alzheimer's disease: a combined structural and resting-state functional MRI study. *Neuroimage* 35:488–500.
- Hedden T, Van Dijk KRA, Becker JA, Mehta A, Sperling RA, Johnson KA, Buckner RL.

2009. Disruption of functional connectivity in clinically normal older adults harboring amyloid burden. *J Neurosci* 29:12686–12694.
- Hejl A, Høgh P, Waldemar G. 2002. Potentially reversible conditions in 1000 consecutive memory clinic patients. *J Neurol Neurosurg Psychiatry* 73:390–404.
- Horwitz B, McIntosh A, Haxby J, Furey M, Salerno J, Schapiro M, Rapoport S, Grady C. 1995. Network analysis of PET-mapped visual pathways in Alzheimer type dementia. *Neuroreport* 2287–2292.
- Iavarone A, Ronga B, Pellegrino L, Loré E, Vitaliano S, Galeone F, Carlomagno S. 2004. The Frontal Assessment Battery (FAB): normative data from an Italian sample and performances of patients with Alzheimer’s disease and frontotemporal dementia. *Funct Neurol* 19:191–195.
- Irish M, Piguet O, Hodges JR, Hornberger M. 2014. Common and unique gray matter correlates of episodic memory dysfunction in frontotemporal dementia and Alzheimer’s disease. *Hum Brain Mapp* 35:1422–1435.
- Jack CR, Knopman DS, Jagust WJ, Shaw LM, Aisen PS, Weiner MW, Petersen RC, Trojanowski JQ. 2010. Hypothetical model of dynamic biomarkers of the Alzheimer’s pathological cascade. *Lancet Neurol* 9:119–128.
- Jack CR, Petersen RC, Xu YC, O’Brien PC, Smith GE, Ivnik RJ, Boeve BF, Waring SC, Tangalos EG, Kokmen E. 1999. Prediction of AD with MRI-based hippocampal volume in mild cognitive impairment. *Neurology* 52:1397–1403.
- Jafri M, Pearlson G, Stevens M, Calhoun V. 2008. A method for functional network connectivity among spatially independent resting-state components in schizophrenia. *Neuroimage* 39:1666–1681.
- Jenkinson M, Bannister P, Brady M, Smith S. 2002. Improved optimization for the robust and accurate linear registration and motion correction of brain images. *Neuroimage* 17:825–841.
- Jernigan TL, Archibald SL, Fennema-Notestine C, Gamst AC, Stout JC, Bonner J, Hesselink JR. 2001. Effects of age on tissues and regions of the cerebrum and cerebellum. *Neurobiol Aging* 22:581–594.
- Jessen F, Amariglio RE, van Boxtel M, Breteler M, Ceccaldi M, Chételat G, Dubois B, Dufouil C, Ellis KA, van der Flier WM, Glodzik L, van Harten AC, de Leon MJ, McHugh P, Mielke MM, Molinuevo JL, Mosconi L, Osorio RS, Perrotin A, Petersen RC, Rabin LA, Rami L, Reisberg B, Rentz DM, Sachdev PS, de la Sayette V, Saykin AJ, Scheltens P, Shulman MB, Slavin MJ, Sperling RA, Stewart R, Uspenskaya O, Vellas B, Visser PJ, Wagner M. 2014. A conceptual framework for research on subjective cognitive decline in preclinical Alzheimer’s disease. *Alzheimers Dement* 10:844–852.
- Jessen F, Feyen L, Freymann K, Tepest R, Maier W, Heun R, Schild H-H, Scheef L. 2006. Volume reduction of the entorhinal cortex in subjective memory impairment. *Neurobiol Aging* 27:1751–1756.

- Jessen F, Wiese B, Bachmann C, Eifflaender-Gorfer S, Haller F, Kölsch H, Luck T, Mösch E, van den Bussche H, Wagner M, Wollny A, Zimmermann T, Pentzek M, Riedel-Heller SG, Romberg H-P, Weyerer S, Kaduszkiewicz H, Maier W, Bickel H. 2010. Prediction of dementia by subjective memory impairment: effects of severity and temporal association with cognitive impairment. *Arch Gen Psychiatry* 67:414–422.
- Jolles J, Houx P, van Boxtel M, Ponds R. 1995. Maastricht Aging Study: determinants of cognitive aging. *Neuropsych Publ*.
- Kalpouzos G, Chételat G, Baron J-C, Landeau B, Mevel K, Godeau C, Barré L, Constans J-M, Viader F, Eustache F, Desgranges B. 2009. Voxel-based mapping of brain gray matter volume and glucose metabolism profiles in normal aging. *Neurobiol Aging* 30:112–124.
- Kantarci K, Senjem ML, Avula R, Zhang B, Samikoglu AR, Weigand SD, Przybelski SA, Edmonson HA, Vemuri P, Knopman DS, Boeve BF, Ivnik RJ, Smith GE, Petersen RC, Jack CR. 2011. Diffusion tensor imaging and cognitive function in older adults with no dementia. *Neurology* 77:26–34.
- Karas G, Burton E, Rombouts S, van Schijndel R, O'Brien J, Scheltens P, McKeith I, Williams D, Ballard C, Barkhof F. 2003. A comprehensive study of gray matter loss in patients with Alzheimer's disease using optimized voxel-based morphometry. *Neuroimage* 18:895–907.
- Khalili-Mahani N, van Osch MJ, de Rooij M, Beckmann CF, Van Buchem MA, Dahan A, van Gerven JM, Rombouts SA. 2014. Spatial heterogeneity of the relation between resting-state connectivity and blood flow: an important consideration for pharmacological studies. *Hum Brain Mapp* 35:929–942.
- Khalili-Mahani N, Zoethout RMW, Beckmann CF, Baerends E, de Kam ML, Soeter RP, Dahan A, van Buchem MA, van Gerven JMA, Rombouts SA. 2012. Effects of morphine and alcohol on functional brain connectivity during “resting state”: a placebo-controlled crossover study in healthy young men. *Hum Brain Mapp* 33:1003–1018.
- Kim D II, Mathalon DH, Ford JM, Mannell M, Turner JA, Brown GG, Belger A, Gollub R, Lauriello J, Wible C, O'Leary D, Lim K, Toga A, Potkin SG, Birn F, Calhoun VD. 2009. Auditory oddball deficits in schizophrenia: an independent component analysis of the fMRI multisite function BIRN study. *Schizophr Bull* 35:67–81.
- King KS, Chen KX, Hulseay KM, McColl RW, Weiner MF, Nakonezny PA, Peshock RM. 2013. White matter hyperintensities: use of aortic arch pulse wave velocity to predict volume independent of other cardiovascular. *Radiology* 267:709–717.
- Klumpers LE, Cole DM, Khalili-Mahani N, Soeter RP, Te Beek ET, Rombouts SA, van Gerven JMA. 2012. Manipulating brain connectivity with δ^9 -tetrahydrocannabinol: a pharmacological resting state fMRI study. *Neuroimage* 63:1701–1711.

- Klunk WE, Engler H, Nordberg A, Wang Y, Blomqvist G, Holt DP, Bergstrom M, Savitcheva I, Huang G, Estrada S, Ausen B, Debnath ML, Barletta J, Price JC, Sandell J, Lopresti BJ, Wall A, Koivisto P, Antoni G, Mathis CA, Langstrom B. 2004. Imaging brain amyloid in Alzheimer's disease with Pittsburgh Compound-B. *Ann Neurol* 55:306–319.
- Koch W, Teipel S, Mueller S, Buerger K, Bokde ALW, Hampel H, Coates U, Reiser M, Meindl T. 2010. Effects of aging on default mode network activity in resting state fMRI: Does the method of analysis matter? *Neuroimage* 51:280–287.
- Krueger CE, Dean DL, Rosen HJ, Halabi C, Weiner M, Miller BL, Kramer JH. 2010. Longitudinal rates of lobar atrophy in frontotemporal dementia, semantic dementia, and Alzheimer's disease. *Alzheimer Dis Assoc Disord* 24:43–48.
- Laird AR, Fox PM, Eickhoff SB, Turner JA, Ray KL, McKay DR, Glahn DC, Beckmann CF, Smith SM, Fox PT. 2011. Behavioral interpretations of intrinsic connectivity networks. *J Cogn Neurosci* 23:4022–4037.
- Li X, Pu F, Fan Y, Niu H, Li S, Li D. 2013. Age-related changes in brain structural covariance networks. *Front Hum Neurosci* 7:1–13.
- Lillo P, Mioshi E, Burrell JR, Kiernan MC, Hodges JR, Hornberger M. 2012. Grey and white matter changes across the amyotrophic lateral sclerosis-frontotemporal dementia continuum. *PLoS One* 7:1–10.
- Lindeboom J, Schmand B, Tulner L, Walstra G, Jonker C. 2002. Visual association test to detect early dementia of the Alzheimer type. *J Neurol Neurosurg Psychiatry* 73:126–133.
- Lipton AM, Ohman KA, Womack KB, Hynan LS, Ninman ET, Lacritz LH. 2005. Subscores of the FAB differentiate frontotemporal lobar degeneration from AD. *Neurology* 65:726–731.
- Liu Y, Wang K, Yu C, He Y, Zhou Y, Liang M, Wang L, Jiang T. 2008. Regional homogeneity, functional connectivity and imaging markers of Alzheimer's disease: a review of resting-state fMRI studies. *Neuropsychologia* 46:1648–1656.
- Lustig C, Snyder AZ, Bhakta M, O'Brien KC, McAvoy M, Raichle ME, Morris JC, Buckner RL. 2003. Functional deactivations: change with age and dementia of the Alzheimer type. *Proc Natl Acad Sci USA* 100:14504–14509.
- Machulda M, Jones D, Vemuri P, McDade E, Avula R, Przybelski S, Boeve B, Knopman D, Petersen R, Jack CJ. 2011. Effect of APOE4 status on intrinsic network connectivity in cognitively normal elderly subjects. *Arch Neurol* 68:1131–1136.
- Madden DJ, Bennett IJ, Burzynska A, Potter GG, Chen N-K, Song AW. 2012. Diffusion tensor imaging of cerebral white matter integrity in cognitive aging. *Biochim Biophys Acta* 1822:386–400.
- Mathers CD, Stevens G a, Boerma T, White R a, Tobias MI. 2015. Causes of international increases in older age life expectancy. *Lancet* 385:540–548.

- McKeith IG, Galasko D, Kosaka K, Perry EK, Dickson DW, Hansen LA, Salmon DP, Lowe J, Mirra SS, Byrne EJ, Lennox G, Quinn NP, Edwardson JA, Ince PG, Bergeron C, Burns A, Miller BL, Lovestone S, Collerton D, Jansen EN, Ballard C, de Vos RA, Wilcock GK, Jellinger KA, Perry RH. 1996. Consensus guidelines for the clinical and pathologic diagnosis of dementia with Lewy bodies (DLB): report of the consortium on DLB international workshop. *Neurology* 47:1113–1124.
- McKhann G, Drachman D, Folstein M, Katzman R, Price D, Stadlan EM. 1984. Clinical diagnosis of Alzheimer's disease: Report of the NINCDS ADRDA work group under the auspices of department of health and human services task force on Alzheimer's disease. *Neurology* 34:939–944.
- McKhann GM. 2011. Changing concepts of Alzheimer disease. *JAMA* 305:2458–2459.
- McMillan CT, Avants BB, Cook P, Ungar L, Trojanowski JQ, Grossman M. 2014. The power of neuroimaging biomarkers for screening frontotemporal dementia. *Hum Brain Mapp* 35:4827–4840.
- Mesrob L. 2012. DTI and structural MRI classification in Alzheimer's Disease. *Adv Mol Imaging* 12–20.
- Mesulam MM. 1998. From sensation to cognition. *Brain* 121:1013–1052.
- Mielke M, Kozauer N, Chan K, George M, Toroney J, Zerrate M, Bandeen-Roche K, VanZijl P, Pekar J, Mori S, Lyketsos C, Albert M. 2009. Regionally-specific diffusion tensor imaging in mild cognitive impairment and Alzheimer's disease. *Neuroimage* 46:47–55.
- Minoshima S, Giordani B, Berent S, Frey KA, Foster NL, Kuhl DE. 1997. Metabolic reduction in the posterior cingulate cortex in very early Alzheimer's disease. *Ann Neurol* 42:85–94.
- Mitchell AJ. 2008a. The clinical significance of subjective memory complaints in the diagnosis of mild cognitive impairment and dementia: a meta-analysis. *Int J Geriatr Psychiatry* 23:1191–1202.
- Mitchell AJ. 2008b. Is it time to separate subjective cognitive complaints from the diagnosis of mild cognitive impairment? *Age Ageing* 37:497–499.
- Möller C, Hafkemeijer A, Pijnenburg YAL, Rombouts SA, van der Grond J, Dopfer E, van Swieten J, Versteeg A, Pouwels PJW, Barkhof F, Scheltens P, Vrenken H, van der Flier WM. 2015. Joint assessment of white matter integrity, cortical and subcortical atrophy to distinguish AD from behavioral variant FTD: a two-center study. *Neuroimage Clin* 9:418–429.
- Möller C, Hafkemeijer A, Pijnenburg YAL, Rombouts SA, van der Grond J, Dopfer E, van Swieten J, Versteeg A, Steenwijk MD, Barkhof F, Scheltens P, Vrenken H, van der Flier WM. 2016. Different patterns of cortical gray matter loss over time in behavioral variant frontotemporal dementia and Alzheimer's disease. *Neurobiol Aging* 38:21–31.

- Möller C, Pijnenburg Y AL, van der Flier WM, Versteeg A, Tijms B, de Munck J, Hafkemeijer A, Rombouts SA, van der Grond J, van Swieten J, Dopper EG, Scheltens P, Barkhof F, Vrenken H, Wink A. 2016. Alzheimer disease and behavioral variant frontotemporal dementia: Automatic classification based on cortical atrophy for single-subject diagnosis. In press. *Radiology*.
- Montejo P, Montenegro M, Fernandez MA, Maestu F. 2011. Subjective memory complaints in the elderly: Prevalence and influence of temporal orientation, depression and quality of life in a population-based study in the city of Madrid. *Aging Ment Heal* 15:85–96.
- Montembeault M, Joubert S, Doyon J, Carrier J, Gagnon J-F, Monchi O, Lungu O, Belleville S, Brambati SM. 2012. The impact of aging on gray matter structural covariance networks. *Neuroimage* 63:754–759.
- Montembeault M, Rouleau I, Provost J-S, Brambati SM. 2015. Altered gray matter structural covariance networks in early stages of Alzheimer’s disease. *Cereb Cortex* 1–13.
- Mormino EC, Smiljic A, Hayenga AO, Onami SH, Greicius MD, Rabinovici GD, Janabi M, Baker SL, V Yen I, Madison CM, Miller BL, Jagust WJ. 2011. Relationships between beta-amyloid and functional connectivity in different components of the default mode network in aging. *Cereb Cortex* 21:2399–2407.
- Morris J. 1993. The Clinical Dementia Rating (CDR): Current version and scoring rules. *Neurology* 43:2412–2414.
- Nichols TE, Holmes AP. 2001. Nonparametric permutation tests for functional neuroimaging: a primer with examples. *Hum Brain Mapp* 15:1–25.
- Niesters M, Khalili-Mahani N, Martini C, Aarts L, van Gerven J, van Buchem M, Dahan A, Rombouts S. 2012. Effect of subanesthetic ketamine on intrinsic functional brain connectivity. *Anesthesiology* 117:868–877.
- Oakes TR, Fox AS, Johnstone T, Chung MK, Kalin N, Davidson RJ. 2007. Integrating VBM into the General Linear Model with voxelwise anatomical covariates. *Neuroimage* 34:500–508.
- Okuizumi K, Onodera O, Tanaka H, Kobayashi H, Tsuji S, Takahashi H, Oyanagi K, Seki K, Tanaka M, Naruse S, Miyatake T, Mizusawa H, Kanazawa I. 1994. ApoE-epsilon4 and early-onset Alzheimer’s. *Nat Genet* 7:10–11.
- Patenaude B, Smith SM, Kennedy DN, Jenkinson M. 2011. A Bayesian model of shape and appearance for subcortical brain segmentation. *Neuroimage* 56:907–922.
- Persson J, Lind J, Larsson A, Ingvar M, Slegers K, Vanbroeckhoven C, Adolfsson R, Nilsson L, Nyberg L. 2008. Altered deactivation in individuals with genetic risk for Alzheimer’s disease. *Neuropsychologia* 46:1679–1687.
- Petersen RC, Smith GE, Waring SC, Ivnik RJ, Kokmen E, Tangalos EG. 1997. Aging, memory, and mild cognitive impairment. *Int Psychogeriatr* 9:65–69.

- Peterson RC, Doody R, Kurz A, Mohs RC, Morris JC, Rabins P V, Ritchie K, Rosser M, Thal L, Winblad B. 2001. Current concepts of mild cognitive impairment. *Arch Neurol* 58:1985–1992.
- Petrella JR, Sheldon FC, Prince SE, Calhoun VD, Doraiswamy PM. 2011. Default mode network connectivity in stable vs progressive mild cognitive impairment. *Neurology* 76:511–517.
- Pievani M, de Haan W, Wu T, Seeley WW, Frisoni GB. 2011. Functional network disruption in the degenerative dementias. *Lancet Neurol* 10:829–843.
- Pihlajamäki M, Sperling RA. 2009. Functional MRI assessment of task-induced deactivation of the default mode network in Alzheimer’s disease and at-risk older individuals. *Behav Neurol* 21:77–91.
- Prvulovic D, Hubl D, Sack AT, Melillo L, Maurer K, Frolich L, Lanfermann H, Zanella FE, Goebel R, Linden DEJ, Dierks T. 2002. Functional imaging of visuospatial processing in Alzheimer’s disease. *Neuroimage* 17:1403–1414.
- Raamana PR, Rosen H, Miller B, Weiner MW, Wang L, Beg MF. 2014. Three-class differential diagnosis among Alzheimer disease, frontotemporal dementia, and controls. *Front Neurol* 5:1–15.
- Rabinovici GD, Seeley WW, Kim EJ, Gorno-Tempini ML, Rascovsky K, Pagliaro TA, Allison SC, Halabi C, Kramer JH, Johnson JK, Weiner MW, Forman MS, Trojanowski JQ, DeArmond SJ, Miller BL, Rosen HJ. 2008. Distinct MRI atrophy patterns in autopsy-proven Alzheimer’s disease and frontotemporal lobar degeneration. *Am J Alzheimers Dis Other Demen* 22:474–488.
- Raichle ME, MacLeod AM, Snyder AZ, Powers WJ, Gusnard DA, Shulman GL. 2001. A default mode of brain function. *Proc Natl Acad Sci USA* 98:676–682.
- Rascovsky K, Hodges JR, Knopman D, Mendez MF, Kramer JH, Neuhaus J, van Swieten JC, Seelaar H, Dopper EGP, Onyike CU, Hillis AE, Josephs KA, Boeve BF, Kertesz A, Seeley WW, Rankin KP, Johnson JK, Gorno-Tempini M-L, Rosen H, Prigleau-Latham CE, Lee A, Kipps CM, Lillo P, Piguet O, Rohrer JD, Rossor MN, Warren JD, Fox NC, Galasko D, Salmon DP, Black SE, Mesulam M, Weintraub S, Dickerson BC, Diehl-Schmid J, Pasquier F, Deramecourt V, Lebert F, Pijnenburg Y, Chow TW, Manes F, Grafman J, Cappa SF, Freedman M, Grossman M, Miller BL. 2011. Sensitivity of revised diagnostic criteria for the behavioural variant of frontotemporal dementia. *Brain* 134:2456–2477.
- Ratnavalli E, Brayne C, Dawson K, Hodges JR. 2002. The prevalence of frontotemporal dementia. *Neurology* 58:1615–1621.
- Raz N, Lindenberger U, Rodrigue KM, Kennedy KM, Head D, Williamson A, Dahle C, Gerstorf D, Acker JD. 2005. Regional brain changes in aging healthy adults: general trends, individual differences and modifiers. *Cereb Cortex* 15:1676–1689.
- Reid AT, Evans AC. 2013. Structural networks in Alzheimer’s disease. *Eur*

- Neuropsychopharmacol 23:63–77.
- Reisberg B, Ferris S, De Leon M, Crook T. 1982. The global deterioration scale for assessment of primary degenerative dementia. *Am J Psychiat* 139:1136–1139.
- Resnick SM, Pham DL, Kraut MA, Zonderman AB, Davatzikos C. 2003. Longitudinal magnetic resonance imaging studies of older adults: a shrinking brain. *J Neurosci* 23:3295–3301.
- Rey A. 1958. *L'examen clinique en psychologie*. Press Univ Fr Paris, Fr.
- Rodda J, Dannhauser T, Cutinha DJ, Shergill SS, Walker Z. 2011. Subjective cognitive impairment: functional MRI during a divided attention task. *Eur Psychiat* 26:457–462.
- Rodda JE, Dannhauser TM, Cutinha DJ, Shergill SS, Walker Z. 2009. Subjective cognitive impairment: increased prefrontal cortex activation compared to controls during an encoding task. *Int J Geriatr Psychiatry* 24:865–874.
- Rombouts SARB, Barkhof F, Goekoop R, Stam CJ, Scheltens P. 2005. Altered resting state networks in mild cognitive impairment and mild Alzheimer's disease: an fMRI study. *Hum Brain Mapp* 26:231–239.
- Rombouts SARB, Damoiseaux JS, Goekoop R, Barkhof F, Scheltens P, Smith SM, Beckmann CF. 2009. Model-free group analysis shows altered BOLD fMRI networks in dementia. *Hum Brain Mapp* 30:256–266.
- Rombouts SARB, Goekoop R, Stam CJ, Barkhof F, Scheltens P. 2005. Delayed rather than decreased BOLD response as a marker for early Alzheimer's disease. *Neuroimage* 26:1078–1085.
- Rosen HJ, Gorno-Tempini ML, Goldman WP, Perry RJ, Schuff N, Weiner M, Feiwell R, Kramer JH, Miller BL. 2002. Patterns of brain atrophy in frontotemporal dementia and semantic dementia. *Neurology* 58:198–208.
- Roth M, Tym E, Mountjoy CQ, Huppert FA, Hendrie H, Verma S, Goddard R. 1986. CAMDEX. A standardised instrument for the diagnosis of mental disorder in the elderly with special reference to the early detection of dementia. *B J Psych* 149:698–709.
- Rytty R, Nikkinen J, Paavola L, Abou Elseoud A, Moilanen V, Visuri A, Tervonen O, Renton AE, Traynor BJ, Kiviniemi V, Remes AM. 2013. GroupICA dual regression analysis of resting state networks in a behavioral variant of frontotemporal dementia. *Front Hum Neurosci* 7:1–10.
- Rytty R, Nikkinen J, Suhonen N, Moilanen V, Renton AE, Traynor BJ, Tervonen O, Kiviniemi V, Remes AM. 2014. Functional MRI in patients with the C9ORF72 expansion associate frontotemporal dementia. *Mol Biol* 3:1–7.
- Sala-Llonch R, Bosch B, Arenaza-Urquijo EM, Rami L, Bargalló N, Junqué C, Molinuevo J-L, Bartrés-Faz D. 2010. Greater default-mode network abnormalities compared

- to high order visual processing systems in amnesic mild cognitive impairment: an integrated multi-modal MRI study. *J Alzheimers Dis* 22:523–539.
- Salat DH, Tuch DS, Greve DN, van der Kouwe AJW, Hevelone ND, Zaleta AK, Rosen BR, Fischl B, Corkin S, Rosas HD, Dale AM. 2005. Age-related alterations in white matter microstructure measured by diffusion tensor imaging. *Neurobiol Aging* 26:1215–1227.
- Salimi-Khorshidi G, Douaud G, Beckmann CF, Glasser MF, Griffanti L, Smith SM. 2014. Automatic denoising of functional MRI data: combining independent component analysis and hierarchical fusion of classifiers. *Neuroimage* 90:449–468.
- Saykin AJ, Wishart HA, Rabin LA, Santulli RB, Flashman LA, West JD, McHugh TL, Mamourian AC. 2006. Older adults with cognitive complaints show brain atrophy similar to that of amnesic MCI. *Neurology* 67:834–842.
- Schouten T, Loitfelder M, de Vos F, Seiler S, van der Grond J, Lechner A, Hafkemeijer A, Moller C, Schmidt R, de Rooij M, Rombouts SA. 2016. Combining anatomical, diffusion, and resting state functional magnetic resonance imaging for individual classification of mild and moderate Alzheimer’s disease. *Neuroimage Clin* 11:46–51.
- Seeley WW, Allman JM, Carlin DA, Crawford RK, Macedo MN, Greicius MD, Dearmond SJ, Miller BL. 2007. Divergent social functioning in behavioral variant frontotemporal dementia and Alzheimer disease: reciprocal networks and neuronal evolution. *Alzheimer Dis Assoc Disord* 21:50–57.
- Seeley WW, Crawford R, Rascofsky K, Kramer JH, Weiner M, Miller BL, Gorno-Tempini ML. 2008. Frontal paralimbic network atrophy in very mild behavioral variant frontotemporal dementia. *Arch Neurol* 65:249–255.
- Seeley WW, Crawford RK, Zhou J, Miller BL, Greicius MD. 2009. Neurodegenerative diseases target large-scale human brain networks. *Neuron* 62:42–52.
- Seeley WW, Menon V, Schatzberg AF, Keller J, Glover GH, Kenna H, Reiss AL, Greicius MD. 2007. Dissociable intrinsic connectivity networks for salience processing and executive control. *J Neurosci* 27:2349–2356.
- Segall JM, Allen EA, Jung RE, Erhardt EB, Arja SK, Kiehl K, Calhoun VD. 2012. Correspondence between structure and function in the human brain at rest. *Front Neuroinform* 6:1–17.
- Sheikh J, Yesavage J. 1986. Geriatric Depression Scale (GDS): a recent evidence and development of a shorter version. *Clin Gerontol* 5:165–173.
- Sheline YI, Morris JC, Snyder AZ, Price JL, Yan Z, D’Angelo G, Liu C, Dixit S, Benzinger T, Fagan A, Goate A, Mintun MA. 2010. APOE4 allele disrupts resting state fMRI connectivity in the absence of amyloid plaques or decreased CSF Abeta42. *J Neurosci* 30:17035–17040.
- Sheline YI, Raichle ME, Snyder AZ, Morris JC, Head D, Wang S, Mintun MA. 2010.

- Amyloid plaques disrupt resting state default mode network connectivity in cognitively normal elderly. *Biol Psychiatry* 67:584–587.
- Silani G, Lamm C, Ruff CC, Singer T. 2013. Right supramarginal gyrus is crucial to overcome emotional egocentricity bias in social judgments. *J Neurosci* 33:15466–15476.
- Slachevsky A, Villalpando JM, Sarazin M, Hahn-Barma V, Pillon B, Dubois B. 2004. Frontal assessment battery and differential diagnosis of frontotemporal dementia and Alzheimer disease. *Arch Neurol* 61:1104–1107.
- Smith CD. 2010. Neuroimaging through the course of Alzheimer’s disease. *J Alzheimers Dis* 19:273–290.
- Smith SM. 2002. Fast robust automated brain extraction. *Hum Brain Mapp* 17:143–155.
- Smith SM, Fox PT, Miller KL, Glahn DC, Fox PM, Mackay CE, Filippini N, Watkins KE, Toro R, Laird AR, Beckmann CF. 2009. Correspondence of the brain’s functional architecture during activation and rest. *Proc Natl Acad Sci USA* 106:13040–13045.
- Smith SM, Jenkinson M, Woolrich MW, Beckmann CF, Behrens TEJ, Johansen-berg H, Bannister PR, Luca M De, Drobnjak I, Flitney DE, Niazy RK, Saunders J, Vickers J, Zhang Y, Stefano N De, Brady JM, Matthews PM. 2004. Advances in functional and structural MR image analysis and implementation as FSL. *Neuroimage* 23:208–219.
- Smith SM, Nichols TE. 2009. Threshold-free cluster enhancement: addressing problems of smoothing, threshold dependence and localisation in cluster inference. *Neuroimage* 44:83–98.
- Sorg C, Riedl V, Mühlau M, Calhoun VD, Eichele T, Läer L, Drzezga A, Förstl H, Kurz A, Zimmer C, Wohlschläger AM. 2007. Selective changes of resting-state networks in individuals at risk for Alzheimer’s disease. *Proc Natl Acad Sci USA* 104:18760–18765.
- Soriano-Mas C, Harrison BJ, Pujol J, López-Solà M, Hernández-Ribas R, Alonso P, Contreras-Rodríguez O, Giménez M, Blanco-Hinojo L, Ortiz H, Deus J, Menchón JM, Cardoner N. 2013. Structural covariance of the neostriatum with regional gray matter volumes. *Brain Struct Funct* 218:697–709.
- Sperling RA, Laviolette PS, O’Keefe K, O’Brien J, Rentz DM, Pihlajamaki M, Marshall G, Hyman BT, Selkoe DJ, Hedden T, Buckner RL, Becker JA, Johnson KA. 2009. Amyloid deposition is associated with impaired default network function in older persons without dementia. *Neuron* 63:178–188.
- Sporns O, Honey CJ, Kotter R. 2007. Identification and classification of hubs in brain networks. *PLoS One* 2:1–14.
- Spreng RN, Turner GR. 2013. Structural covariance of the default network in healthy

- and pathological aging. *J Neurosci* 33:15226–15234.
- Steinberg BA, Bieliauskas LA, Smith GE, Ivnik RJ. 2005. Mayo's Older Americans Normative Studies: age- and IQ-adjusted norms for the Trail-Making Test, the Stroop test, and MAE controlled oral word association test. *Clin Neuropsychol* 19:329–377.
- Stewart R, Godin O, Crivello F, Maillard P, Mazoyer B, Tzourio C, Dufouil C. 2011. Longitudinal neuroimaging correlates of subjective memory impairment: 4-year prospective community study. *Br J Psychiatry* 198:199–205.
- Striepens N, Scheef L, Wind A, Popp J, Spottke A, Cooper-Mahkorn D, Suliman H, Wagner M, Schild HH, Jessen F. 2010. Volume loss of the medial temporal lobe structures in subjective memory impairment. *Dement Geriatr Cogn Disord* 29:75–81.
- Strittmatter WJ, Saunders AM, Schmechel D, Pericak-vance M, Enghild J, Salvesen GS, Roses AD. 1993. Apolipoprotein E: high-avidity binding to beta-amyloid and increased frequency of type 4 allele in late-onset familial Alzheimer disease. *Proc Natl Acad Sci USA* 90:1977–1981.
- Stroop JR. 1935. Studies of interference in serial verbal reactions. *J Exp Psychol* 18:643–662.
- Sui J, He H, Yu Q, Chen J, Rogers J, Pearlson GD, Mayer AR, Bustillo JR, Canive J, Calhoun VD. 2013. Combination of resting state fMRI, DTI, and sMRI data to discriminate schizophrenia by N-way MCCA + jICA. *Front Hum Neurosci* 7:1–14.
- Supekar K, Menon V, Rubin D, Musen M, Greicius MD. 2008. Network analysis of intrinsic functional brain connectivity in Alzheimer's disease. *PLoS Comput Biol* 4:1–11.
- Talelli P, Waddingham W, Ewas A, Rothwell JC, Ward NS. 2008. The effect of age on task-related modulation of interhemispheric balance. *Exp Brain Res* 186:59–66.
- Thurstone L, Thurstone T. 1962. Primary mental abilities. *Sci Res Assoc Chicago*.
- Tijms BM, Moller C, Vrenken H, Wink AM, De Haan W, Van der Flier WM, Stam CJ, Scheltens P, Barkhof F. 2013. Single-subject grey matter graphs in Alzheimer's disease. *PLoS One* 8:1–9.
- Tomasi D, Volkow ND. 2012. Aging and functional brain networks. *Mol Psychiatry* 17:549–558.
- Tondelli M, Wilcock GK, Nichelli P, De Jager CA, Jenkinson M, Zamboni G. 2012. Structural MRI changes detectable up to ten years before clinical Alzheimer's disease. *Neurobiol Aging* 33:25–36.
- Van der Flier WM, van Buchem MA, Weverling-Rijnsburger AWE, Mutsaers ER, Bollen ELEM, Admiraal-Behloul F, Westendorp RGJ, Middelkoop HAM. 2004. Memory complaints in patients with normal cognition are associated with smaller

- hippocampal volumes. *J Neurol* 251:671–675.
- Van Dijk KRA, Sabuncu MR, Buckner RL. 2012. The influence of head motion on intrinsic functional connectivity MRI. *Neuroimage* 59:431–438.
- Vestberg S, Passant U, Elfgren C. 2010. Stability in the clinical characteristics of patients with memory complaints. *Arch Gerontol Geriatr* 50:e26–e30.
- Wang K, Liang M, Wang L, Tian L, Zhang X, Li K, Jiang T. 2007. Altered functional connectivity in early Alzheimer’s disease: a resting-state fMRI study. *Hum Brain Mapp* 28:967–978.
- Wang L, Zang Y, He Y, Liang M, Zhang X, Tian L, Wu T, Jiang T, Li K. 2006. Changes in hippocampal connectivity in the early stages of Alzheimer’s disease: evidence from resting state fMRI. *Neuroimage* 31:496–504.
- Wang Z, Xia M, Dai Z, Liang X, Song H, He Y, Li K. 2015. Differentially disrupted functional connectivity of the subregions of the inferior parietal lobule in Alzheimer’s disease. *Brain Struct Funct* 220:745–762.
- Wechsler D. 1945. A standardised memory scale for clinical use. *J Psychol* 19:87–95.
- Wechsler D. 1997. WAIS–III administration and scoring manual. Psychol Corp San Antonio, TX.
- Wen W, Sachdev PS, Chen X, Anstey K. 2006. Gray matter reduction is correlated with white matter hyperintensity volume: a voxel-based morphometric study in a large epidemiological sample. *Neuroimage* 29:1031–1039.
- Westlye ET, Lundervold A, Rootwelt H, Lundervold AJ, Westlye LT. 2011. Increased hippocampal default mode synchronization during rest in middle-aged and elderly APOE4 carriers: relationships with memory performance. *J Neurosci* 31:7775–7783.
- Whitwell JL, Jack CR, Parisi JE, Knopman DS, Boeve BF, Petersen RC, Ferman TJ, Dickson DW, Josephs KA. 2007. Rates of cerebral atrophy differ in different degenerative pathologies. *Brain* 130:1148–1158.
- Whitwell JL, Josephs KA, Avula R, Tosakulwong N, Weigand SD, Senjem ML, Vemuri P, Jones DT, Gunter JL, Baker M, Wszolek ZK, Knopman DS, Rademakers R, Petersen RC, Boeve BF, Jack CR. 2011. Altered functional connectivity in asymptomatic MAPT subjects: a comparison to bvFTD. *Neurology* 77:866–874.
- Wishart HA, Saykin AJ, McAllister TW, Rabin LA, McDonald BC, Flashman LA, Roth RM, Mamourian AC, Tsongalis GJ, Rhodes CH. 2006. Regional brain atrophy in cognitively intact adults with a single APOE ϵ 4 allele. *Neurology* 67:1221–1224.
- Wishart HA, Saykin AJ, Rabin LA, Santulli RB, Flashman LA, Guerin SJ, Mamourian AC, Belloni DR, Rhodes CH, McAllister TW. 2006. Increased brain activation during working memory in cognitively intact adults with the APOE epsilon4 allele. *Am J Psychiat* 163:1603–1610.

- Woodward M, Jacova C, Black SE, Kertesz A, Mackenzie IR, Feldman H. 2010. Differentiating the frontal variant of Alzheimer's disease. *Int J Geriatr Psychiatry* 25:732–738.
- Wu K, Taki Y, Sato K, Kinomura S, Goto R, Okada K, Kawashima R, He Y, Evans AC, Fukuda H. 2012. Age-related changes in topological organization of structural brain networks in healthy individuals. *Hum Brain Mapp* 33:552–568.
- Wu K, Taki Y, Sato K, Qi H, Kawashima R, Fukuda H. 2013. A longitudinal study of structural brain network changes with normal aging. *Front Hum Neurosci* 7:1–12.
- Wu X, Li R, Fleisher AS, Reiman EM, Guan X, Zhang Y, Chen K, Yao L. 2011. Altered default mode network connectivity in alzheimer's disease—a resting functional MRI and bayesian network study. *Hum Brain Mapp* 32:1868–1881.
- Xu L, Groth KM, Pearson G, Schretlen DJ, Vince D. 2009. Source-based morphometry: the use of independent component analysis to identify gray matter differences with application to schizophrenia. *Hum Brain Mapp* 30:711–724.
- Yan C, Craddock RC, Zuo X-N, Zang Y-F, Milham MP. 2013. Standardizing the intrinsic brain: towards robust measurement of inter-individual variation in 1000 functional connectomes. *Neuroimage* 80:246–262.
- Yassa MA, Stark SM, Bakker A, Albert MS, Gallagher M, Stark CEL. 2010. High-resolution structural and functional MRI of hippocampal CA3 and dentate gyrus in patients with amnesic mild cognitive impairment. *Neuroimage* 51:1242–1252.
- Zhang D, Raichle ME. 2010. Disease and the brain's dark energy. *Nat Rev Neurol* 6:15–28.
- Zhang H-Y, Wang S, Liu B, Ma Z-L, Yang M, Zhang Z-J, Teng G-J. 2010. Resting brain connectivity: changes during the progress of Alzheimer Disease. *Radiology* 256:598–606.
- Zhang H-Y, Wang S-J, Xing J, Liu B, Ma Z-L, Yang M, Zhang Z-J, Teng G-J. 2009. Detection of PCC functional connectivity characteristics in resting-state fMRI in mild Alzheimer's disease. *Behav Brain Res* 197:103–108.
- Zhang Y, Brady JM, Smith SM. 2001a. An HMRf-EM algorithm for partial volume segmentation of brain MRI. FMRIB Tech Rep TR01YZ1 from www.fmrib.ox.ac.uk/analysis/techrep Last accessed June 26, 2015.
- Zhang Y, Brady M, Smith S. 2001b. Segmentation of brain MR images through a hidden Markov random field model and the expectation-maximization algorithm. *IEEE Trans Med Imaging* 20:45–57.
- Zhou B, Yao H, Wang P, Zhang Z, Zhan Y, Ma J, Xu K, Wang L, An N, Liu Y, Zhang X. 2015. Aberrant functional connectivity architecture in Alzheimer's disease and mild cognitive impairment: a whole-brain, data-driven analysis. *Biomed Res Int* 2015:1–9.

- Zhou J, Greicius MD, Gennatas ED, Growdon ME, Jang JY, Rabinovici GD, Kramer JH, Weiner M, Miller BL, Seeley WW. 2010. Divergent network connectivity changes in behavioural variant frontotemporal dementia and Alzheimer's disease. *Brain* 133:1352–1367.
- Zielinski BA, Anderson JS, Froehlich AL, Prigge MBD, Nielsen JA, Cooperrider JR, Cariello AN, Fletcher PT, Alexander AL, Lange N, Bigler ED, Lainhart JE. 2012. scMRI reveals large-scale brain network abnormalities in autism. *PLoS One* 7:e49172–e49172.

Dankwoord

Dit proefschrift is mede tot stand gekomen dankzij waardevolle bijdragen van velen. Graag wil ik iedereen die bij mijn promotieproject betrokken is geweest bedanken.

Ten eerste bedank ik alle deelnemers van de verschillende studies voor hun vrijwillige medewerking.

Speciale dank gaat uit naar mijn promotor prof. dr. S.A.R.B. Rombouts en copromotor dr. J. van der Grond. Beste Serge, beste Jeroen, bedankt voor de mogelijkheden die jullie me hebben geboden, het regelmatige en laagdrempelige contact en jullie steun.

Geachte leden van de promotiecommissie, prof. dr. M.J. de Rooij, prof. dr. H.A.M. Middelkoop, prof. dr. J.C. van Swieten en prof. dr. W.M. van der Flier, bedankt voor het beoordelen van mijn proefschrift en voor jullie bereidheid om bij mijn verdediging aanwezig te zijn.

Christiane Möller, Wiesje van der Flier, Hugo Vrenken en Yolande Pijnenburg van het VU Medisch Centrum Amsterdam, bedankt voor de samenwerking. Ideaal dat onze projecten zo nauw verweven waren en dat we onze data en kennis met elkaar hebben mogen delen. Ik ben trots op het eindresultaat dat we hebben weten te bereiken.

Elise Dopper, Lize Jiskoot en John van Swieten van het Erasmus Universitair Medisch Centrum Rotterdam, bedankt voor jullie bijdrage bij het includeren van de studiedeelnemers. Elise, bedankt voor je tomeloze inzet en je hulp tijdens de scanweekenden. Lize, bedankt voor het afnemen van de neuropsychologische testen. En John, bedankt dat we gebruik mochten maken van je klinische expertise.

Daarnaast wil ik het ondersteunend personeel van het Leids Universitair Medisch Centrum - Michèle Huijberts, Michel Villerius, Wouter Teeuwisse, Joost Doornbos, Mattanja Latuhihin en de K4-receptionisten - bedanken voor de hulp om het project soepel te laten verlopen.

Additionally, I want to thank Gabriel Rivera from InfoCortex UG for his help with the XNAT server, which gives us great opportunities to share our data.

Alle coauteurs, de verschillende studenten - in het bijzonder Wendy de Leng en Vicky Chalos - en de collega's van K4.44, bedankt voor jullie bijdragen en zeer gewaardeerde discussies.

Beste paranimfen, Annette van den Berg-Huysmans en Mischa de Rover, bedankt voor jullie steun en het proofreaden. Fijn dat jullie er altijd voor mij zijn, zowel vakinhoudelijk als ook daar buiten.

Renske, bedankt voor je vriendschap en in het bijzonder voor het ontwerpen van de omslag van dit proefschrift.

Frank, Ton, Bart en in het bijzonder Martin, bedankt voor jullie steun, liefde en de mogelijkheden die jullie bieden voor de nodige ontspanning.

Allen bedankt!

Curriculum vitae

Anne Hafkemeijer was born on the 26th of August 1986 in Tilburg and grew up in Esbeek, the Netherlands. After finishing high school at *Koning Willem II College* in Tilburg in 2004, she received her bachelor's degree in Medical Biology in 2007 from the *Radboud University Nijmegen*. Because of her interest in neurobiology and neuropathology, Anne applied for the research master Cognitive Neuroscience. In 2009, Anne received her master's degree in Cognitive Neuroscience and in 2010 her master's degree in Medical Biology both from the



Radboud University Nijmegen. As part of her graduation, Anne performed two neuroimaging studies. The first study was conducted under supervision of Dr. Amanda Kiliaan and Dr. Diane Jansen at the department of Anatomy and Cognitive Neuroscience, Radboud University Medical Center, Nijmegen. In this MRI study, she investigated the effects of nutritional lipids on cognition and cerebral hemodynamics in aging and dementia. In the second study, under supervision of Dr. Tineke van Rijn, she used EEG to investigate the sedating effects of cannabinoids at the Biological Psychology department, Donders Institute for Brain, Cognition, and Behaviour, Nijmegen. In November 2010, Anne started her PhD research at *Leiden University, Leiden Institute for Brain and Cognition, and Leiden University Medical Center* under supervision of professor Serge Rombouts and Dr. Jeroen van der Grond. In her PhD project, Anne used in addition to the commonly studied functional brain networks, a relatively new approach based on structural covariance to study structural brain networks. Her findings resulted in more insights in brain networks in healthy aging and dementia as described in this thesis. In April 2016, Anne started as MRI research coordinator and consultant at *Leiden University Medical Center and Leiden University*.

List of publications

2016

Hafkemeijer A, Möller C, Dopper EGP, Jiskoot LC, van den Berg-Huysmans AA, van Swieten JC, van der Flier WM, Vrenken H, Pijnenburg YAL, Barkhof F, Scheltens P, van der Grond J, Rombouts SA (2016) Differences in structural covariance networks between behavioral variant frontotemporal dementia and Alzheimer's disease. *Human Brain Mapping 37*: 978-988

Möller C, **Hafkemeijer A**, Pijnenburg YAL, Rombouts SA, van der Grond J, Dopper EGP, van Swieten JC, Versteeg A, Steenwijk M, Barkhof F, Scheltens P, Vrenken H, van der Flier WM (2016) Different patterns of cortical gray matter loss over time in behavioral variant frontotemporal dementia and Alzheimer's disease. *Neurobiology of Aging 38*: 21-31

Schouten TM, Loitfelder M, de Vos F, Seiler S, van der Grond J, Lechner A, **Hafkemeijer A**, Schmidt R, de Rooij M, Rombouts SA (2016) Combining anatomical, diffusion, and resting state magnetic resonance imaging for individual classification of mild and moderate Alzheimer's disease. *Neuroimage Clinical 11*: 46-51

De Vos F, Schouten TM, **Hafkemeijer A**, Dopper EGP, van Swieten JC, de Rooij M, van der Grond J, Rombouts SA (2016) Combining multiple anatomical MRI measures improves Alzheimer's disease classification. *Human Brain Mapping: in press*

Möller C, Pijnenburg YAL, van der Flier WM, Versteeg A, Tijms B, de Munck JC, **Hafkemeijer A**, Rombouts SA, van der Grond J, van Swieten JC, Dopper EGP, Scheltens P, Barkhof F, Vrenken H, Wink AM (2016) Alzheimer disease and behavioral variant frontotemporal dementia: Automatic classification based on cortical atrophy for single-subject diagnosis. *Radiology: in press*

2015

Hafkemeijer A, Möller C, Dopper EGP, Jiskoot LC, Schouten TM, van Swieten JC, van der Flier WM, Vrenken H, Pijnenburg YAL, Barkhof F, Scheltens P, van der Grond J, Rombouts SA (2015) Resting state functional connectivity differences between behavioral variant frontotemporal dementia and Alzheimer's disease. *Frontiers in Human Neuroscience 9*: 1-12

Möller C, **Hafkemeijer A**, Pijnenburg YAL, Rombouts SA, van der Grond J, Dopper EGP, van Swieten JC, Versteeg A, Pouwels PJW, Barkhof F, Scheltens P, Vrenken H, van der Flier WM (2015) Joint assessment of white matter integrity, cortical and subcortical atrophy to distinguish AD from behavioral variant FTD: a multi-center study. *Neuroimage Clinical* 9: 418-429

2014

Hafkemeijer A, Altmann-Schneider I, de Craen AJ, Slagboom PE, van der Grond J, Rombouts SA (2014) Associations between age and gray matter volume in anatomical brain networks in middle-aged to older adults. *Aging Cell* 13: 1068-1074

2013

Hafkemeijer A, Altmann-Schneider I, Oleksik AM, van de Wiel L, Middelkoop HA, van Buchem MA, van der Grond J, Rombouts SA (2013) Increased functional connectivity and brain atrophy in elderly with subjective memory complaints. *Brain Connectivity* 3: 353-362

Jansen D, Zerbi V, Janssen CI, Dederen PJ, Mutsaers MP, **Hafkemeijer A**, Janssen AL, Nobelen CL, Veltien A, Asten JJ, Heerschap A, Kiliaan AJ (2013) A longitudinal study of cognition, proton MR spectroscopy and synaptic and neuronal pathology in aging wild-type and AbetaPP^{swe-PS1dE9} mice. *Plos One* 8: 1-17

2012

Hafkemeijer A, van der Grond J, Rombouts SA (2012) Imaging the default mode network in aging and dementia. *Biochimica et Biophysica Acta – Molecular Basis of Disease* 1822: 431-441

Jansen D, Janssen CI, Vanmierlo T, Dederen PJ, van Rooij D, Zinnhardt B, Nobelen CL, Janssen AL, **Hafkemeijer A**, Mutsaers MP, Doedée AM, Kuipers AA, Broersen LM, Mulder M, Kiliaan AJ (2012) Cholesterol and synaptic compensatory mechanisms in Alzheimer's disease mice brain during aging. *Journal of Alzheimers Disease* 31: 813-826

Hafkemeijer A, van der Grond J, van Buchem M, Rombouts SA (2012) FMRI bij veroudering en dementie: het 'default-mode netwerk'. *Memorad Neuro fMRI* 17: 40-44

Manuscripts under review

Hafkemeijer A, Möller C, Dopper EGP, Jiskoot LC, van den Berg-Huysmans AA, van Swieten JC, van der Flier WM, Vrenken H, Pijnenburg YAL, Barkhof F, Scheltens P, van der Grond J, Rombouts SA (submitted) A longitudinal study on resting state functional connectivity in behavioral variant frontotemporal dementia and Alzheimer's disease.

Dopper EGP, Jiskoot LC, den Heijer T, **Hafkemeijer A**, de Koning I, Seelaar H, Veer IM, van Buchem MA, van Minkelen R, Rombouts SA, van Swieten JC (submitted) Longitudinal brain changes in presymptomatic familial frontotemporal dementia.

Dopper EGP, Chalos V, Ghariq E, den Heijer T, **Hafkemeijer A**, Jiskoot LC, de Koning I, Seelaar H, van Minkelen R, van Osch MJP, Rombouts SA, van Swieten JC (submitted) Cerebral blood flow in presymptomatic familial frontotemporal dementia: a longitudinal arterial spin labeling study.

Foster-Dingley JC, **Hafkemeijer A**, van den Berg-Huysmans AA, Moonen JE, de Ruijter W, de Craen AJ, van der Mast RC, Rombouts SA, van der Grond J (submitted) Integrity of structural covariance networks is associated with cognitive functioning independently of cerebral small vessel disease in older persons.

Coppen EM, van der Grond J, **Hafkemeijer A**, Rombouts SA, Roos RA (submitted) Early cortical changes in structural covariance networks in Huntington's disease.

